PRODIAG

Combined Expert System/Neural Network
for Process Fault Diagnosis

Volume 1: THEORY

J. Reifman
T. Y. C. Wei
J. E. Vitela

September 1995

Argonne National Laboratory
9700 South Cass Avenue
Argonne, Illinois 60439

TABLE OF CONTENTS

TABLE OF CONTENTS (Cont'd)

TABLE OF CONTENTS (Cont'd)

LIST OF FIGURES

LIST OF FIGURES (Cont'd)

LIST OF FIGURES (Cont'd)

LIST OF TABLES

LIST OF TABLES (Cont'd)

GLOSSARY OF ACRONYMS

AI	Artificial Intelligence
ANN	Artificial Neural Network
BC	Boundary Condition
CCD	Component Classification Dictionary
CV	Control Volume
EOS	Equation of State
ECS	External Connected System
ES	Expert System
FTRS	Faster-than-real-time Simulator
HX	Heat Exchanger
ICS	Internal Connected System
JC	Junction Component
LHS	Left-hand side
PID	Piping Instrumentation Diagram
PORV	Pressure Operated Relief Valve
PRD	Physical Rules Database
RHS	Right-hand side
SS	Secondary System
T-H	Thermal-hydraulic
TW	Time Window
TWS	Time Window Selector
V&V	Verification and Validation

NOMENCLATURE

A	cross sectional area
Δp_{pump}	pump head
c	specific heat
c_p	specific heat at constant pressure
h	enthalpy
$h_{s\ell}$	liquid saturation enthalpy
k	momentum loss coefficient
k_{pipe}	pipe coefficient
k_{valve}	valve coefficient
ℓ	level
L	length
m	mass
Min	minimum
p	pressure
Q_{mass}	mass source or sink strength
Q_{mom}	momentum source or sink strength
Q_{eng}	energy source or sink strength
t	time
T	temperature
$T_{s\ell}$	liquid saturation temperature
V	volume
w	flow

w_a	component average flow
x	signal variable

Greek symbols

α	thermal expansion coefficient
δ	increment
Δ	differential
ϵ_x	signal x threshold
ε_p	primary threshold
ε_s	secondary threshold
ρ	density
τ	time constant
$\tau_{hydslop}$	hydraulic slop time constant
$\tau_{transport}$	transport time constant
$\rightarrow$	then
,	or

superscripts

-	constant
$\bar{}$	nondimensionalized
/	negation
$\uparrow$	increasing
$\downarrow$	decreasing
'	first derivative

''	second derivative
o	steady state

subscripts

down	down stream
g	gas
EC	end condition
HX	heat exchanger
i	inlet
in	inlet
inst	instrument.
ℓ	liquid
m	metal
ntfd	natural feedback
o	outlet
out	outlet
up	upstream

TERMINOLOGY INDEX

1.0 SYSTEM DESIGN DEFINITION

1.1 Introduction

The function of the PRODIAG code is to diagnose on-line the root cause of a thermal-hydraulic (T-H) system transient with trace back to the identification of the malfunctioning component using the T-H instrumentation signals exclusively. The code methodology is based on the AI techniques of automated reasoning/expert systems (ES) and artificial neural networks (ANN). The research and development objective is to develop a generic code methodology which would be plant- and T-H-system-independent. For the ES part the only plant or T-H system specific code requirements would be implemented through input only and at that only through a Piping and Instrumentation Diagram (PID) database [1.1]. For the ANN part the only plant or T-H system specific code requirements would be through the ANN training data for normal component characteristics and the same PID database information. PRODIAG would, therefore, be generic and portable from T-H system to T-H system and from plant to plant without requiring any code-related modifications except for the PID database and the ANN training with the normal component characteristics. This would give PRODIAG the generic feature which numerical simulation plant codes such as TRAC or RELAP5 have. As the code is applied to different plants and different T-H systems, only the connectivity information, the operating conditions and the normal component characteristics are changed, and the changes are made entirely through input. Verification and validation of PRODIAG would, therefore, be T-H system independent and would be performed only "once". With each different application, verification would only be performed for the input deck which is the specific T-H system model [1.2].

To achieve the driving technical objective of a generic feature, several novel theoretical concepts in intelligent database knowledge structuring had to be introduced and developed in detail. This Theory Manual, Volume 1, describes those concepts and those details. It forms the basis for the practical implementation of the diagnostic algorithm as described in the PRODIAG Code Manual, Volume 2. In summary, in contrast to a traditional event-oriented knowledge base [1.3-1.5], the knowledge structure used by PRODIAG is based on T-H first-principles [1.6-1.7]. System functions (such as heat or mass transfer) are used in conjunction with equipment characteristics (such as pressure-versus-flow curves that define the operating ranges of pumps and valves). Together these provide a two-level approach to diagnosing process system faults. The PRODIAG concept has therefore a two-level, hierarchical knowledge structure. At the first level, an expert system uses T-H functions to determine physical occurrences (i.e., water added or lost, heat added or lost). At the second level, artificial neural networks pinpoint the source of the transient by classifying the functional misbehavior of the system through specific component characteristics [1.8].

An effort has been made in Volume 1 to document the theoretical concepts and structure of the PRODIAG diagnostic algorithm in a systematic and comprehensive manner. Given the available resources and the available data, priority in the implementation of those concepts in the PRODIAG code was given to these concepts which would provide for the proof-of-concept laboratory testing with the test cases detailed in Volume 3 on Applications. Certain approximations to the theory could also be made in the practical implementation and were made to improve the time performance without sacrificing accuracy performance. These approximations are described in the PRODIAG Code Manual, which is Volume 2. As future resources and data become available, expansion of the implementation of the theoretical concepts detailed here will be carried out. Chief among these is

the second level of the diagnostic approach, the network of ANNs. Due to the general limited availability of component characteristics data, in particular, transient (high frequency band) characteristics, and the efficiency of the first level, the ES, in diagnosing the malfunctions of the selected test cases, the major implementation of the second level, the ANNs, has been deferred to future work. A limited implementation of ANNs has been carried out to aid the ES at the first level of diagnosis. It is the stated intent that this theory volume form the comprehensive and systematic basis of the concepts for the future implementation work which will expand the range of PRODIAG.

The knowledge based structuring concepts have been developed for the current laboratory-scale version of PRODIAG for the following range of applicability:

- single-phase liquid plus noncondensible gas T-H systems;
- non-neutronic heat sources;
- coolants with bulk moduli and thermal expansion coefficients similar to water;
- single fault initiated transient scenarios;
- transient severity should be sufficient for instrumentation in single-phase liquid components to respond;
- use of instrumentation signal data which has been filtered for noise;
- diagnostic window closure upon initiation of control action.

The issue of optimization for time performance has been deferred to future work. Future work will also extend this range of applicability so that two-phase saturated T-H systems, multiple faults, and neutron fission power feedback can be treated.

The next section describes the overall diagnostic strategy which forms the framework for the two-level hierarchical structuring of the PRODIAG knowledge database.

1.2 System Diagnostic Strategy

Thermal-hydraulic phenomena play a major role with a wide range of behavior for many different fields of application. The physics of thermal-hydraulics is, therefore, a complex area. Initially, it would appear not to be possible to develop a generic AI-based system for process diagnosis where the only plant- and thermal-hydraulic system-application dependent input requirement is the piping and instrumentation information. However, it should be pointed out that there already exists a universal description of thermal-hydraulics regardless of the type of the application. This is the mathematical description inscribed in the calculus form of the Navier-Stokes conservation equations with various equations of state and transport properties for use with the different materials encountered. Furthermore, this mathematical description has been generalized further with the introduction of nondimensional groups, similarity solutions and length-scaling to universalize the effects of materials, thermal-hydraulic conditions, and geometrical configurations. Decades ago when numerical computer simulation of thermal-hydraulic systems was being introduced, a different simulation code was written or 'hard-wired' for each thermal-hydraulic system. It was then realized that the universal equations permitted the usage of basic elements, volumes, junctions/pipes and heat slabs which then allowed the development of a "few" simulation codes which could model a wide variety of thermal-hydraulic systems. The field of expert systems for process diagnostics has reached a similar point. Canonical structuring of this T-H knowledge base into a process diagnostics language with a number of key abstractions and general concepts transformed into language

constructs (mass source, energy sink, ..., momentum imbalance), will allow this generic thermal-hydraulic system independent generalization.

The canonical structuring has to be grounded on the universal mathematical description. If not, heuristics would inevitably creep in and render the concept of thermal-hydraulic system independence meaningless. The mathematical description has to be transformed into the AI system construct of rules, representations, and supervisory flow logic. This is a first-principles approach. The mathematical description consists of the three mass, momentum, and energy conservation equations, transport properties, correlations for viscosities and conductivity and, usually, the pressure equation of state. Process diagnostics at this research stage will be restricted to the identification of faulty T-H system components during an off-normal event. This starting point fuzzifies the required output from the expert system. For instance, the precise extent of component failure will not be initially required. This lack of precision on the output decreases the requirements on the transformation of the mathematical description, but the transformation is still very demanding. We divide the transformation into parts by using the taxonomy of Fig. 1.1, which assumes no chemical reactions.

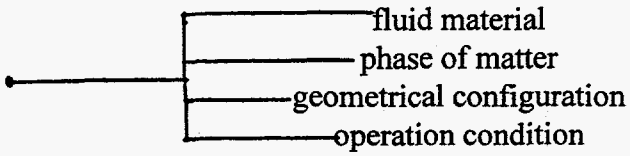

Fig. 1.1. Thermal-Hydraulic System Classification

At this stage of the research, we choose to focus on subcooled liquid water. Future research will reexamine the effect of fluid material and phase selection on the generalization of the expert system. Currently, it appears that the bulk modulus and the thermal expansion coefficient are the only fluid material properties which affect the generalization for subcooled liquids. The bulk modulus determines incompressibility which is extensively used in the transformation of the mathematical description. A low thermal expansion coefficient allows the decoupling of the energy equations from the mass and momentum equations in the transformation. This still leaves the effect of geometrical configuration and operating condition. To permit the generalization, the taxonomy of Fig. 1.1 is broken down further in Chapters 3 and 4.

The knowledge base structuring which forms the framework for the PRODIAG methodology emulates the analytic decomposition strategy for root cause fault diagnosis followed by the system designer using first-principles engineering. This is in contrast to the intuitive heuristic strategy of the plant operator which uses the recognition of previous patterns. The overall decomposition strategy is summarized below [1.8].

- Use a prescribed formula with a set of the T-H signal data to detect the presence or absence of a specific key T-H feature. Then,

- check a predetermined classification list of components classified by the key T-H feature to obtain a candidate list of potential malfunctioning components using the previously detected present or absent specific key T-H features. Then,

- check the system connectivity information contained in the PID to see what match and reduction can be made against the previous candidate list of potential malfunctioning components. If a single unique match can be made, then the malfunctioning component has been identified. Otherwise, repeat the process with other formulas and other key T-H features.

This overall strategy is necessary to allow the generic portability from T-H system to T-H system without major code modifications. It is, however, by itself not sufficient. The key T-H features used for the classification and the classified components have to be generic and not unique to specific T-H systems. Figure 1.2 shows the details of the analytic decomposition strategy. The notation [w p h ℓ] is used for the set of T-H signal variables [flow pressure enthalpy level] utilized exclusively for the diagnostics. It can be seen that three sets of T-H formulas are used with the set of T-H signal data to detect the presence or absence of key T-H features. There are, in order of diagnostic sequence,

(1) The three conservation equations of mass, momentum, and energy to detect changes in the features of the three key T-H functions; mass momentum, and energy transfer.

(2) The normal operation quasi-static component T-H characteristics to detect generic and specific component characteristics changes.

(3) The normal operation transient component T-H characteristics to detect specific component characteristics changes.

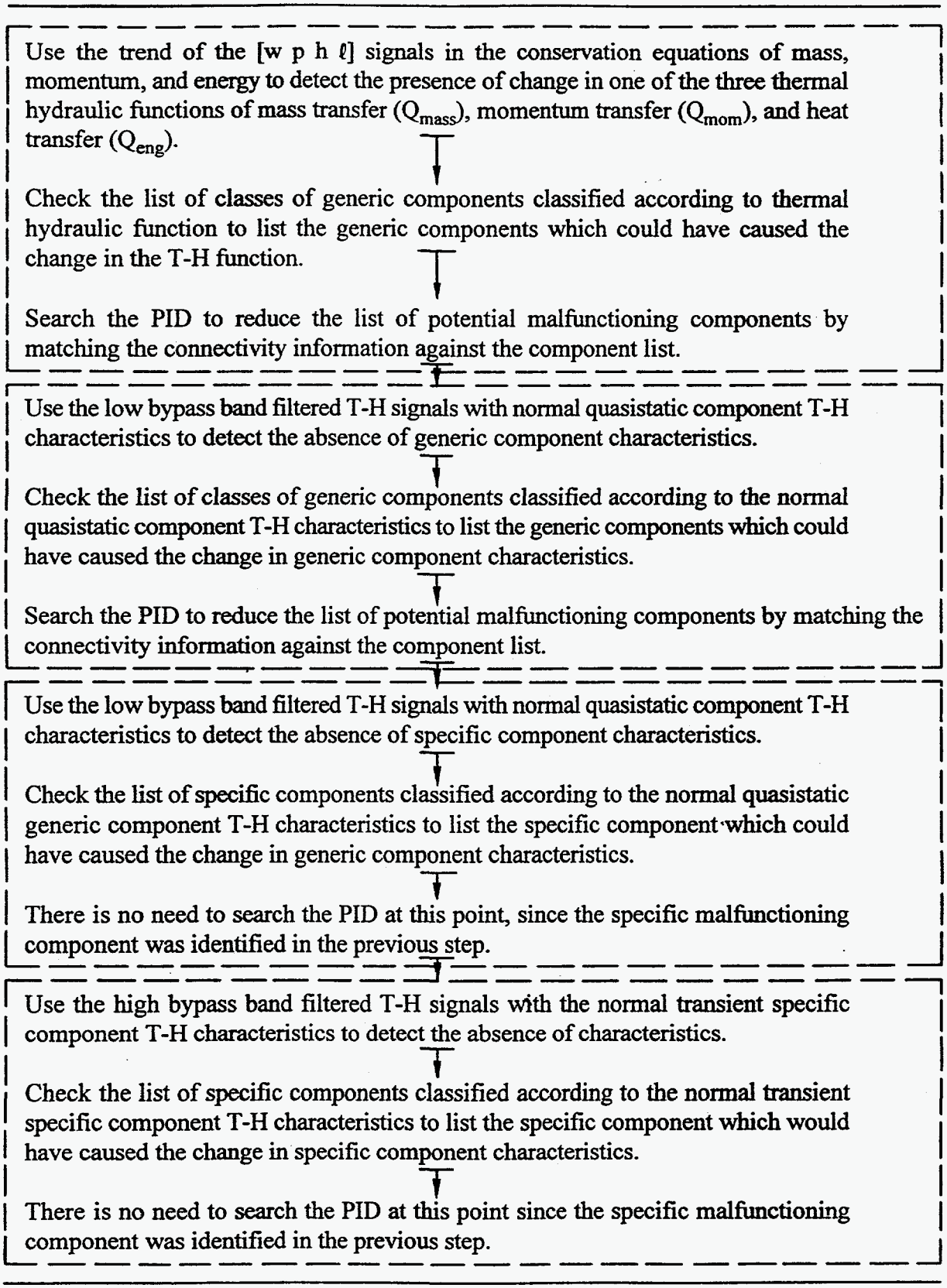

Fig. 1.2. Analytic Decomposition Strategy

Dynamic effects in the transient response of a T-H system are complex and coupled. The PRODIAG methodology is to decompose the temporal data into first-order initial trends, low-bypass band (low frequency) data, and high-bypass band (high frequency) data. The proposed route is to analyze dynamic effects and correlate them before the initiation of the diagnostic reasoning with the sets of T-H formulas (1)-(3). Additional details are available in Chapters 2 and 3. In accordance with the strategy, the conservation equations formulas (1) used to detect imbalances in the three key T-H functions are then applied to control volumes in quasistatic form. Control volumes can include one or several T-H components. Qualitative analysis theory is utilized to convert the conservation equations into "simple" first principles correlations which tie the trend of the T-H signals from different components across the plant system to infer imbalances in one of the T-H functions, mass (Q_{mass}), momentum (Q_{mom}), or energy (Q_{eng}) in that control volume. Q is used to represent source strength, either numerically in the balance equations as actual values, or symbolically in the ES rules as signal trends. This is diagnostics at the plant level and begins to localize the identification of the component malfunction. These correlations utilize only the initial trends of the T-H signal variables which is, therefore, only the first-order perturbation of the temporal data. Figure 1.2 shows that after the application of the conservation formulas (1), the next step is to apply the normal operation quasistatic component characteristic formulas (2) which utilize the low bypass band data. While these formulas can be applied to the plant T-H system as one control volume, practically, it becomes more difficult and the control volumes need to shrink to a few or one component. This is diagnostics at the component level. Detailed spatial correlations are replaced by detailed temporal correlations. A smaller number of signals at different locations are used in the diagnostics, but more detail from the time signature of each of these signals is utilized. This signal data when utilized with the quasistatic component characteristics will detect the absence of generic or specific component T-H

characteristics. The final set of T-H formulas (3) are the correlations for the normal operation transient T-H component characteristics. These are applied one specific component by one specific component and utilize the complete high-bypass band temporal signal data. Each component which has a unique T-H characteristic spectrum will have the absence of that spectrum detected. This completes the diagnostics at the component level [1.9].

As can be seen from Fig. 1.2, the overall strategy can be summarized as a three-step process used repeatedly with the three sets of T-H formulas:

(1) Apply a T-H formula using the T-H signal data;

(2) Check a predetermined list of component classifications;

(3) Search the PID.

The "simpler" T-H formulas in step (1) can be expressed in terms of IF-THEN rules, but the more "complicated" formulas required the additional flexibility of the ANN knowledge base structure. Table 1.1 shows the diagnostic strategy of Fig. 1.2 translated into a tree structure. The entries of the tree form the entries of a database, the Component Classification Dictionary. Each level of the tree is the application of 'a' T-H formula and the branches (i.e., entries) leading from the level are the corresponding list of components classified by the key T-H feature. The set of formulas form a rule database, the Physical Rules Database. The T-H physics formulas which are utilized in this set are shown in the second column of Table 1.1. It will be recognized that these are the formulas discussed

Table 1.1. Analytic Decomposition Strategy Tree Structure

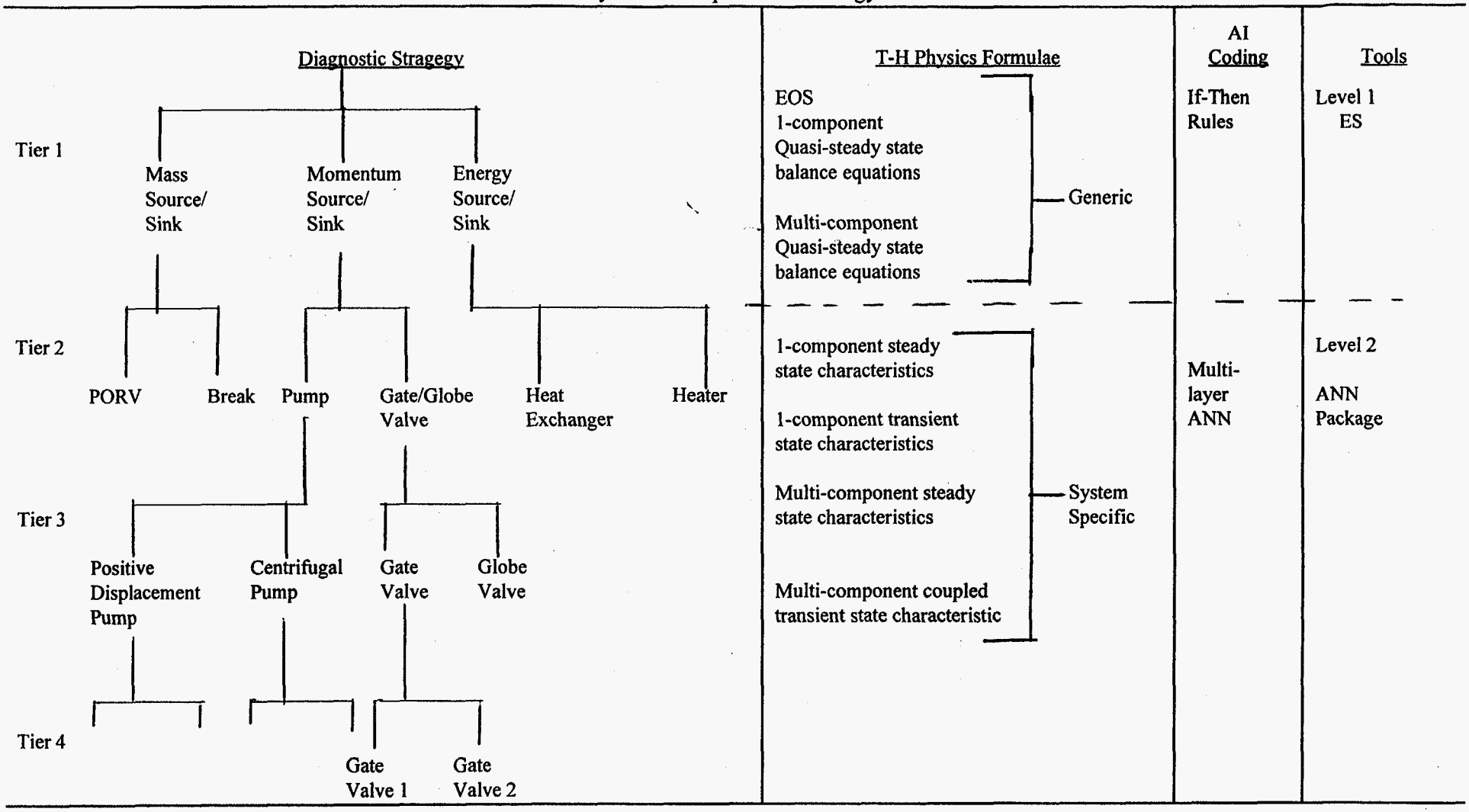

previously as (1) the three conservation equations, (2) the normal operation quasi-static component T-H characteristics, and (3) the normal operation transient component characteristics. Table 1.1 also shows the main boundary between the implementation of the T-H formulas in the ES and the implementation of the T-H formulas in the ANNs. The diagnostic knowledge base structure is a two-level hierarchical system. The classification by component T-H function, Q_{mass}, Q_{mom}, or Q_{eng}, is performed in the ES with the formulas of the conservation balances implemented as IF-THEN rules. The classification by component characteristics is performed in the network of ANNs where the formulas for the quasistatic and transient component curves are implemented. The plant-level diagnostics are, therefore, carried out in the ES. Component-level diagnostics are carried out in the network of ANNs. Table 1.1 is summarized in Fig. 1.3. It shows the two-level hierarchical structure for the diagnostic strategy. Figure 1.4 shows the internal database structure of the ES and the network of ANNs which implements the diagnostic strategy. In the ES, it can be seen that the three-step process can be transformed into a three-knowledge database structure. The three databases, Physical Rules Database (PRD), Component Classification Dictionary (CCD), and PID, are independent of each other. Based on the three conservation equations, qualitative analysis theory yields a set of first-principles IF-THEN rules which are plant- and T-H system-independent. These are grouped in the PRD. The CCD contains the classification of generic component types by the three T-H functions. This database is, therefore, also plant- and T-H system-independent. The PID groups the component and instrumentation locations in the T-H system. This database is, therefore, the only plant- and T-H system-dependent database in the ES. These databases and the diagnostic logic flow connecting them are described in further detail in Chapter 3. In the ANN network, Fig. 1.4 shows the hierarchy is further divided into two sublevels. The generic component characteristics formulas used to classify components by the absence of generic characteristics are grouped in the

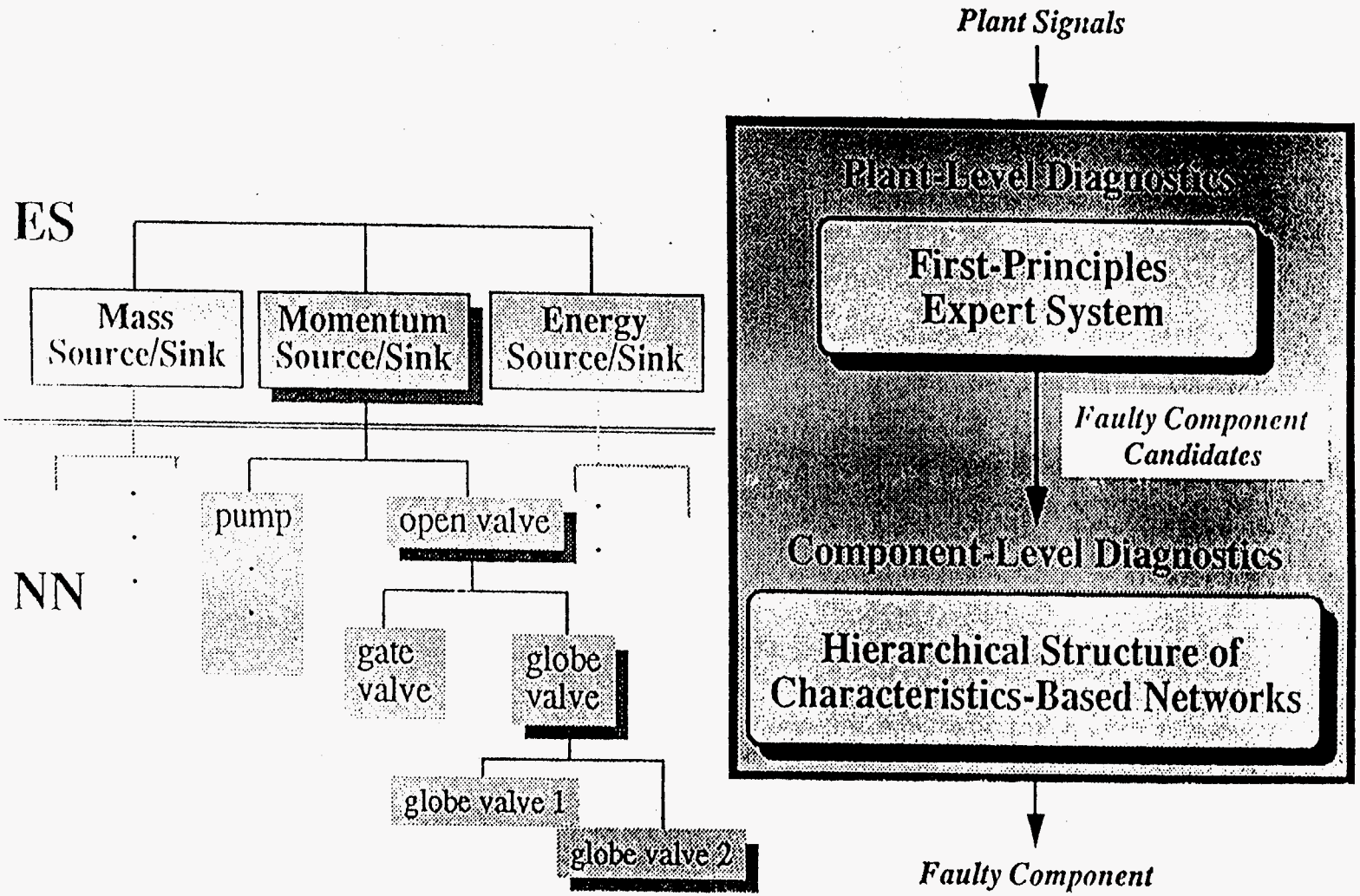

Fig. 1.3. Two-Level Hierarchical Structure

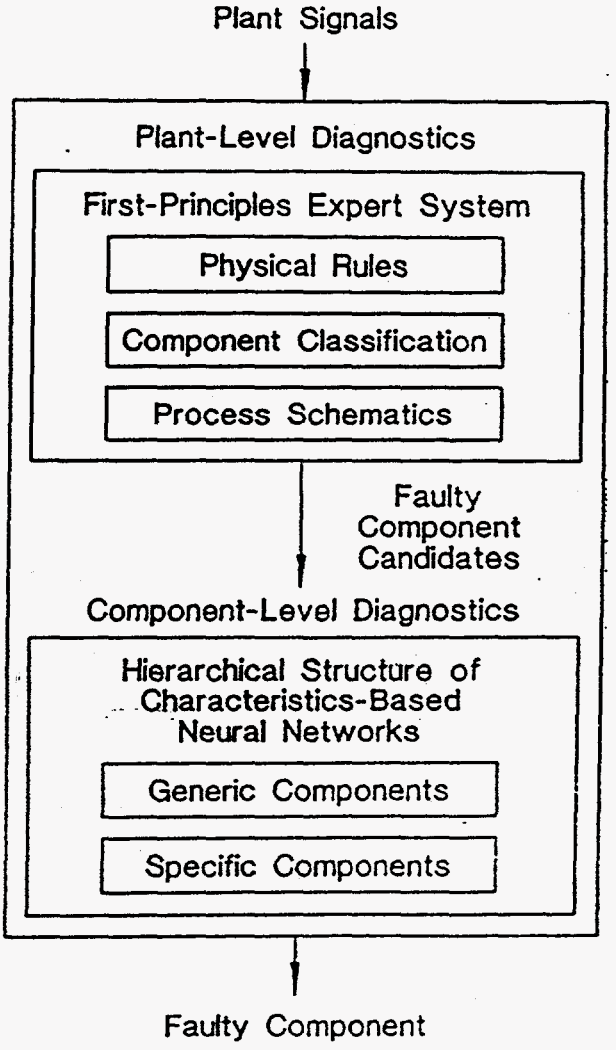

Fig. 1.4. Expert System/Neural Network Internal Structure

network of generic component ANNs. Specific component characteristics formulas are grouped in the network of specific component ANNs. These ANNs are not necessarily plant and T-H system independent. In addition to the ANN training data required, the ANN topologies may also vary from plant to plant and T-H system to T-H system. Further details are available in Chapter 4. While the main division between the ES and the network of ANNs is as discussed here, there are places where IF-THEN rules can be used for component-level diagnostics and places where ANNs can be used for plant-level diagnostics. Where these occasions arise, they are addressed further in Chapters 3 and 4.

Due to the limited availability of component characteristics data, implementation of the ANN part of the diagnostic strategy has actually only been performed at the plant-level diagnostics. The theory for the implementation is described in Section 4.2, while the details of the implementation are presented in Volume 3 on Applications. Component steady-state characteristics have been utilized. In our approach, the component steady-state characteristics are used to construct quasi-static "part-of-a-plant" models. A "part-of-a-plant" model is a model which could not only be restricted to a limited portion of the plant configuration but could also be limited to part of the T-H physics. It codifies the approximate "back-of-the-envelope" calculations used by analysts to confirm "semi-quantitatively" certain general numerical features of a transient response. It can therefore also be used to narrow the diagnostic focus of the conclusions from the ES. Implementation has been through the utilization of ANNs which then allows the pattern recognition comparisons of malfunction data against model data to be made in one step. However, in the case of the use of component transient characteristics which would be the next step in the diagnostic strategy, merely modifying the quasi-static part-of-a-plant model approach may not be the optimum route. Two other

possibilities already exist and will be utilized in future work on PRODIAG. These are faster-than-real-time plant numerical simulator (FTRS) and the area of noise signature analysis. Work in the area of FTRS would utilize the standard simulator practice of incorporating the component transient characteristics into numerical dynamic models of the plant. The research would then concentrate on multiprocessor algorithms to improve the computing time performance of these numerical models. The area of noise signature analysis is also a field where there is extensive on-going work of using component transient characteristics to diagnose component malfunctions. Pattern recognition techniques other than ANNs are being used, but ANNs have also been utilized. Future PRODIAG work in this area will involve either incorporating proven techniques from this area as PRODIAG modules or investigating the use of ANNs as a potential improvement.

REFERENCES

[1.1] T. Y. C. Wei, "Diagnostic/Control System Work," Memorandum to J. Reifman and L. L. Briggs, October, 1989.

[1.2] J. Reifman, T. Y. C. Wei, R. G. Abboud, and T. M. Chasensky, "Cooperative Research and Development for Artificial Intelligence Based Reactor Diagnostic System," Proc. of the American Power Conference, pp. 365-370, Chicago, Illinois, April 25-27, 1994.

[1.3] M. C. Majundar, D. Majundar, and J. I. Sackett, Artificial Intelligence and Innovative Computer Applications in the Nuclear Industry, Plenum Press, 1988.

[1.4] J. A. Bernard and T. Washio, Expert Systems Applications Within the Nuclear Industry, American Nuclear Society, 1989.

[1.5] D. B. Kirk and A. E. Murray, "Verification and Validation of Expert System for Nuclear Power Plant Applications," EPRI-NP-5978, Electric Power Research Institute, 1988.

[1.6] J. Reifman, L. L. Briggs, and T. Y. C. Wei, "A First-Principles General Methodology for Representing the Knowledge Base of a Process Diagnostic Expert System," Proc. of the Fourth International Conference on Industrial and Engineering Applications of Artificial Intelligence and Expert System, pp. 255-265, Kauai, Hawaii, June 2-5, 1991.

[1.7] J. Reifman, L. L. Briggs, and T. Y. C. Wei, "Nuclear Power Plant Diagnostics Using Qualitative Analysis and Component Functional Classification," Proc. of the AI91: Frontiers in Innovative Computing for the Nuclear Industry, pp. 227-236, Jackson, Wyoming, September 15-18, 1991.

[1.8] Project Staff, "Combined Expert System/Neural Network for Process Fault Diagnosis," Annual Status Report for FY93, September 1993.

[1.9] Project Staff, "Combined Expert System/Neural Network for Process Fault Diagnosis," Annual Status Report for FY94, September 1994.

2.0 DYNAMIC EFFECTS

2.1 Introduction/Overall Methodology

The transient response of a thermal-hydraulic system incorporates several dynamic effects driven by various thermal-hydraulic phenomena [2.1]. These effects can be complicated to decompose or to separate and are further complicated by coupling of the phenomena. Timescales for these phenomena can also vary from the very short to the very long. Identification of a unique component malfunction from the transient response requires a classification of the various dynamic effects. One generic classification of these dynamic effects is the following:

(1) Natural T-H Response

With an initial perturbation or disturbance, the thermal-hydraulic variables of flow, pressure, temperature and level naturally readjust to preserve the conservation of mass, momentum, and energy. This dynamic response of the various T-H phenomena to the initial perturbation with the corresponding changes in [w p h ℓ] is termed natural feedback. Further classification into Q_{mass}, Q_{mom}, or Q_{eng} malfunctions requires an overall methodology which is presented in Chapter 3.

(2) Control System Response

Control systems are normally designed to react to T-H system disturbances to maintain various setpoints. These control system actions in response to the initial disturbance also change [w p h ℓ] dynamically as the transient progresses. The dynamic effects and changes in the T-H system variables due to control system actions are classified as control system feedback.

(3) Instrumentation Response

Each instrument has an associated time constant or constants of its own. Dynamic changes in the T-H variables due to either natural or control system feedback are further convolved with the instrumentation dynamic response to produce the dynamic changes in the T-H signals. These dynamic effects have also to be accounted for in the transient diagnostic methodology.

This decomposition of the response into classes of dynamic effects is necessary if identification of a unique component malfunction or initiator of the transient is to occur, but it is not sufficient. Some methodology has to be invoked to use the dynamic features of the T-H signals to map the T-H response into these three classes. Each signal has a complete Fourier spectrum of dynamic frequencies. As stated in Chapter 1, each T-H signal can be decomposed into the following classes of dynamic features.

$$x(r,t) = x(r,t_o) + \frac{d}{dt}x(r,t)\Big|_{t_o} \Delta t + \text{---} \qquad (2.1)$$

namely

change in signal		
from steady	=	signal trend + low bypass part (low frequency)
state value		+ high bypass part (high frequency)

Each signal is therefore decomposed into an initial trend, low-frequency and high-frequency oscillations, as stated in Chapter 1. The initial signal trend information is used in the plant-level ES diagnosis, while the frequency-driven oscillations are used in the component-level ANN diagnosis. The methodology used to map these dynamic features of the signals to the three classes of dynamic effects requires the following signal processing procedure [2.2] detailed in Section 2.1.1.

2.1.1 Signal Processing Procedure

Recognition of the occurrence of a component malfunction from the dynamic features is first required. Currently, a threshold criterion is used

If $|\delta x| > \epsilon_x$ threshold → component malfunction has occurred.

The development of PRODIAG is at the laboratory proof-of-concept stage. Full-scope operator training simulator data are being used for the development. These data are noise-free. At some stage

in the PRODIAG development, other signal processing techniques will be assessed and selected to provide a greater degree of resolution for the recognition of the malfunction.

The thresholds are in general set independently of each other. In particular, the coolant temperature thresholds have to be set high enough for resolution purposes but low enough so that the temperature driven expansion of the coolant does not drive the coolant pressures significantly. This then decouples mass and momentum dynamic effects from energy effects. It simplifies the identification of Q_{mass} or Q_{mom} or Q_{eng} malfunctions. This is explained in Section 3.2.

Once it has been established that a malfunction has occurred and a transient has been initiated, that is, a previously "constant" variable x (x^-) at steady state has now become "nonconstant" ($x^{/-}$), then all the transient signals have to be classified into the three classes of signal information presented in Eq. (2.1): initial signal trends, fuzzified to just increasing x ($x^{\uparrow}$) or decreasing x ($x^{\downarrow}$) for the ES, and the low and high frequency information for the ANNs. However, this is not always possible for the ES. The extent of the malfunction and the timescale of the malfunction determine the extent of the change in the signal variable x (δx) and depending upon the variable, the timescale of the response. In some malfunction cases, the δx's are so small that the detection threshold criteria used are never met, so it appears that x^- even though a malfunction has occurred. In the case of other variables, the thresholds are met only after a considerable period of time. Section 2.2 shows that the set of T-H variables [p w ℓ h] can be divided into two sets [p w] and [ℓ h] based on the generic dynamic response time. The variables [p w] are regarded as "instantaneous" variables, while the variables [ℓ h] are regarded as "cumulative" or "integrated" variables. In general, the instantaneous set has a fast time response while the integrated set has a slow time response. This will be detailed

in Section 2.2. Based upon these sets of T-H variables, the transients which have to be diagnosed for specific malfunctions can be classified as:

(i) Long-time Transients: These are the mild transients where all [p w] are x^- forever, but the [ℓ h] eventually reach the threshold malfunction criteria and become $x^{/-}$. In essence, the failure extents are so small that the instantaneous variables [δp δw] cannot be detected but at some point, the integrated variables [$\delta\ell$ δh] have to reach the thresholds by definition. Even though it may be difficult to pinpoint the initiation of such a malfunction this class of mild transients can be recognized by rate criteria.

$$\text{If } \frac{d\ell}{\ell^{o}dt} < \frac{\epsilon_{\text{threshold}}}{\tau_{\text{tank}}} \rightarrow \text{long-time transient} \tag{2.2}$$

$$\text{If } \frac{dT}{T^{o}dt} < \frac{\epsilon_{\text{threshold}}}{\tau_{\text{thermal inertia}}} \rightarrow \text{long-time transient} \tag{2.3}$$

where in the notation "→" replaces "then".

Section 2.2 presents the derivation for these criteria where τ_{tank} is the time constant of the tank level and $\tau_{thermal\ inertia}$ is the time constant of the temperature of a particular mass [2.6]. These long-time transients cannot be practically diagnosed by the ES rules strategy presented in this report and detailed in Chapter 3.0, as these ES rules and strategies were specifically developed for the class of short-time transients. The short-time ES rules specifically focus on the short-time part of the transient for larger extent malfunctions. These rules are still correct for long-time transients, but they will not activate since, in mild transients, many of

the signal variables will not reach the threshold criteria. The diagnosis of the long-time transients in the ES part of the diagnostic hierarchy will require future development of additional long-time ES rules.

(ii) Intermediate-time Transients: These are the transients where the instantaneous variables [p w] do respond but the extent of the malfunction is such that not all these variables reach the threshold criteria. The integrated variables will by definition reach the threshold criteria at some point in time. The short-time ES rules/strategy presented in this report do also apply to intermediate time transients. However, additional rules are needed to provide a comprehensive set of trends for the ES diagnostic strategy. For example, if $w^{/-}$ is detected somewhere in a loop, but, due to the limited extent of the transient the flowmeters elsewhere do not reach the threshold criteria, then additional rules are required to extrapolate from that $w^{/-}$ detection to establish w trends elsewhere in the loop. These are extrapolation rules to compensate for differing sensitivities of the variables in different parts of a loop. The definition of a loop will be further discussed in Chapter 3. Other rules are also possible to compensate for the different variable sensitivities in the different parts of a loop, but extrapolation rules for p are not used. This is because in the ES diagnostic strategy detailed in Chapter 3, the differing sensitivities of various pressure signals in a loop are treated through further classification by boundary conditions (in tanks, etc. where the pressure response is slow) and non-boundary conditions (in pipes etc. where the pressure response is faster). Dynamic effects are thus implicitly factored into this treatment of the varying sensitivities of the pressure signals.

(iii) Short-time Transients

These are the transients where the affected [p w] variables all reach the threshold criteria. The integrated variables may reach the criteria at longer times but within the short-time period of the transient all the x' trends necessary for the ES diagnostic strategy are established. The short-time ES rules and strategy presented in this report were specifically developed for this class of transients. The entire diagnosis is aimed at the identification of the malfunctioning component early so that later natural coupling feedback in the T-H variables and effects from control actions will not complicate the decomposition of the signal.

Once the transient signals have been decomposed into initial signals trends, low frequency and high frequency information, and before the mapping into the three classes of dynamic effects can occur it must be first established that the malfunction is not an instrumentation malfunction [2.3]. This is the classic area of signal validation. Well established techniques of varying degrees of sophistication are readily available to determine that the transient is driven not by a spurious instrument failure but rather by a specific T-H component malfunction. To these classical techniques a number of rules based upon the PRODIAG first-principle approach can also be added. These are discussed in Section 2.1.2. The derivations for the rules are presented in Section 2.2 and Chapter 3.

2.1.2 Instrumentation Failure

Diagnosis of instrumentation failure is the area of signal validation with its own special techniques. It is difficult to apply the first-principles based diagnostic method to detect instrumentation error.

One ends up with too many hypotheses and too many unknowns. For the method to succeed, a first-principles based inference has to be drawn and compared against an instrumentation reading to arrive at consistency or inconsistency. Instrumentation is generally limited. However, some success can be obtained because instrumentation failure can be divided into two classes. To illustrate the division into the two classes, suppose we have three instrumented variables x_1, x_2, and x_3. We then have the two possiblities,

(a) Instrumentation failure which initiates a transient signal $[x_1^{-}x_2^{-}x_3^{/-}]$

(b) Instrumentation failure which does not lead to a transient signal $[x_1^{-}x_2^{-}x_3^{-}]$, but is waiting for a transient initiated by other malfunctions.

Class (b) is of much lower probability than class (a), since it is a double failure. Class (a) is the more likely type of instrumentation failure. Class (a) is also easier to diagnose than class (b) with the first-principles based diagnostic technique. If we focus on class (a), the situation is initially, $x_1^{-}x_2^{-}x_3^{/-}$ before control system action and natural feedback starts, and the hypothesis is one of a bad instrument. This situation should be more amenable than class (b) where the bad instrument appears to give a normal response. If nothing else happened and $x_1^{-}x_2^{-}x_3^{/-}$ continued forever, one would suspect that x_3 is a bad instrument. However, this is not a generically true statement. It depends upon the number, type, and location of the instruments. The first-principles based rules presented below are specific examples of this statement for specific combinations of instruments.

One generic possibility is to cross-correlate $x_1^- x_n^{/-}$ where the x's are instrumentation at different locations for p's, ℓ's, w's or T's only. Conventional validation and verification techniques (V&V) use redundant instrumentation at the same location. Cross correlations are an extrapolation on that. However, due to different variable sensitivity, ambiguous results can not be ruled out except for possibly, where h is used and that depends upon time constants. After the Time Window Selector defined in Section 2.2 has opened the window for x^- signals, then the following rules which are essentially cross-correlations for instrument error (IE) are applicable. By definition, if IE is deduced, $x_n^{/-}$ is the bad instrument. The rules are written in shorthand form with the "IF" and "AND" on the left-hand side deleted.

For a non-separated volume,

Hydraulic element (pipe, etc.) $\quad \Delta p^- w^{/-} \rightarrow IE$

$\Delta p^{/-} w^- \rightarrow IE$

where $\Delta p = p_i - p_o$ is the pressure drop across the hydraulic element. The pressure drop across a hydraulic element such as a pipe is correlated to the flow in the pipe. If one variable physically changes, the other should also change. If this does not occur, then an instrumentation error is indicated. This rule works in practice because practical control systems have deadbands and can not produce null exactly.

Similarly for a heat exchanger (HX), the outlet enthalpies h_o on the cold and hot sides are correlated. These enthalpies are also correlated to the flow through the heat exchanger. Dynamic effects have to be accounted for.

HX

$$h_{ohot}{}^{/-}\, h_{ocold}{}^{-} \rightarrow IE$$

$$h_{ohot}{}^{-}\, h_{ocold}{}^{/-} \rightarrow IE$$

$$w_{cold}{}^{-}\, w_{hot}{}^{-}\, h_{i\ cold}{}^{-}\, h_{i\ hot}{}^{-}\, h_{o\ hot\ or\ cold}{}^{/-} \rightarrow IE$$

In the case of a pipe where no heat transfer is occurring, we similarly have,

Pipe

$$w^{-}\, h_{up}{}^{-}\, h_{down}{}^{/-} \rightarrow IE$$

For a separated volume such as a tank the gas space pressure p and the liquid level ℓ are closely correlated, so we have,

$p^{/-}\ \ell^{-} \rightarrow IE$

$p^{-}\ \ell^{/-} \rightarrow IE$

(If more than one separated volume exists in the system. In the case of only one separated volume, liquid incompressibility could invalidate this rule.)

The equal sensitivities of p and ℓ to perturbations is an advantage in this case, because they would reach the malfunction threshold criteria "simultaneously." Other ES rules are possible, but more complicated formulas could be required to detect other instances of instrument failure. Implementation of this knowledge in neural networks and detailed simulation models could then be

needed. One example of using neural networks for such a possibility is the following one for a non-separated volume type component. For a passive hydraulic element where ˉ indicates non-dimensionalization to reference conditions,

$$\overline{\Delta p} = \overline{w^2} \tag{2.4}$$

Signal trend analysis with the ES rules is sometimes insufficient to detect IE. Rearranging Eq. (2.4) to become

$$\overline{\Delta p} - \overline{w^2} = 0. \tag{2.5}$$

For Eq. (2.5) to be true, Fig. 2.1 shows that the pair of $\left[\overline{\Delta p}, \overline{w^2}\right]$ data points must fall on the straight line of Fig. 2.1. However, due to non-ideality of physics laws incorporated in Eq. (2.5), every hydraulic element is different. There will be an uncertainty band. Instrumentation uncertainties will also contribute. Fuzziness is an inherent feature of neural nets and can be put to good use here. The proposal here is to implement a two-input/two-output neural net to divide the region into three areas: A, B, and C.

This is shown in Fig. 2.2. The net can be trained with data to self-set this fuzziness. This is the equivalent of an analyst doing a simple back of envelope "order of magnitude" calculation to satisfy ranges of parameters after the analysis process has gone through with the trend analysis. The conclusion of consistency will be taken to mean IE can not be definitively concluded. The conclusion of inconsistency would mean either IE or $Q_{mass}{}^{/-}$ or $Q_{mom}{}^{/-}$. Neural networks can be and have been used with other approaches to identify instrumentation malfunctions. The area of signal validation is a well established one and other techniques are available.

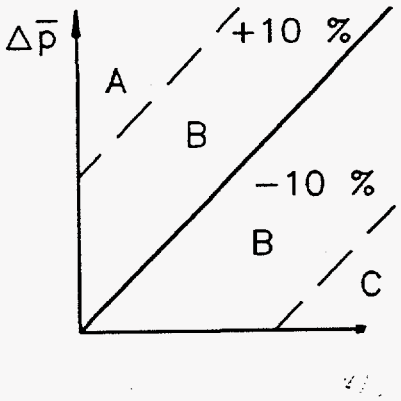

Fig. 2.1 Δp/w Operating Space

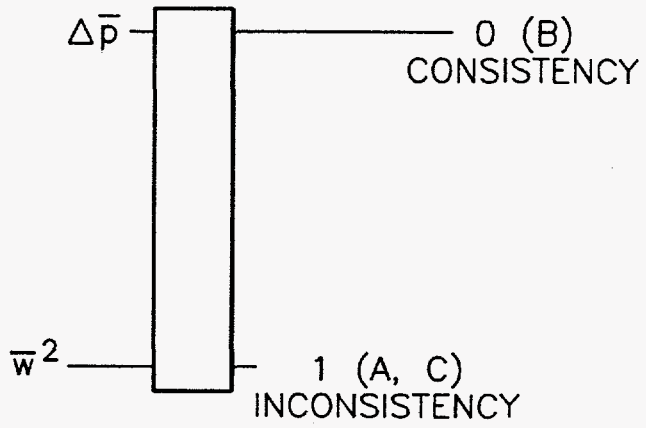

Fig. 2.2 ANN representation for Δp/w IE

Obviously, there are many other formulas along the lines of Eq. (2.4) which can be implemented as neural nets. Basically, these neural net representations are more detailed representations of the balance equations and component characteristics which are simplified into the ES IF-Then trend rules, but at this point the boundary with classical signal validation techniques is beginning to blur. Eventually it may be necessary to proceed further and implement certain detailed mathematical models in FORTRAN as part of the FTRS (Faster Than Real-time Simulation), but at that stage, use of classical signal validation techniques may be more beneficial. We have presented here a number of ES rules, based on the PRODIAG first principles apparoch, to identify instrument failure. However, in the main, the intent is to use the techniques of signal validation and not to pursue development of new techniques to identify instrument failure.

2.2 Time Window Selector

Once it has been established that a transient has occurred, the signals have been decomposed into initial trends and high frequency oscillations, and it has been established that the driving source is

not a spurious instrument malfunction, the mapping of the signal components into the three classes of dynamic effects can proceed. The ES, which uses the initial signal trend, and the part of the ANN hierarchy which utilizes the quasisteady component characteristics definitely require the usage of the mapping into the three classes of dynamic effects. The mapping is carried out by defining a time window where signals can be correlated in the ES rules or in the ANN representations [2.4]. In our treatment of the dynamic effects the correlations are no longer applicable outside the time window. In this way changes in the signals due to subsequent plant actions or "later" T-H phenomena are prevented from masking the signal changes due to the initial malfunction. The Time Window Selector (TWS) algorithms perform the task of defining this time window. The hierarchy of ANNs also uses the high frequency part of the signal information so the TWS algorithm described in this Theory Volume may have to be modified for usage with that part of the diagnostic strategy.

To reiterate there are three classes of dynamic effects: (i) natural T-H response; (ii) control system response; (iii) instrumentation response. Separation of signal components into these classes allows decoupling of these three effects on the plant parameters. However, it simplifies the discussion of the treatment of these effects to combine the natural T-H response together with the instrumentation response. The control system response will be discussed separately as it cannot be analyzed simply as a matter of time delays.

For the general time window opening which begins the diagnostic process, reference should be made to Fig. 2.3. Analysis is started at time t_o when some variable or signal x_1 reaches its primary threshold ε_p. Then, variable x_2, which has reached its secondary threshold ε_s before t_o and which

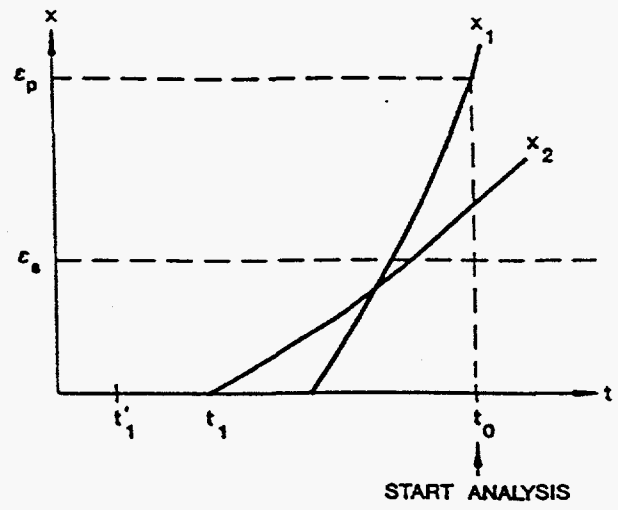

Fig. 2.3. Opening of the Time Window for Thermal-Hydraulic Variables

has the earliest deviation time t_1, is used to determine the TW opening. The TW opens on variable x_2 at

$$t_{open} = t'_1 = t_1 - \tau_{inst} - \tau_{ntfd} , \tag{2.6}$$

where τ_{inst} and τ_{ntfd} are the time constants for x_2 associated with instrumentation response and natural T-H feedback, respectively. The thresholds ε_p and ε_s are selected for each variable on the basis of the T-H system being diagnosed and the sensitivity of the particular variable to malfunctions. The window is now open from this time on for accepting all signals (trends) to be sent to the PRD except for signals with constant (-) trend x^-. For all constant T-H variables, the signal trend is x^-. The prime difficulty with "constant" signals is in accounting for x^- when it actually is $x^{/-}$ with a delay [2.5]. For all constant T-H variables, w^-, p^-, h^-, ℓ^-, another special TW opens at the corresponding t_{open} according to

$$t_{open} = t'_1 + \tau_{inst} + \tau_{ntfd} . \tag{2.7}$$

One way of implementing this method for treating "constant" signals is to consider the trend of x to be unknown (?) if x has a normal trend x^-, until Eq. (2.7) is satisfied. Equation (2.7) allows us to

use x^- information after an approximate time delay $\tau_{inst} + \tau_{ntfd}$. This method makes use of the fact that the initial condition at the onset of the transient is steady-state. If the initial condition is not steady-state, adjustments should be made accordingly. This special TW for constant signals is an example of other special TWs which are used for some of the variables. The general TW initiates the diagnostic process, but the multiple special TWs allow for special treatment of specific variables.

To close the TW, we need to account for all three types of time constants. The general TW closes as soon as the first one of two closing times is reached, i.e.,

$$t_{close} = Min(t_{close\ control}, t_{close\ inst/ntfd}) . \quad (2.8)$$

We lump instrumentation and natural feedback dynamic effects together in $t_{close\ inst/ntfd}$ since in our concept they are both treated as effective time delays. However, each T-H natural feedback phenomenon has its own $t_{close\ inst/ntfd}$. Equation (2.9) shows how the TW for thermal phenomena is closed with the thermal feedback time constant $\tau_{thermal}$:

$$t_{close\ inst/ntfd} = t'_1 + \tau_{inst} + \tau_{thermal} . \quad (2.9)$$

Analogous equations can be written for the other natural feedback phenomena, and the related time constants are discussed in detail in the following sections. The window closing by $t_{close\ control}$ is discussed in Section 2.2.2.

2.2.1 Natural Feedback/Instrument Response

We present here the derivations which show the dynamic natural feedback relationships between different T-H variables in a first order perturbation theory sense. The various time constants which determine the timescale of each dynamic relationship is also derived. This will permit the separation

of dynamic effects by time delays. The difficulty of translating these dynamic relationships into IF-THEN ES rules is then illustrated. A method for treating these dynamic relationships through the TWs is then presented. This consequently allows the use of the quasistatic relationships presented in Chapter 3 for the construction of the necessary IF-THEN rules correlating the various T-H variables.

The first principles dynamic T-H equations which govern the response of the T-H variables [p w ℓ h] to perturbations for a control volume in one dimension are

$$\frac{dm}{dt} = w_i - w_o + Q_{mass} \tag{2.10}$$

$$\frac{L}{A}\frac{dw}{dt} = \frac{w_i^2}{2A^2\rho_i} - \frac{w_o^2}{2A^2\rho_o} + p_i - p_o + \Delta p_{pump} - k_{valve}\frac{w^2}{2\rho A^2}$$

$$= \frac{w_i^2}{2A^2\rho_i} - \frac{w_o^2}{2A^2\rho_o} + \Delta p + Q_{mom} \tag{2.11}$$

$$\frac{dmh}{dt} = w_i h_i - w_o h_o + Q_{eng} \tag{2.12}$$

$$p = p(\rho, h) \tag{2.13}$$

where Eqs. (2.10) - (2.12) are the three conservations equations of mass, momentum and energy, Eq. (2.13) is the equation of state (EOS). We use the following notation

m	= LAρ = mass	ρ	= density	Q_{mass}	= mass source
L	= length	i	= inlet	Q_{mom}	= momentum source

A	= cross section area	o	= outlet	Q_{eng}	= energy source
k_{valve}	= valve loss coefficient			Δp	= $p_i - p_o$

Since the topic in this section is the natural dynamic response of a T-H system, it is assumed for the derivations presented here that the source/sink driving terms, the Q's, remain constant (Q^-). This means $\delta Q = 0$ and it removes the unnecessary complication of the time constants of the Q's. For single phase systems with noncondensible gas, two types of control volumes can be identified.

(i) completely single phase flow volumes termed non-separated volumes,

(ii) a noncondensible gas space over single phase liquid denoted as separated volumes.

The initial dynamic T-H response of these control volumes for "small" changes in boundary conditions can be obtained by using first-order perturbation theory. Although the three balance equations and the EOS are common for the entire T-H system, the natural feedback time response, and therefore time constants, can be quite different for different configurations. For these two broad categories of T-H control volumes in a loop, differing time constants can be identified.

In the case of a non-separated volume, the balance equations can be divided into two sets to represent two broad phenomena; hydraulic coupling between p and w, i.e., {p,w} coupling and energy coupling $\{h_i, h_o, w\}$. We have for the hydraulic coupling in a finite volume the mass and momentum equations

$$\frac{dm}{dt} = w_i - w_o = LA \frac{dp}{dt}\left(\frac{d\rho}{dp}\right) \qquad (2.14)$$

$$\frac{L}{A}\frac{dw}{dt} = \frac{w_i^2}{2A^2\rho_i} - \frac{w_o^2}{2A^2\rho_o} + \Delta p \qquad (2.15)$$

Friction and gravity have been neglected in the momentum equation, Eq. (2.15). The EOS enters through $d\rho/dp$ and for simplification the process is assumed to be isothermal. Manipulation of Eqs. (2.14) - (2.15) for small perturbation from a uniform steady state where p_o is kept constant and w_i is changed externally gives

$$\frac{d\delta w_o}{dt} = \frac{\delta w_i}{\tau_T} + \frac{A}{L}\delta p_i - \frac{\delta w_o}{\tau_T} - \frac{A}{L}\delta p_o \qquad (2.16)$$

$$\frac{d\delta p_i}{dt} = -\frac{\delta w_o}{\tau_s^2}\frac{L}{A} + \frac{\delta w_i}{\tau_s^2}\frac{L}{A} \qquad (2.17)$$

where

$$\tau_T = \frac{\rho^o LA}{w_o} \qquad (2.18)$$

$$\tau_S = L\left(\frac{d\rho}{dp}\right)^{1/2} \qquad (2.19)$$

This gives simplistically in the limit of small perturbations

$$\delta w_o \simeq \frac{\delta w_i}{\tau_T}\,dt \quad \text{for small times and } \tau_T >> \tau_S \qquad (2.20)$$

Equation (2.20) is a dynamic first order coupling for the variables [p w] in a non-separated volume for the assumed boundary conditions.

For the energy coupling using

$$h = cT, \tag{2.21}$$

we have

$$m_m c_m \frac{dT}{dt} = wc\,(T_i - T_o) \tag{2.22}$$

where for one side of a heat exchanger (HX)

m_m = metal mass T = temperature

c_m = metal specific heat c = fluid specific heat.

For simplicity, we take $T = T_o$. Solving the differential equation and expanding the solution gives for constant w,

$$\delta T_o = \delta T_i \left(\frac{dt}{\tau_{Hx}} \right), \tag{2.23}$$

where

$$\tau_{Hx} = \frac{m_m c_m}{wc}. \tag{2.24}$$

Equation (2.23) is the dynamic first order coupling for $\{h_i, h_o, w\}$ for the assumed boundary condition.

Now in the case of a separated volume, the main couplings are {w,ℓ} liquid mass balance; {p,ℓ} gas EOS; and {h_i, h_o, w} liquid energy balance. The momentum equation internal to the volume is not used, as internal flows are not important for this application. The liquid mass balance gives for liquid

$$\frac{1}{m^{\circ}}\frac{dm}{dt} = \frac{d\ell}{\ell^{\circ}dt} = \frac{1}{\tau_{tank}}\left(\frac{w_i}{w_i^{\circ}} - 1\right) \tag{2.25}$$

where for a tank superscript o = initial value and $w_o = w_i^{\circ}$ as w_o is held initially constant and w_i is perturbed.

So

$$\frac{\delta\ell}{\ell^{\circ}} = \frac{\delta w_i}{w_i}\frac{dt}{\tau_{tank}} \tag{2.26}$$

with

$$\tau_{tank} = \frac{m^{\circ}}{w_i^{\circ}} . \tag{2.27}$$

Equation (2.26) is the dynamic first order coupling for [w ℓ] for the assumed boundary condition. If heat transfer is neglected, the gas EOS for a low inertia gas volume V gives

$$\frac{\delta p(t)}{p} = \frac{\delta V(t)}{V} = \frac{\delta\ell(t)}{\ell} \tag{2.28}$$

Therefore,

$$\delta p = K\, \delta \ell \qquad (2.29)$$

$$\text{and } K = p^o/\ell^o$$

There is no time constant involved here, so the dynamic first order coupling for $\{p\ \ell\}$ in Eq. (2.28) is an instantaneous one for a separated volume. The liquid energy balance gives

$$\frac{dmcT}{mcT\,^o dt} = \frac{1}{T^o}\frac{dT}{dt} = \frac{1}{\tau_{thermal}}\left(\frac{w_i h_i}{w_i{}^o h_i{}^o} - 1\right) \qquad (2.30)$$

where the outlet flow and enthalpy are kept initially constant while the inlet enthalpy is perturbed.

Therefore,

$$\frac{\delta T}{T^o} = \frac{\delta w_i h_i}{w_i h_i}\frac{dt}{\tau_{thermal}} \qquad (2.31)$$

with

$$\tau_{thermal} = \frac{mcT^o}{w_i{}^o h_i{}^o} = \frac{mcT^o}{w_o{}^o h_o{}^o} \quad . \qquad (2.32)$$

For the assumed boundary conditions, Eq. (2.31) is a dynamic first order coupling for the variables $[h_i\ h_o\ w]$, since $h = cT$ and $T = T_o$.

The dynamic first-order couplings describing the natural feedback response expressed in Eqs. (2.20), (2.23), (2.26), (2.28), and (2.31) are summarized in Table 2.1. The equations show that the initial trends of coupled variables follow each other but with a time lag expressed as a time constant. As can be seen from the equations, the time constant for each coupling is T-H system dependent. Geometric dimensions are a factor. However, in general, for most T-H systems, the time constants are either small leading to a fast time coupling response or large leading to a slow time coupling response. Table 2.1 shows the division of time couplings into fast and slow classes. It can be seen that the integrated or cumulative couplings $\{\ell,w\}$, Eq. (2.26), and $\{h_i,h_o,w\}$, Eqs. (2.23) and (2.31) are slow while the "instantaneous" couplings $\{p,\ell\}$, Eq. (2.29) and $\{p,w\}$, Eq. (2.20), are fast. The corresponding time constants are given in Eq. (2.27), Eq. (2.24), Eq. (2.32), and Eq. (2.18).

Table 2.1. Theoretical Dynamic Coupling Between Thermal-Hydraulic Variables Based on Natural Feedback

Control Volume	Non-Separated		Separated		
Coupled Variables	$\{p,w\}$	$\{h_i,h_o,w\}$	$\{p,\ell\}$	$\{\ell,w\}$	$\{h_i,h_o,w\}$
Correlating Equation	mass and momentum balance	energy balance	gas equation of state	liquid mass balance	liquid energy balance
Time Coupling	fast	slow	fast	slow	slow

This division and Eqs. (2.25) and (2.30) are useful in defining the class of long-term mild transients introduced in Section 2.1. It can be seen that

$$\frac{1}{\tau_{tank}}\left(\frac{w_i}{w_i^{\,o}} - 1\right) = \frac{1}{\tau_{tank}}\left(\epsilon_{threshold}\ \text{on}\ w\right) \tag{2.33}$$

So the criteria for mild transients become naturally using Eq. (2.25),

$$\frac{1}{\ell_o}\frac{d\ell}{dt} < \frac{\epsilon_{threshold}}{\tau_{tank}}\ , \tag{2.34}$$

which is Eq. (2.2) of Section 2.1. Similarly, it can be seen that

$$\frac{1}{\tau_{thermal}}\left(\frac{w_i h_i}{w^{\,o}_i h^{\,o}_i} - 1\right) = \frac{1}{\tau_{thermal}}\left(\epsilon_{threshold}\ \text{on}\ wh\right) \tag{2.35}$$

which naturally leads to the mild transient criteria using Eq. (2.30)

$$\frac{1}{T_o}\frac{dT}{dt} < \frac{\epsilon_{threshold}}{\tau_{thermal\ inertia}} \tag{2.36}$$

which is Eq. (2.3) of Section 2.1.

The logical next step would be to transform Eqs. (2.19), (2.23), (2.26), (2.28), and (2.31) into the IF-THEN ES rules for the plant-level diagnosis by the ES. These are the first-principles T-H correlations based on conservation equations which relate the initial trends in [p w ℓ h] to the perturbations in the Q source terms. From the time-dependent Eq. (2.23) and the fact that energy is being conserved in the heat exchanger, we may infer the following "dynamic" ES rule:

$$\bar{w}(t)\ \bar{w}(t+dt)\ \bar{T}^{\,l}_{\,i}(t)\ \bar{Q}_{eng}(t)\quad \bar{Q}_{eng}(t+dt) \Rightarrow \bar{T}^{\,l}_{\,o}(t+dt)\ , \tag{2.37}$$

which expresses the fact that if T_i is increasing ($\uparrow$) at time t, and both w and Q_{eng} are constant at times t and t+dt, then T_o must be increasing at time t+dt. Q^{-}_{eng} means that the energy source/sink does not change from the initial steady state value. From Eq. (2.23) it can be seen that dt in Eq. (2.37) is equal to τ_{Hx}. It takes τ_{Hx} seconds for δT_o to reach the threshold criterion after $\delta_i T$ has reached it. The dynamic ES rule has to explicitly account for the period τ_{Hx} during which the status of T_o is ambiguous. The rule would also have to explicitly track the dynamic status of Q_{eng} and w while freezing the value of T_i. This shows the difficulty of writing a dynamic ES rule which fully incorporates the dynamic response of thermal inertia. If we used quasistatics instead, the equation corresponding to Eq. (2.23) would be

$$\delta T_o = \delta T_i \ .$$

Equation (2.37) would then be changed to the following ES rule with no time delay,

$$T^{\uparrow}_i \; Q^{-}_{eng} \rightarrow T^{\uparrow}_o \ ,$$

which illustrates the simplifications made possible by using quasistatic diagnostic rules and treating dynamic effects separately.

Equations (2.23) and (2.37) are simple derivations which show that if we used the dynamic balance equations instead of the static/quasistatic versions to derive qualitative physics rules of the PRD, complications would arise. Equations (2.20) - (2.31) are the corresponding derivations which draw the same conclusions for all the other PRD rules. However, these dynamic perturbation equations do show that each rule derived from a balance equation should have a time constant associated with it. The lagging variable is delayed with respect to the leading variable. We will, therefore, utilize quasi-static rules derived from quasi-static balance equations in the ES and treat dynamic effects in the TWS. The TW concept approximates the dynamic effects by associating time constants/delays

with each signal variable instead of with each PRD rule. One exception is the enthalpy transport phenomenon which is not treated in the TWS, but as an explicit time delay rule in the PRD. In the case of transport phenomena, a simple IF THEN rule incorporating time delay can be written to correlate upstream and downstream changes. Associating natural feedback with time constants/lags then rationally allows the inclusion of the instrumentation time constants/lags.

The theory of natural feedback and instrument time delays is simple and consistent. However, because of slop due to uncertainties in τ_{inst}, approximations in simulation models, assumptions of incompressibility in the rules of the PRD, etc., we need to derive slop formulas to approximate the concepts described above. The time window is opened and closed for acceptance or rejection of each signal variable and its associated initial trend in accordance with these formulas which treat the associated time constant/delay. These formulas account for the physical fact that certain hydraulic variables are dynamically tied together with delay times. The chief difficulty is in the treatment of x^- when it is used to activate rules. In the slop formulas, a general TW is opened in accordance with the procedure for Eq. (2.6). After the general TW is opened, however, specific slop formulas for specific window openings and closings are applied in accordance with the natural feedback couplings shown in Table 2.1. These are discussed next.

For a non-separated volume, we start with {p,w} coupling. Once the first p or w signals with not normal (/-), i.e., $p^{/-}$ and $w^{/-}$, trend occur, then we do not use a constant trend for any of the other p and w variables until a period $\Delta t_{pw} = \tau_{hydslop} + \tau_{inst}$ has passed. This is a "slop formula". In essence, Δt_{pw} is the window which opens after the first $p^{/-}$ or $w^{/-}$ reach their corresponding ϵ_s. Reference should be made to Fig. 2.4. During Δt_{pw}, all $p^{/-}$ and $w^{/-}$ are used in the {p,w} rules or in other

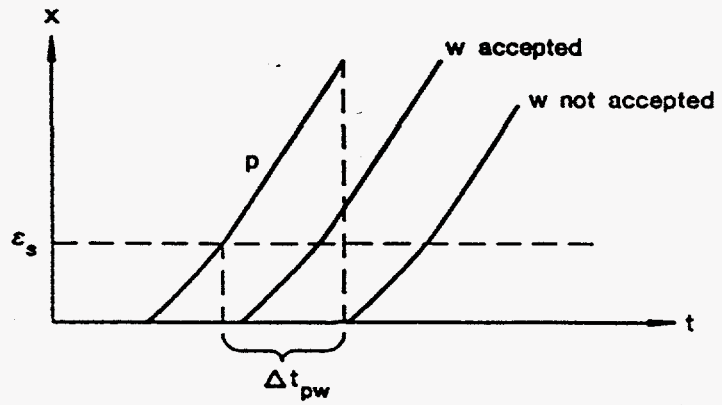

Fig. 2.4. Slop Time for the {p,w} Coupling

hydraulic coupling rules between {p,p} and {w,w} for non-separated volumes. This includes $p^{/-}$ in the separated volumes. However, p^- and w^- are not used in those rules until the window is closed. After Δt_{pw}, no more new occurrences of $p^{/-}$ and $w^{/-}$ are used in the rules.

For the heat exchanger energy rules relating $\{h_i,h_o,w\}$, once the general window is opened, it is never closed for h_o unless $t_{close\ control}$ closes it. However, h_o^- is not used until a heat exchanger slop time $\Delta t_{hx} = \tau_{inst} + \tau_{thermal}$ has passed after the general time window was opened at t_{open}. For h_i, Δt_{hx} is also used, but the thermal time constant $\tau_{thermal}$ is not needed if at the onset of the transient the plant is at steady-state. The constant flows w^- are treated as discussed for the {p,w} coupling. The dynamic coupling between h_i and h_o for a pipe is treated through enthalpy transport outside the TWS.

In the case of separated volume rules, the analogous procedure to that for non-separated volumes is used. In the case of {p,ℓ}, the slop time period is $\Delta t_{p\ell}$, and for {ℓ,w} rules, the corresponding period is $\Delta t_{w\ell}$. There is a corresponding period Δt for the $\{h_i,h_o,w\}$ coupling, but that will not be discussed further here, as it is similar to that for non-separated volumes. The {p,ℓ} coupling is then treated in the same way as the {p,w} coupling for non-separated volumes. The {p,ℓ} coupling and the $\{h_i,h_o,w\}$ are both treated similarly to the $\{h_i,h_o,w\}$ coupling for non-separated volumes.

2.2.2 Control System Action

We now turn to the procedure for the control system response [2.7]. The ES plant-level diagnosis uses the initial signal trend. The treatment of the dynamic natural feedback effects discussed in Section 2.2.1 should account for these effects prior to changes in trend due to this natural feedback. However, control system actions could be taken early and change these initial trends complicating the diagnosis. Trend changes masking the effect of the initial malfunction could also occur if multiple malfunctions occurred. This is the major reason for restricting the current diagnostic methodology to single T-H system faults. If the control system completely suppresses a signal response, there is not much that can be done. However, in most cases, once control action takes place, there are breaks in the signal history as illustrated in Fig. 2.5. The breaks are characterized by a discontinuity in dx/dt that is consistent with the first-order time dependence of the conservation equations. A discontinuity in dx/dt, particularly a "sharp" one, indicates control action. A "soft" discontinuity is more indicative of natural feedback, but including that here is consistent with the approach. Oscillations could also be treated here. What is not treated as a break is a discontinuity from steady-state. This could be a control action, but we will not use it to close the window. We

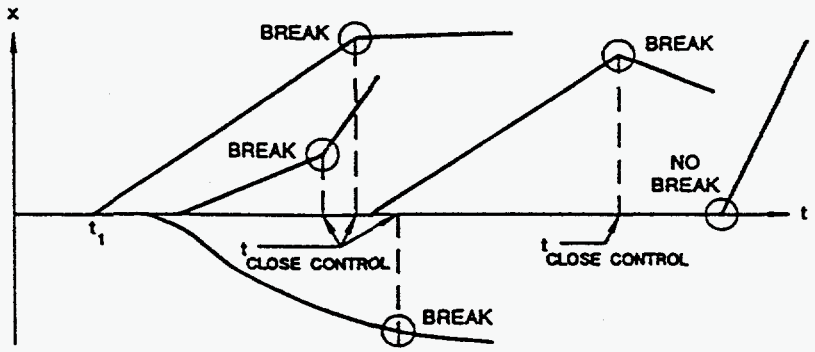

Fig. 2.5. Effects of Control System Action on the Thermal-Hydraulic Variables

will rely on the $t_{close\ inst/ntfd}$ to reject any control action from steady-state. This should simplify the logic. There may be cases when this is not sufficient, but they should be in the minority. Theoretically, the correct thing to do once a break is encountered is to move the diagnosis point to the break point, reinitialize, and start the diagnosis to determine what control system action was taken. This could be done by using the same rules as the diagnosis for the initiating component malfunction and then comparing the $Q^{/-}$ malfunction [2.5] with the control system algorithms and the PID to determine which control system reacted. The control system algorithm would be written as a set of IF-THEN rules to be conveniently used along with the diagnostic rules. Having determined the specific control system action, one could then subtract it out and complete the diagnosis for the initial component malfunction. This is a complicated process, and we will not attempt to resolve it here.

We try to close the TW on control action in a manner which makes the longest use of the signals. This is a rule-dependent procedure. Closing the TW means that no more new occurrences of $x^{/-}$ are accepted for the specific rule and that some post-closure trend for the previous $x^{/-}$ needs to be

defined. For the rules relating tightly coupled variables {p,w} and {p,ℓ}, after a break is first encountered in the signal variables for the rules, the TW is simultaneously closed for all non-separated volume rules relating {p,w} and separated volume rules relating {p,ℓ}. In a non-separated volume, p and w are dynamically very closely tied together. Similarly, in a separated volume when the wall temperature effects are ignored, there is not much delay between ℓ and p. In essence, we only use the initial trend of these signals in the rules of the PRD.

The closing of the TW on the tightly coupled variables does not close the window for rules relating $\{h_i,h_o,w\}$ and {ℓ,w}. This is because h and ℓ normally have much longer natural time constants than the other variables, since they are integrated variables. Some of the $t_{close\ inst/ntfd}$ formulas close the windows for h or T, and ℓ signals. For the variables h_i and w, if there are no breaks in either of the variables, as illustrated in Fig. 2.6, we continue to use the initial trend of the variables in the rules. For each variable, if there is a break but the break is not the opposite of the initial trend, as shown in Fig. 2.7, we continue to use the initial trend of the variable in the rules. For each variable, if there is a break but the break acts against the initial trend, as shown in Fig. 2.8, we continue to use the

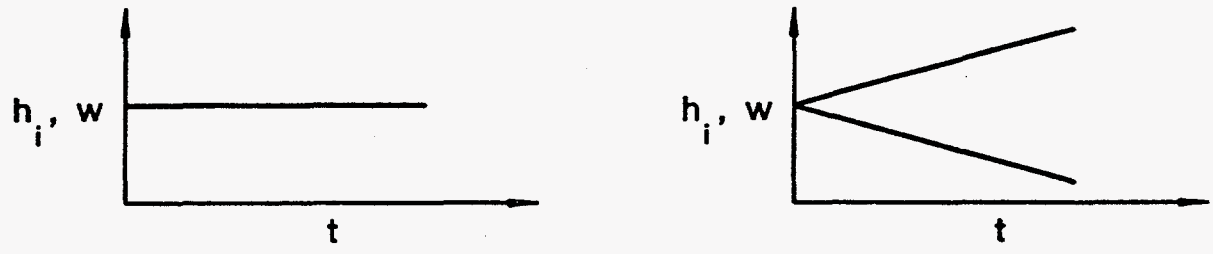

Fig. 2.6. Control System Actions with No Effects on Inlet Enthalpy h_i and Flow w

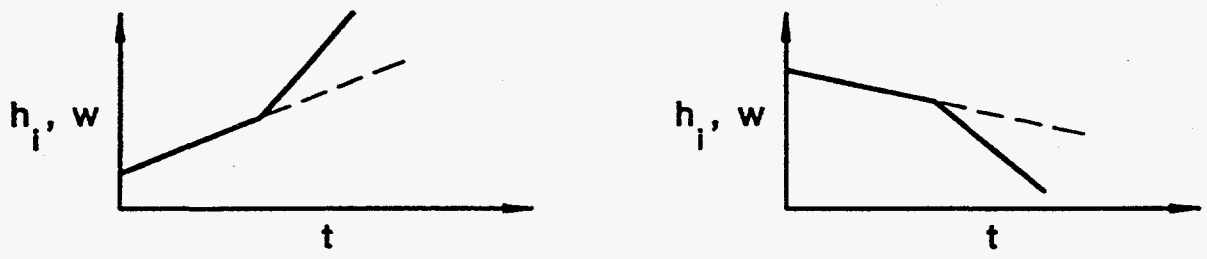

Fig. 2.7. Control System Actions that Cause Monotonic Trend Behavior on Inlet Enthalpy h_i and Flow w

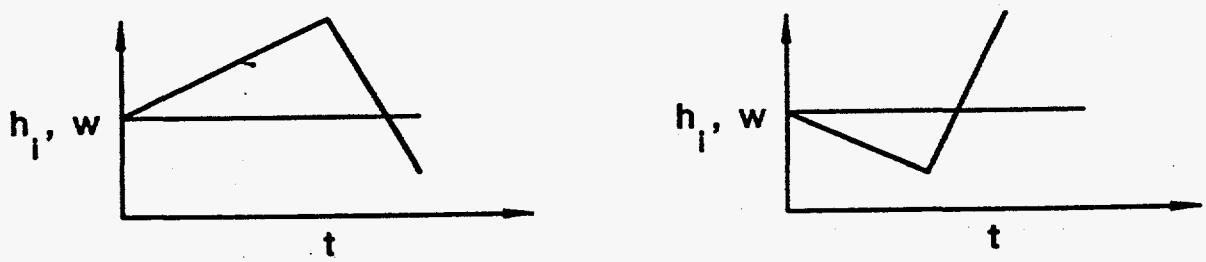

Fig. 2.8. Control System Actions Close the Time Window at $t_{close\ control}$ Due to Nonmonotonic Trend Behavior on Inlet Enthalpy h_i and Flow w

variable in the rules with the initial trend until the initial value is reached. At this point, the trend is treated as unknown and the TW closes. Since the qualitative trend in h_0 and ℓ will remain the same until the h_i and w reach the initial value this will keep the time window open as long as possible before breaks occur in h_0 and ℓ. For the integrated variable ℓ and h_0, for each variable, if there is a break, we stop using the initial trend in the variables. It may be possible to be less restrictive and keep the time window open longer but integrated variables are the "slowest" variables in the system and it may be advantageous to be cautious in this case. At this point, the trend is treated as unknown and the TW closes. This is shown in Fig. 2.9.

2.2.3 Stopping Criteria

In addition to governing the opening and closing of the TW for the T-H variables, the evolution in time of the T-H variables during a transient can also be used as criteria for the ES to stop the

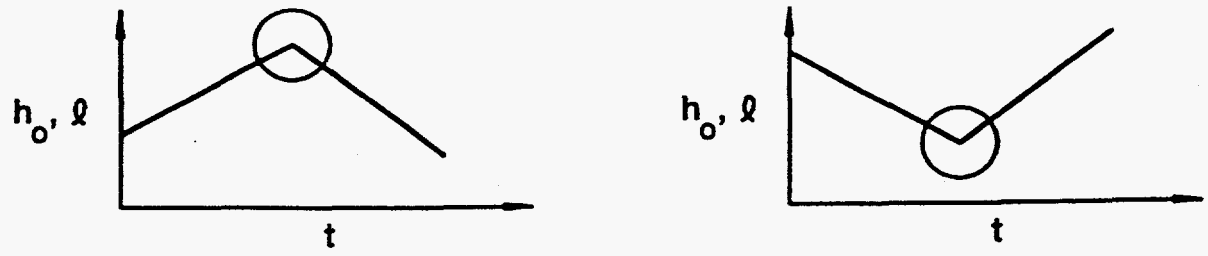

Fig. 2.9. Control System Actions Close the Time Window at $t_{close\ control}$ Due to Nonmonotonic Trend Behavior on Outlet Enthalpy h_0 and Level ℓ

diagnostics. For instance, diagnostics should be stopped after the window has closed for all variables, after all h_o's and ℓ's have initially responded, reverse flow occurs, and initiation of two-phase conditions. The difficulty with this procedure is that some w may not be monitored. The control system may also activate a $Q^{/-}$ function. Stopping criteria for the diagnosis are important. They define the limits of the applicability of the diagnostic technique. The following stopping criteria should be used:

- After the time window has closed for all variables. Once the time window is closed for all variables no new signal information is accepted for processing. The diagnosis will therefore not change from that point on.

- After all h_o's and ℓ's have initially responded. These integrated variables are the "slowest" variables in the system. Once they have responded, all the information that can be obtained for the malfunction should have already been obtained. Closing the time window at this point is conservative as it decreases the possibility of misinterpreting new information.

- Reverse flow occurs. The ES rules, in particular, the energy rules have been derived assuming that the initial flow direction remains the direction of the flow during the transient. If, for example, the flow reverses in a heat exchanger during a transient, the ES supervisory logic will have to become much more complex with the interchanging of h_i and h_o, etc. The benefits of such complexity appear to be marginal.

- Initiation of two-phase conditions. Currently the ES is restricted to single phase/noncondensible gas T-H systems. Two phase ES rules will have to be developed in the future.

- After the malfunctioning component has been identified. This includes instrumentation error. The objective of the diagnostics has been accomplished with the identification of the malfunctioning component.

- If the list of hypothesized component malfunctions becomes larger. If this case should occur the supervisory logic of the ES will have to be reviewed as the algorithm is supposed to narrow the focus of the diagnostics with increasing signal information and not widen the range of possibilities.

With the definition of these stopping criteria, we complete the description of the approach taken to account for dynamic effects. T-H dynamic effects are complex and difficult to model in terms of IF-THEN rules. By introducing the concept of the TWS and performing the signal processing and validation prior to entering the ES part of the diagnostic strategy, we allow the utilization of quasi-static T-H physics in the derivation of "simpler" ES rules.

This chaper described the theory behind the concept of the TWS. In the actual implementation of the TWS in the PRODIAG, it was found necessary to make a number of approximations. Reference should be made to Section 2.4.2 of Volume 2, the PRODIAG code manual, for a discussion of the approximations and the accompanying rationale.

REFERENCES

[2.1] Project Staff, "Combined Expert System/Neural Network for Process Fault Diagnosis," Annual Status Report for FY93, September 1993.

[2.2] Project Staff, "Combined Expert System/Neural Network for Process Fault Diagnosis," Annual Status Report for FY94, September 1994.

[2.3] T. Y. C. Wei, "Instrumentation Error/Signal Validation," Memorandum to J. Reifman, December 1, 1993.

[2.4] T. Y. C. Wei, "Time Window Selector," Memorandum to J. Reifman, December 1, 1993.

[2.5] T. Y. C. Wei, "Clarification of Some Issues Relating to First PRODIAG Results," Memorandum to J. Reifman, December 1, 1993.

[2.6] T. Y. C. Wei, "Switching Criteria to Long-time Rules," Memorandum to J. Reifman, November 10, 1994.

[2.7] J. Reifman and T. Y. C. Wei, "PRODIAG - Dynamic Qualitative Analysis for Process Fault Diagnosis," Proc. of the Ninth Power Plant Dynamics, Control and Testing Symposium, pp. 40.01-40.15, Knoxville, Tennessee, May 24-26, 1995.

3.0 PLANT-LEVEL ES DIAGNOSTICS

3.1 ES Taxonomy

Chapter 2 discussed the dynamic effects involved during T-H transients, the accompanying complications for diagnostics of malfunctioning components, and the proposed route to solve these dynamic complications in the context of the expert system. As discussed, the proposed route is to analyze dynamic effects and correlate them before initiation of the diagnostic reasoning with the ES. The ES will, therefore, focus only on quasi-static T-H effects. The rules and correlated reasoning in the ES for the diagnosis of the T-H response are, therefore, based upon the quasi-static approximations of the three conservation equations of mass, momentum, and energy [3.1]. Figure 1.1 and Chapter 1.0 initiated the discussion on the taxonomy of T-H systems at the first level of classification. This classification of T-H systems will allow the classification of these T-H effects which are describable by the quasi-static conservation equations. Further details are now added to the taxonomy of Fig. 1.1. The geometrical configuration class and the operation condition class are further decomposed as shown in Fig. 3.1.

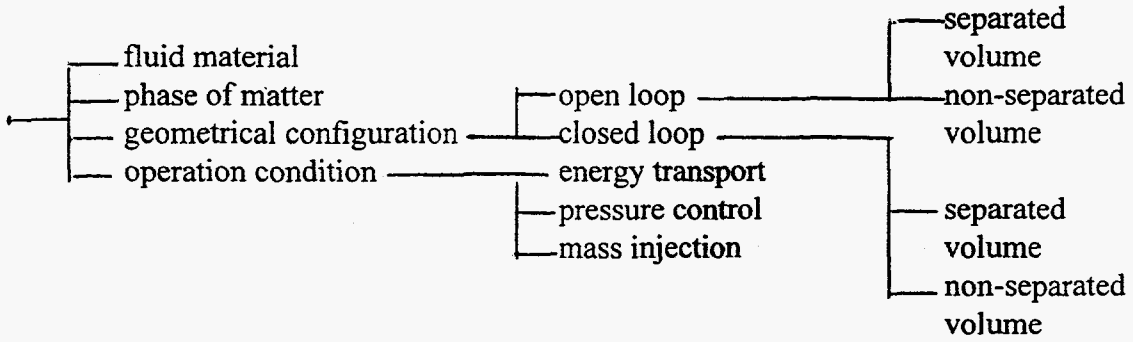

Fig. 3.1. Thermal-Hydraulic System Classification

In accordance with the system design strategy laid out in Chapter 1, the plant-level ES diagnostics utilize only the initial trend of the temporal T-H signals but correlate them spatially across the plant to identify the component malfunction. This requires ES rules or correlations to be developed for a wide set of geometrical configurations. For these rules to be generic, the geometrical configurations have to be generic. This then necessitates the definition of a few basic configurations which have to be "simple" to enable them to be used as building blocks [3.2]. All T-H systems should then be decomposable into these building blocks, which will be termed as loops. To decompose a T-H system into "independent" loops requires the identification of end conditions with flows or pressures, which are "essentially" constant during a T-H transient, and allows a loop-by-loop decoupling to be performed during the diagnostic reasoning. A loop is defined as a continuous fluid circuit of monodirectional incompressible flow between two end conditions. This is in the direction of the monotonically decreasing pressure gradient, except across a pump. Allowances are made for the step pressure discontinuity at the pump. The ES rules are then applied to one loop at a time. They correlate the initial trends of the signals spatially along the loop to allow an inference to be drawn.

A number of concepts are introduced here which pertain to loop interfacing, loop connections, and loop ends:

(a) External Connected System (ECS)

(b) Internal Connected System (ICS)

(c) Secondary System (SS)

(d) Junction Component (JC)

(e) Boundary Condition (BC)

There can be hydraulic interfaces and thermal interfaces between loops. Loops can be hydraulically connected at an ECS, at an ICS, or through a junction component (JC). An ECS is a T-H system which is hydraulically connected to the specific T-H system under diagnosis but it is valved off at normal steady state. Attributes of ECSs which need to be recorded are the normal steady state p and T. If any instrument data are available for those systems (in particular, those dealing with inventory; level, etc.), those will also be utilized in the diagnosis. An ICS is a T-H subsystem which is hydraulically part of the specific T-H system under diagnosis and is not valved off at normal steady state, but at normal steady state, the interconnecting flow is zero. An example of this is a pressurizer connected to the reactor primary system. A junction is an intersection of three or more pieces of piping. We restrict ourselves to three-way junctions. Loops can be hydraulically connected through junctions. Junctions are classified as components with a mass source or mass sink capability for the loop which is being diagnosed. A boundary condition is defined as an end condition of constant w or p. Another example of an end condition is a tank which is a volume with separated liquid and gas phases (i.e., a level exists). At present only noncondensible gas phases will be considered. Saturation conditions and bubbles will not be considered. However, the onset of saturation conditions will be diagnosed. Thermal interfacing of loops is treated by using the concept of an SS. A SS is a T-H system which is coupled to the specific T-H system thermally but not hydraulically at normal steady state. Attributes of these concepts which need to be known in our approach are indicated in Table 3.1. These will have to be included in the PID or an equivalent database with system-specific information in it.

Table 3.1. PID Attribute Data

ECS	Normal Steady State P, T
SS	Normal Steady State P, T
JC	Connectivity data

With these concepts, the simple hydraulic loops of Fig. 3.2 can now be presented. These are the model loops into which the specific T-H system is decomposed. These loops perform the T-H function of energy transport. Future work will treat loops with the T-H functions of pressure control and mass injection. Volume 2 refers to these energy transport loops as "normal" loops. The geometrical configuration of the energy transport function loops is further decomposable into loops which are classified as being of two types: open and closed. An open loop starts and ends at two boundary conditions. This is shown in Figs. 3.2(a) and (c). A closed loop starts and ends at the same location. This is shown in Figs. 3.2(b) and (d). This decomposition into open and closed loops of specific T-H function makes it sufficient to transform the balance equations into ES rules for only a finite number of model geometries. All T-H systems can then be constructed from these model geometries. With the one identified exception of the three-way direct valve discussed in Section 3.3, the ES rules and supervisory flow logic for the process fault diagnosis of each of these model geometries is configuration independent. Each of the model geometries is decomposed into a number of control volumes each of which is associated with a specific component or group of connected components in that model geometry. The associated rules for the specific component are then configuration independent.

(a) OPEN LOOP/ENERGY TRANSPORT

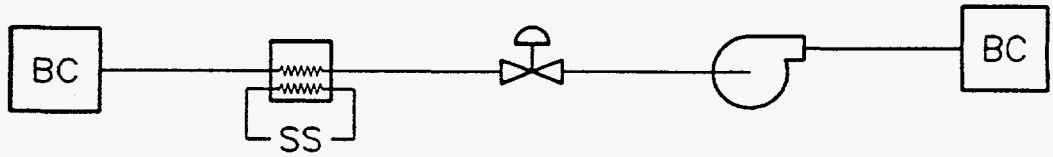

(b) CLOSED LOOP/ENERGY TRANSPORT

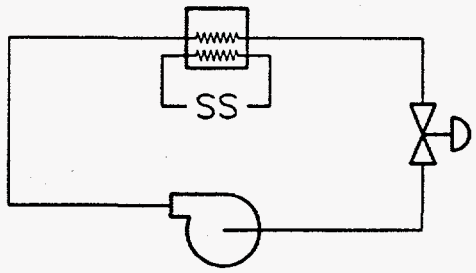

(c) OPEN LOOP/ENERGY TRANSPORT

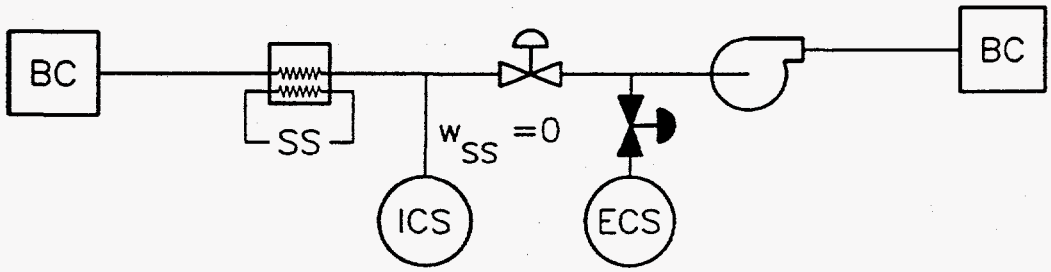

(d) CLOSED LOOP/ENERGY TRANSPORT

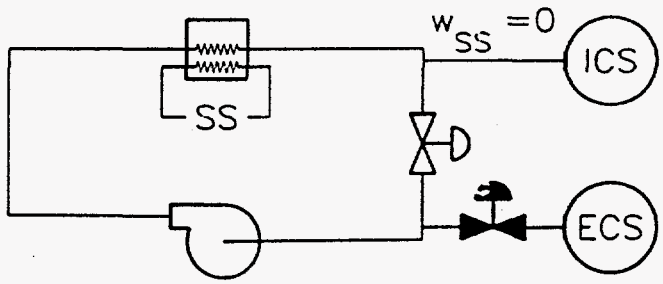

Fig. 3.2. Loop Configuration

Control volumes can be further classified into two classes: non-separated volumes and separated volumes. A separated volume consists of a non-condensible gas space over a liquid volume, while a non-separated volume consists entirely of subcooled liquid. Two sets of ES rules can be derived for the two types of control volumes. Table 3.2 repeats the classification of Table 2.1 and the associated structured taxonomy for the related equations by volume class. The thermal-hydraulic variables are pressure (p), flow (w), enthalpy (h), and Level (ℓ).

Table 3.2. Classification of Volumes and First-Principles Equations

Control Volume	Non-Separated		Separated		
Coupled Variables	{p,w}	$\{h_i,h_o,w\}$	$\{p,\ell\}$	$\{\ell,w\}$	$\{h_i,h_o,w\}$
Correlating Equation	mass and momentum balance	energy balance	gas equation of state	liquid mass balance	liquid energy balance

The diagnostic strategy tree is shown in Fig. 3.3. It is clear that the diagnostic strategy tree is a classification system, or taxonomy, whereby a T-H system is partitioned into smaller and smaller groups of components until ultimately the single failure component becomes the focus of the search and is finally identified. The Component Classification Dictionary (CCD) of Fig. 1.3 is the lower part of the diagnostic tree of Fig. 3.3. To perform the partitioning of the T-H system at each level of the tree requires formulae or criteria to distinguish among the different branches. In the lower part of the tree or the CCD, which is further developed in Section 3.3, these formulae or criteria are the first-principles rules of the Physical Rules Database (PRD) which was introduced in Section 1.2 for

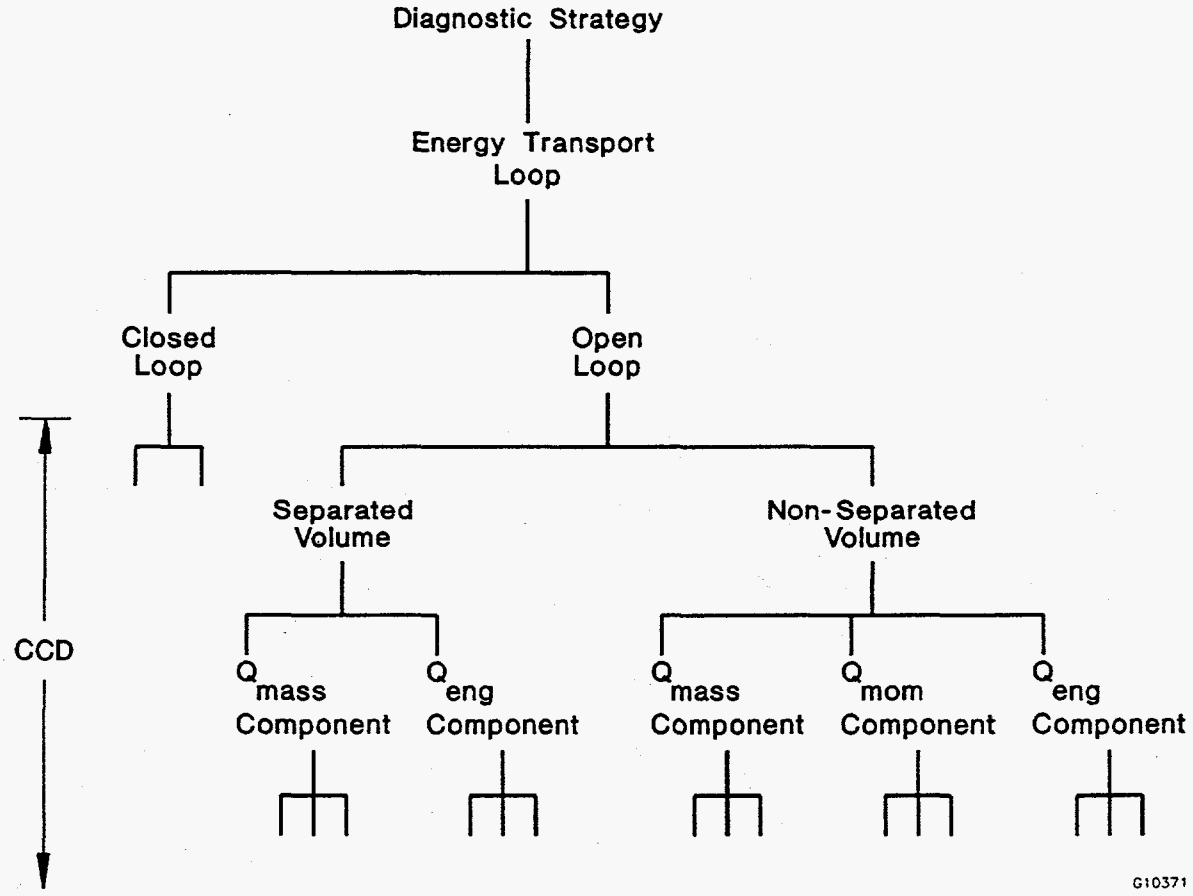

Fig. 3.3. Diagnostic Strategy Tree

the plant-level ES. Further down the tree at the component-level ANNs, these formulae or criteria are the component characteristics used for the ANN representations

3.2 PRD Rules

We concentrate on the energy transport loop. Malfunctions due to imbalances in energy sources/sinks can lead to coolant volumetric changes. The resultant flow changes, particularly in surge lines, would be difficult to diagnose if mass and momentum malfunctions were not decoupled from energy malfunctions. This decoupling is effected by the usage of a coolant, water, with a "small" coefficient of thermal expansion α, and the selection of a threshold for T deviations (i.e., h deviations) of ~2°F. This leads to "small" expansions and changes in expansion flow which are still large enough to provide for early detection of energy source/sink malfunctions. For a volume V,

$$\frac{\delta V}{V} = \alpha \delta T \tag{3.1}$$

For subcooled water $\delta V/V = 10^{-4} \times 2 = 0.02\%$. This expansion is well below the diagnostic thresholds discussed in Chapter 2 and allows us to focus on deriving rules for the energy transport loop with energy malfunctions decoupled from mass and momentum malfunctions. Other types of coolants will require further investigation.

Equations (2.10) - (2.12) in Chapter 2 are the dynamic forms of the three conservation equations integrated over a control volume. The corresponding quasistatic forms are as follows:

$$\Sigma w_i - \Sigma w_o + Q_{mass} = 0 \tag{3.2}$$

$$p_i - p_o - \Sigma_j \frac{k_j w_j^2}{\rho_j A_j^2} + \Delta p_{pump} = 0 \tag{3.3}$$

$$\Sigma h_i w_i - \Sigma w_o h_o + Q_{eng} = 0 \tag{3.4}$$

with the equation of state

$$p = f(\rho, T). \tag{3.5}$$

To simplify the resultant qualitative analysis the momentum equation has been written in one-dimensional form with neglect of the gravity term and the acceleration term. In addition, the energy equation neglects mechanical work and kinetic energy.

The PRD rules which correlate signals from different components using the balance equations (3.2)-(3.4), and the EOS (3.5), are denoted as primary rules. These are used by the plant-level diagnostics work. In the diagnostic system design strategy outlined in Section 1.2, the component-level diagnostics work is to be performed by the network of ANNs. However, some component-level rules can be derived for the ES to perform the same type of diagnostics. These rules are denoted as secondary rules. In addition, the secondary and primary rules of the PRD are of two classes [3.3]: Q rules and CV (Control Volume) rules. A Q rule indicates the type and trend of the imbalance in a control volume inferred from the trends in the measured T-H variables. Corresponding to the three balance equations of mass, energy, and momentum, we have three types of Q rules: Q_{mass}, Q_{eng}, and Q_{mom}, respectively, to infer the Q status of a control volume. The Q status can have one of three trends or qualitative values, increasing (↑), decreasing (↓), and unchanging (-). Thus, if a control

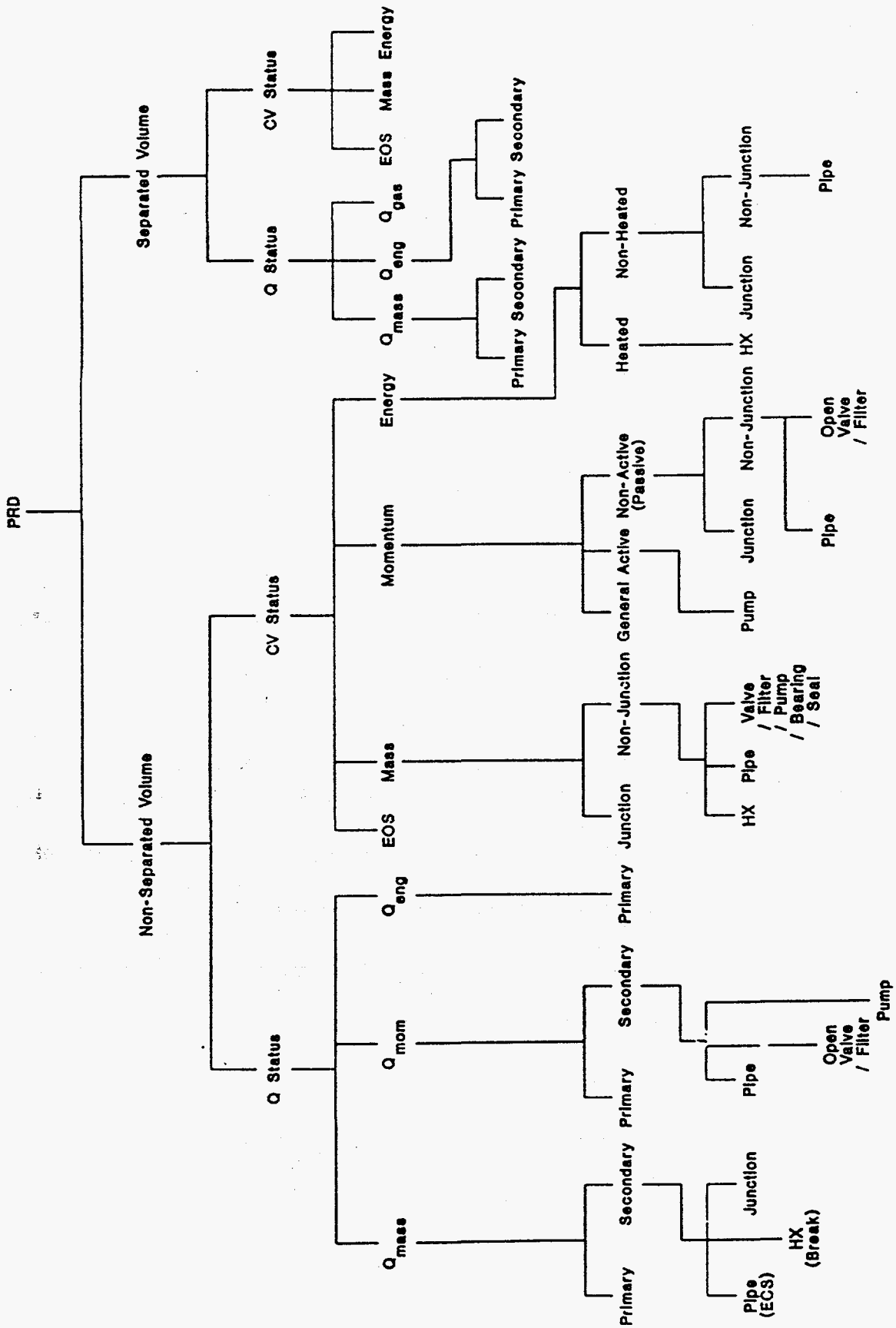

Fig. 3.4. PRD Database Structure

volume is experiencing a loss of mass, a Q rule identifying such imbalance would characterize the Q status of the control volume as $Q\downarrow_{mass}$. A CV rule infers the trend status of nonmeasured T-H variables, pressure p, flow w, temperature T, and level ℓ, in a process component, from the other T-H variables and the Q status of the component. In the following sections we provide the derivations of the Q rules and CV rules. Figure 3.4 shows the taxonomy of the PRD rules.

3.2.1 Primary Q Rule Derivation

The primary Q rules derived here, since they are at the plant-level diagnostics and are based on the balance equations, apply equally well to control volumes composed of both separated and non-separated volumes. However, different classes of primary Q rules, with varying degree of diagnostic precision, can be derived as a function of the type, trend, and number of T-H variables. Specific groups of three-signal variables with specific trends are required to form the minimum set for *unique* identification of an increasing or decreasing Q status in a control volume. For instance, the three-signal variables $[p^{\downarrow}_{out}\ w^{\uparrow}_{in}\ w^{\downarrow}_{out}]$, can uniquely identify $Q\downarrow_{mass}$ in the control volume defined by the two flow measurements in both open and closed T-H loop configurations. In the above notation, $p^{\downarrow}$ indicates a pressure decrease measurement anywhere in the T-H loop, $w^{\uparrow}_{in}$ represents an increase in the control volume inlet flow and $w^{\downarrow}_{out}$ represents a decrease in the control volume outlet flow. Unique Q status identification can also be obtained for Q_{mom} and Q_{eng} if the specific variable trends are available for the sets $[w\ p_{in}\ p_{out}]$ and $[w\ T_{in}\ T_{out}]$, respectively. However, in many practical situations, the instrumentation set is insufficient to provide this minimum set. There are cases where only two- or one-signal variables are available in a loop. In such cases, Q rules can also be constructed to provide some malfunction Q diagnostics. But, as can be expected, the precision of

the diagnostics decreases, with a larger number of possible Q malfunctions being inferred. For instance, if only the two-signal variable set [p w] is available in the loop, then a Q rule would indicate the possibility of either Q_{mass} or Q_{mom} problems.

In the following sections, we derive Q rules with both three- and two-variable sets. Also, we show that three-variable rules can be systematically constructed through the logical intersection of two two-variable rules, and that two-variable rules can be constructed through the logical union of two three-variable rules.

It is important to note that an inference of a nonchanging Q^- status can be of as much value as a changing $Q^{/-}$ status, since it rules out malfunction possibilities. Furthermore, as will be seen, the application of CV rules may require the knowledge of Q^- for the particular control volume. By the assumption of single failure if $Q^{/-}$ is identified for a particular location, then all other Q functions at this location as well as in the rest of the system are normal. We derive Q^- rules as well as $Q^{/-}$ rules.

3.2.1.1 Three-Variable Rules

We start the derivation of three-variable rules for Q rules that infer imbalances in the conservation of mass inventory.

Mass Conservation

For the open loop with no junctions, there is only one outlet and one inlet, so the summation signs will be dropped. Focusing on the mass conservation equation Eq. (3.2), it can be seen that if $w_i(t)$ and $w_o(t)$ are measured then $Q_{mass}(t)$ is completely determined for a control volume in the open loop. This conclusion is also reflected in the corresponding ES rule derived from Eq. (3.2). Using DeKleer and Brown's methodology [3.10] to transform Eq. (3.2) into a qualitative differential expression for the geometry of Fig. 3.5, gives the following confluence for the control volume with single input/output ports.

$$[dw_{in}] - [dw_{out}] = -[dQ_{mass}] , \tag{3.6}$$

where the square brackets [·] represent the qualitative value or trend (↑,↓,-), of the argument basic quantity, i .e., w_{in}, w_{out}, and Q_{mass}. Equation (3.6) represents the general confluence, from which Q rules characterizing imbalances in Q_{mass} can be derived by applying the different trend

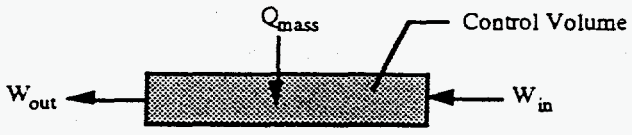

Fig. 3.5. Control Volume with Moveable Boundaries Defined by the Location of the Flow Measurements w_{in} and w_{out}

combinations of w_{in} and w_{out} and using the operations of qualitative algebra. Table 3.3 shows all the combinations. The symbol A is used to indicate an ambiguous trend, i.e., ↑,-,↓, could all be possible. For the case where inlet flow into the control volume is increasing and outlet flow is decreasing, the confluence in Eq. (3.6) infers that Q_{mass} is decreasing ($Q^{\downarrow}_{mass}$), or equivalently, that the control volume is losing mass, represented through the rule:

rule (B.1) If $w^{\uparrow}_{in}$ and $w^{\downarrow}_{out}$, then $Q^{\downarrow}_{mass}$.

Table 3.3. Q_{mass} Trend

w_{out} \ w_{in}	↑	-	↓
↑	A	↑	↑
-	↓	-	↑
↓	↓	↓	A

While Q_{mass} in the actual balance equation is the source/sink term, in the qualitative analysis rule (B.1), it should be thought of as a conservation imbalance indicator, viz. a malfunction status indicator characterizing the fact that one of the components within the control volume is malfunctioning and causing the mass inventory to decrease. Physically speaking, rule (B1) is a consequence of the fact that the pressure distribution determines the flow distribution. The only case where the changes in a control volume inlet and outlet flow are not in tandem is when changes in the control volume internal pressure is the driver. Changes in the pressure distribution external to

the control volume will not have this effect. A Q_{mass} malfunction in the control volume is the only possible initiator of such a pressure driver.

Similarly, we can also derive a rule from the general confluence in Eq. (3.6) corresponding to rule (B.1), for the case where Q_{mass} is increasing,

Rule (B.2) If $w^{\downarrow}_{in}$ and $w^{\uparrow}_{out}$, then $Q^{\uparrow}_{mass}$.

Trend combinations that cause ambiguous inference in Eq. (3.6), e.g., both w_{in} and w_{out} increasing, are not represented in the PRD. These two rules (B.1) and (B.2), formed with two variables of the same type, i.e., w, in the condition part of the rule, uniquely identify Q_{mass} imbalances in open loops. Two instrumentation locations for flow will pinpoint Q_{mass} imbalances occurring between the two locations. As in the case of the analytical equation, only two flow measurements are required for unique Q malfunction identification.

We now move to closed-loop geometries. If the control volume of Fig. 3.5 is in a closed loop, ambiguities arise. In a closed loop, the definition of "in" (upstream) and "out" (downstream) has two possible combinations. Both rules would be simultaneously activated regardless of the fault locations and type of mass problem ($\uparrow$ or $\downarrow$). This undesirable situation can be eliminated by the addition of information if a p instrument measurement is available. Through perturbation analysis of the single-phase equation of state $p = p(\rho,T)$, where ρ is the liquid density, we obtain

$$dp = \frac{\partial p}{\partial \rho} d\rho + \frac{\partial p}{\partial T} dT \ . \qquad (3.7)$$

We now move to a control volume with multiple inlet and outlet ports. The rules derived previously can be thought of as correlating signals along one loop. With multiple inlet and outlet ports, those rules should still be valid for any selection of an inlet and an outlet port as part of a single loop. For mass malfunctions within the control volume, all inlet flows should respond with the same trend and all outlet flows should respond the same way. However, since a control volume with multiports could contain a number of junctions, junctions need to be classified as Q_{mass} components in the CCD. This is because the initiating pressure disturbance is not necessarily within the control volume. For the plant-level diagnostics, the key is that the flow distribution is driven by an initiating pressure disturbance caused either by a Q_{mass} malfunction or a Q_{mom} malfunction. The synchronous or asynchronous behavior of the trends in the pressure spatial distribution or the flow spatial distribution is then used to diagnose the malfunction. For a control volume containing junctions, a pressure disturbance initiator in the part of a loop outside the control volume would lead to the same spatial flow distribution in the other loops connected through junctions within the control volume as a pressure disturbance within the control volume [3.5]. The previous rules would therefore also be activated for this malfunction. Defining a "junction" as a Q_{mass} component in the CCD would be a simple resolution for this situation. Furthermore, rules can be derived which correlate signals from different loops in contrast to the previous rules which correlated signals along one loop. Based upon experience, it appears that the multiport control volumes of Figs. 3.6 and 3.7 are frequently encountered. For these control volumes, the following inter-loops Q rules can be derived. Since initiating pressure disturbances can be either Q_{mass} or Q_{mom} driven, the rules lead to two possible inferences. The rules depend upon the type of junction being considered. For type (a) as depicted in Fig. 3.6, if we initiate a pressure disturbance in each of the ports in turn we obtain from the resulting flow patterns, the example

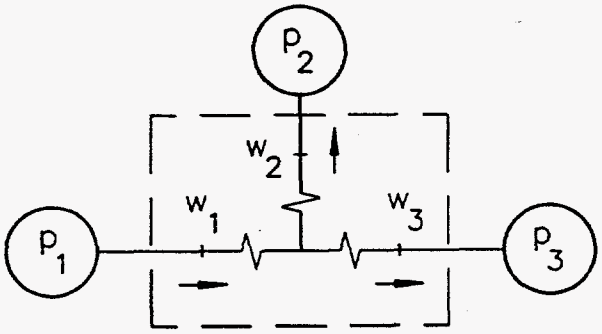

Fig. 3.6. Type (a) Junction/ Multipleport Control Volume

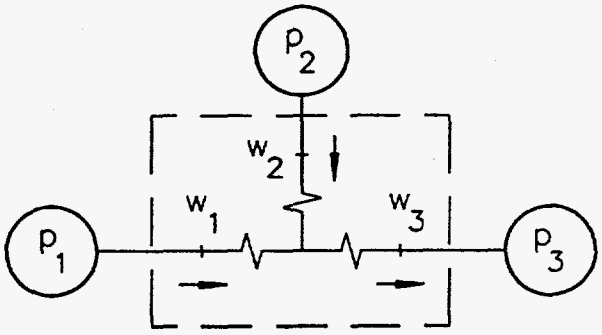

Fig. 3.7. Type (b) Junction/ Multipleport Control Volume

$$w_1^{\uparrow}\ w_2^{\uparrow}\ w_3^{\uparrow} \rightarrow Q_1{}^{\uparrow}{}_{mass},\ Q_1{}^{\uparrow}{}_{mom}$$

For type (b) as depicted in Fig. 3.7, we obtain similarly by initiating a pressure disturbance in each of the ports in turn, the example

$$w_1^{\uparrow}\ w_2^{\downarrow}\ w_3^{\uparrow} \rightarrow Q_1{}^{\uparrow}{}_{mass},\ Q_1{}^{\uparrow}{}_{mom}$$

Future work will use and develop other possible examples of this type of a rule.

These Q_x's are located in the respective loop "x" outside the control volume measurements. The multiports need to be independent and not connected outside the control volume. We also have within the control volumes (a) and (b) for synchronized flow trends,

$$w_1^{\uparrow}\ w_2^{\uparrow}\ w_3^{\uparrow} \rightarrow Q^{-}_{mass}$$

$$w_1^{\downarrow}\ w_2^{\downarrow}\ w_3^{\downarrow} \rightarrow Q^{-}_{mass}$$

Some of these rules can be derived by applying the two variable rules described later in Section 3.2.1.2 and then taking the union of the conclusions for the various single loops.

Momentum Conservation

To obtain the corresponding quasistatic qualitative differential expression for the momentum equation, Eq. (3.3), we need to think of the junction friction term and the pump head term as source/sink terms

$$\frac{kw^2}{\rho A^2} = \frac{w^2}{Q_{mom}} \tag{3.9}$$

$$\Delta p_{pump} = Q_{mom} f_{pump}\ (w) \tag{3.10}$$

With this redefinition, using the De Kleer and Brown's methodology on Eq. (3.3) and evaluating changes in the two Q_{mom} separately gives us for the configuration of Fig. 3.2(A), assuming negligible density changes.

$$dp_{in} - dp_{out} - \frac{2w\,dw}{Q_{mom}} = -\frac{w^2}{Q^2_{mom}}\,dQ_{mom} \tag{3.11}$$

or

$$[dQ_{mom}] = [dw] + [dp_{out}] - [dp_{in}] \tag{3.12}$$

for the valve. For the pump we have similarly

$$dp_{in} - dp_{out} + Q_{mom}\, f'(w)dw = -f(w)dQ_{mom}$$

using generic pump characteristics (f (w) = positive, derivative f ′(w) = negative) we obtain also

$$[dQ_{mom}] = [dw] + [dp_{out}] - [dp_{in}] \tag{3.14}$$

As in the case of the mass conservation equation, search of the possible trend combinations gives us the following three variable rules derived from the momentum conservation equation.

Rule (A.3) $\quad w^{\uparrow}\ p_{in}^{\downarrow}\ p_{out}^{\uparrow} \rightarrow Q_{mom}^{\uparrow}$

Rule (A.4) $\quad w^{\downarrow}\ p_{in}^{\uparrow}\ p_{out}^{\downarrow} \rightarrow Q_{mom}^{\downarrow}$

where $Q^{\uparrow}_{mom}$ is downstream of p_{in} and upstream of p_{out} and w is measured anywhere in the loop. As in the case of the mass conservation rules these rules show that only three signal variables, the set [w p_{in} p_{out}] are required to form the minimum set to uniquely identify a Q_{mom} malfunction for a control volume in both an open loop or a closed loop.

Moving over to the multiport control volume, any single loop which can be formed from a combination of an input port and an output port will obey the above momentum rules. For inter-loops correlations the previous discussion in the section on mass conservation rules should be referred to. The rules presented there give both a possible Q_{mom} as well as a possible Q_{mass} inference. It can be seen from the discussion on the two conservation equations while it is true that three signal variables uniquely identify the imbalancing Q function of the malfunction, there are unique sets of variables which have this property. The canonical sets are [w w p] for the mass equation and [w p p] for the momentum equation. The reason for this is evident from the structure of the equations, Eq. (3.2) and Eq. (3.3).

Energy Conservation

For the single input/output port control volume shown in Fig. 3.8, the energy conservation equation, Eq. (3.4), becomes, with the summation signs deleted,

$$Q_{eng} = w_a(h_{out} - h_{in}) \tag{3.15}$$

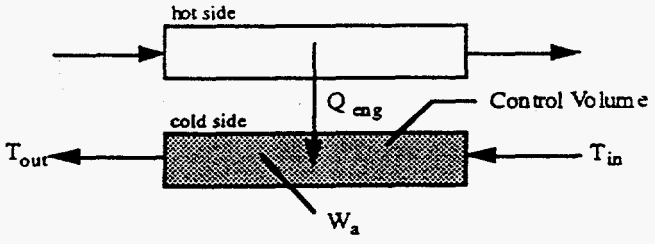

Fig. 3.8. Single Input/Output Port Control Volume

The subscript a indicates that w_a is the average flow between the locations "in" and "out."

Since $T = c_p h$ and c_p is the specific heat we will use h and T interchangeably in this report. Transforming Eq. (3.15) into a qualitative differential expression and solving for Q_{eng} yields the confluence

$$[dQ_{eng}] = [dw_a] - [dh_{in}] + [dh_{out}] \tag{3.16}$$

As with the mass and momentum conservation equations, examination of the possible trend combinations gives the following rules which should apply for both closed and open loops.

$$w_a^{-}\ h_{out}^{\uparrow}\ h_{in}^{/\downarrow} \rightarrow Q_{eng}^{\uparrow}$$

$$w_a^{-}\ h_{out}^{\downarrow}\ h_{in}^{/\uparrow} \rightarrow Q_{eng}^{\downarrow}$$

Once again as with the other conservation equations the malfunction is located downstream of "in" and upstream of "out." Physically speaking, in the case of heat exchangers, the Q_{eng} malfunction is caused by a flow or an inlet temperature change on the secondary side (SS). This then causes the Q_{eng} to change also. The rules can be shown to be equally valid for these cases as long as care is exercised in the definition of the physical direction of the heat transfer; heat is entering the system (q^+) or heat is being removed from the system (q^-).

For a multiport control volume the situation is more complex than with the mass and momentum equations. Concentrating on a single loop formed from one input and output port is insufficient. There is a need to know the h_{in} for all the inlet ports. Furthermore the w_{in} also need to be known for all the inlet ports; otherwise conclusions regarding Q_{eng} cannot be drawn. In light of this, multiport rules with only three variables are not useful here.

For the energy equation the following three-variable rule to infer Q_{eng} can be used.

$$w_a \; h_{out} \; h_{in} \rightarrow Q_{eng}$$

The corresponding rules from the mass and momentum equations are not used because of the dynamic effects involved.

3.2.1.2 Two-Variable Rules

When only two signal variables are available in a loop, rules can also be constructed to provide some Q malfunction diagnostics. But as can be expected the precision of the diagnostics decreases with a larger number of possible Q malfunctions being inferred.

Mass Conservation

Some of the two-variable rules for mass conservation were previously derived in the section on three-variable rules. These are repeated here for comprehensiveness.

Rule (B.1) $w_{in}^{\uparrow}\ w_{out}^{\downarrow} \rightarrow Q_{mass}^{\downarrow}$

Rule (B.2) $w_{in}^{\downarrow}\ w_{out}^{\uparrow} \rightarrow Q_{mass}^{\uparrow}$

As noted previously this provides a unique malfunction location for an open loop. However for a closed loop there is an ambiguity since both rules would simultaneously fire. The ambiguity is with the definition of 'in' and 'out' in a closed loop [3.6]. One possible solution is to define a unique starting and end point and "break" the closed loop into an open loop at that point. Since these rules infer mass source/sink malfunctions it is natural to consider a mass source/sink or location as a possible start/end point. Unlike the closed valve component from the CCD the junction component does not require any action to function as a mass source or sink. So junctions may appear to be a good candidate for the start/end point. Since there may be a number of junctions the best choice for "breaking" would appear to be junctions connected to large inventories of liquid. A closed loop with no surge tank junction should be "broken" at the pump. However such a T-H system would quickly develop two-phase conditions placing it outside the assumptions of the current PRODIAG diagnostic system.

We now consider the case when only two-signal variables [pw], are available and show how rules can be constructed. For the case where [$p^{\downarrow}$ $w^{\uparrow}$], rule (A.1) could be activated, if another flow meter downstream of w was present with a decreasing trend, or rule (A.3) could be activated, if another pressure transducer downstream of p was present with an increasing trend. Since either rule could be activated in this [$p^{\downarrow}$ $w^{\uparrow}$] combination, then the logic union of rules (A.1) and (A.3), could be applied

Rule (C.1) If $p^{\downarrow}$ and $w^{\uparrow}$, Then $Q^{\downarrow}_{mass}$ or $Q^{\uparrow}_{mom}$,

where $Q^{\downarrow}_{mass}$ is located downstream of the w instrument and $Q^{\downarrow}_{mom}$ is located downstream of the p instrument. Thus, when two-variable rules with different T-H variables are activated, the location of one of the variables (w for Q_{mass} and p for Q_{mom}) is used to define one boundary of the control volume with the other boundary defined by either end of the loop.

The construction of rule (C.1) shows that there is a systematic procedure using Boolean logic, logic union in the case of two-signal variables, to derive Q rules with two- or one-signal variables from the set of rules which uses the minimum three-variable sets [p w_{in} w_{out}] and [w p_{in} p_{out}]. However, the two-variable rules can also be used to reconstruct the three-variable rules, if the signal variables can be grouped in blocks of two. For instance, if we consider a two-variable rule analogous to rule (C.1), i.e.,

Rule (C.2) If $p^{\downarrow}$ and $w^{\downarrow}$, Then $Q^{\downarrow}_{mass}$ or $Q^{\downarrow}_{mom}$,

and a signal set [$p^{\downarrow}$ $w^{\uparrow}_{in}$ $w^{\downarrow}_{out}$] is available, it can be grouped as two two-variable sets [$p^{\downarrow}$ $w^{\uparrow}$] and [$p^{\downarrow}$ $w^{\downarrow}$]. This would mean the activation of both rules (C.1) and (C.2), where the logical intersection of these rules yields $Q^{\downarrow}_{mass}$, which is the identical conclusion of the activation of rule (A.1). This shows the logical consistency between the derivation of the sets of the different-variable-number rules. We apply logical union when we construct two-variable rules from two three-variable rules and logical intersection when we construct three-variable rules from two two-variable rules. In shorthand the remaining rules for this set of two variables are

Rule (C.3) $p^{\uparrow}$ $w^{\downarrow}$ → $Q^{\uparrow}_{mass}$, $Q^{\downarrow}_{mom}$

Rule (C.4) $\quad p^{\uparrow} w^{\uparrow} \rightarrow Q^{\uparrow}_{mass}, Q^{\uparrow}_{mom}$

where in the case of rule (C.3) the momentum malfunction is downstream of the p location and in the case of rule (C.4) it is upstream. In the case of the mass malfunction the corresponding position is relative to the w location. Future work will include the possibility of malfunctions in the end condition.

To date there are no useful inter-loops rules for the multiport control volume but there are important Q^{-}_{mass} rules. For an open loop these are

$$w^{\uparrow}_{in}\, w^{\uparrow}_{out} \rightarrow Q^{-}_{mass}$$

$$w^{\downarrow}_{in}\, w^{\downarrow}_{out} \rightarrow Q^{-}_{mass}$$

The difficulty with closed loops occurs again. The avoidance of junctions in applying these rules across any part of a closed loop would be sufficient for their validity. However this would limit the usefulness of these rules. A pump should be used to "break" the closed loop into an open loop but it should also be made certain that the rules are not applied across a junction which leads to a closed loop. Reference should be made to Section 3.3 for additional clarification when the configuration dependence classification of the three-way divert valve is discussed. Certain configurations where branch-off piping is reconnected back to a loop could lead to ambiguities.

Momentum Conservation

The logical union of the three-variable momentum rules, rules (A.3) and (A.4), gives the following two-variable rules.

Rule (B.3) $\quad p^{\uparrow}_{in}\, p^{\downarrow}_{out} \rightarrow Q^{\downarrow}_{mom}$

Rule (B.4) $\quad p^{\downarrow}_{in}\, p^{\uparrow}_{out} \rightarrow Q^{\uparrow}_{mom}$

The location is uniquely defined for an open loop. For a closed loop, as was the case for mass conservation, the situation is ambiguous. Resolution is provided by using a pump or set of pumps as the start/end point for "breaking" the closed loop into an open loop. The pressure distribution is then monotonically decreasing around the loop. The two-variable set rules for [p w] have been previously discussed in the section on mass conservation.

To date there are no useful inter-loop rules for the multiport control volume but there are important Q^{-}_{mom} rules. For the open loop these are

$$p^{\uparrow}_{in}\, p^{\uparrow}_{out} \rightarrow Q^{-}_{mom}$$

$$p^{\downarrow}_{in}\, p^{\downarrow}_{out} \rightarrow Q^{-}_{mom}$$

The difficulty with closed loops is resolved here as with rules (B.3) - (B.4) by starting at the pump or set of pumps [3.7].

Energy Conservation

Future work will be performed for these rules.

3.2.1.3 One-Variable Rules

When only one signal variable trend is available it may be thought to be difficult to infer anything about Q_{mass}, Q_{mom}, and Q_{eng}. By decoupling energy-malfunction-driven flow and pressure effects from the diagnostics through the use of a small δT threshold we have the following rules

$$w^{/-} \rightarrow Q^{/-}_{mass}, Q^{/-}_{mom}$$

$$w^{-} \rightarrow Q^{-}_{mass}\, Q^{-}_{mom}$$

End condition malfunctions ($Q^{/-}_{EC}$) will have to be considered in the future.

3.2.2 Secondary Q Rules Derivation

Secondary Q rules are derived from generic component characteristics. In the diagnostic strategy outlined in Chapter 1, diagnosis is first performed at the plant level in the ES using conservation equation balances across control volumes expressed as rules. Subsequent to that, diagnosis is performed at the component-level using T-H component characteristics such as pump-head curves expressed in terms of neural network representations. However for a number of generic component types some of these component characteristics can be used to derive ES rules to distinguish among

Q_{mass}, Q_{mom}, and Q_{eng} malfunctions. These rules are by definition then only applicable to components of these types and not to general control volumes. We present here secondary Q rules for

(1) non-separated volumes (2) separated volumes.

3.2.2.1 Non-Separated Volume

As with the primary rules, the secondary rules are presented in the order: mass conservation malfunction, momentum conservation malfunction and energy conservation malfunction.

Mass Conservation

For pipes which are connected to ECS's (Externally Connected Systems), Q rules are presented here for liquid flow systems where the notation is that [w h] are ECS variables and [Q] pertains to the T-H system under diagnosis. If it is known that the fault is located in the system under diagnosis, then given the fact that the ECS is only hydraulically connected to the system under diagnosis through a closed valve, then any change in ECS variables must be due to fluid entering the ECS from the system under diagnosis. This means,

$$h^{/-} \rightarrow Q_{mass}{}^{/-}$$

$$w^{/-} \rightarrow Q_{mass}{}^{/-}$$

Other combinations when the signal trends are known lead to

$w^{\downarrow} \rightarrow Q_{mass}{}^{\uparrow}$ $\quad$ $w^{\uparrow} \rightarrow Q_{mass}{}^{\downarrow}$ $\quad$ (define positive flow as being into ECS)

$\ell^{\downarrow} \rightarrow Q_{mass}{}^{\uparrow}$ $\quad$ $h^{\uparrow} \rightarrow Q_{mass}{}^{\downarrow}$ $\quad$ (if enthalpy of T-H system > h)

$\ell^{\uparrow} \rightarrow Q_{mass}{}^{\downarrow}$ $\quad$ $h^{\downarrow} \rightarrow Q_{mass}{}^{\uparrow}$ $\quad$ (if enthalpy of T-H system < h)

For gas flow systems, where there is no liquid level, the liquid flow ECS rules apply except that Q_{mass} is replaced by Q_{gas}.

Across a heat exchanger (HX) by correlating the inlet and outlet enthalpies on the hot and cold sides we have for conditions where the initial trends on the outlet are not synchronized,

$h'^{\downarrow}{}_{i\ cold}\ h'^{\uparrow}{}_{i\ hot}\ h^{\downarrow}{}_{o\ cold}\ h^{\uparrow}{}_{o\ hot} \rightarrow Q'^{-}{}_{mass}$ (uses assumption of single failure)

$h'^{\uparrow}{}_{i\ cold}\ h'^{\downarrow}{}_{i\ hot}\ h^{\uparrow}{}_{o\ cold}\ h^{\downarrow}{}_{o\ hot} \rightarrow Q'^{-}{}_{mass}$

With the assumption of a single failure, if flow on either the cold side or hot side of the HX alone malfunctioned the outlet temperatures on both sides would follow the same trend. Similarly, if malfunctions affecting either of the inlet temperatures occurred the outlet temperatures on both sides would once again act in unison, after time delays are accounted for. The possibility of instrumentation failure can be ruled out since in our rules both outlet temperature measurements respond and we are limited to single failures. The only possibility is a mass malfunction or break within the HX which affects both hot side and cold side flow and also changes the "effective" heat

transfer coefficient. The sensitivity of the responses in reaching the threshold criteria will be dependent upon HX design, in particular, whether a countercurrent or a parallel heat exchanger is being considered, and the break location. This rule should be used before the CV rules for heated components.

Momentum Conservation

Across an open valve or a filter using the valve/pipe momentum confluence Eq. (3.12) and deriving the corresponding Q_{mom} trend table similar to Table 3.3 for the mass confluence Eq. (3.6), we have

$$Q^{-}_{mass}\ \Delta p^{\downarrow}\ w^{\uparrow} \rightarrow Q^{\uparrow}_{mom}$$
$$Q^{-}_{mass}\ \Delta p^{\uparrow}\ w^{\downarrow} \rightarrow Q^{\downarrow}_{mom}$$

Similarly, across a pipe also using the valve/pipe momentum confluence Eq. (3.12) gives

$$Q^{-}_{mass}\ \Delta p^{\downarrow}\ w^{\uparrow} \rightarrow Q^{\uparrow}_{mom}$$
$$Q^{-}_{mass}\ \Delta p^{\uparrow}\ w^{\downarrow} \rightarrow Q^{\downarrow}_{mom}$$

The Q^{-}_{mass} term is required since in our algorithm, these components can have $Q^{/-}_{mass}$ (i.e., leak or break).

Across a pump using the pump momentum confluence Eq. (3.14) we have

$$Q^{-}_{mass}\,\Delta p^{\downarrow}\;w^{\downarrow} \rightarrow Q^{\downarrow}_{mom}$$

$$Q^{-}_{mass}\,\Delta p^{\uparrow}\;w^{\uparrow} \rightarrow Q^{\uparrow}_{mom}$$

The open valve, filter and pipe are passive momentum components in the CCD. The pump is an active momentum component. Since Δp is defined as positive in these rules, the qualitative analysis equations (3.9) - (3.14) for momentum conservation use

$\Delta p = p_i - p_o$ valve

$\Delta p = p_o - p_i$ pump

This change in sign due to the difference between active and passive component characteristics then leads to these rules based on the equations (3.12) and (3.14).

Energy Conservation

To date no secondary rules of importance for energy conservation have been derived. The primary rules presented in Section 3.2.1.1 also represent component characteristics.

3.2.2.2 Separated Volume

The Q state vector for a separated volume is [Q_{mass}, Q_{eng}, Q_{gas}]. The CV state vector is [w p h ℓ]. We restrict our discussion of separated volume components to tanks. A tank can have a number of inlet and outlet connections. As discussed in Section 3.1, tanks form end-conditions for loops.

Mass Conservation

Using the liquid mass balance equation for a volume containing a gas space over liquid inventory,

$$\ell A \frac{d\rho}{dt} + \rho A \frac{d\ell}{dt} + (w_i - w_o) + (w_i - w_o)^o = Q_{mass} - Q^o_{mass}. \qquad (3.17)$$

where ρ = liquid density

superscript o = steady state value

A = tank cross-sectional area

$w_i = \sum_k w_{ik}$ for a multiport configuration

We have to first generate a confluence equation similar to Eq. (3.6) for the non-separated volume from which "all" rules can be derived. Obviously, Eq. (3.17) is already in differential form so evidently the confluence is, using [$d\rho$] = -[dT] for "incompressible" water,

$$-[dT] + [d\ell] - \text{sign}\{(w_i - w_o) - (w_i - w_o)^o\}\,[dt] = \text{sign}(Q_{mass} - Q^o_{mass})\,[dt] \qquad (3.18)$$

This gives the following rules,

$$T_{\ell}^{/\uparrow}\ \ell^{\uparrow}\ w_i^{/\uparrow}\ w_o^{\uparrow} \rightarrow Q_{mass}^{\uparrow}$$

$$T_{\ell}^{/\uparrow}\ \ell^{\uparrow}\ w_i^{\downarrow}\ w_o^{-} \rightarrow Q_{mass}^{\uparrow}$$

and

$$T_{\ell}^{/\downarrow}\ \ell^{\downarrow}\ w_i^{/\downarrow}\ w_o^{\downarrow} \rightarrow Q_{mass}^{\downarrow}$$

$$T_{\ell}^{/\downarrow}\ \ell^{\downarrow}\ w_i^{\uparrow}\ w_o^{-} \rightarrow Q_{mass}^{\downarrow}$$

If we only have one inlet port and one outlet port the ℓ can be dropped from the L.H.S.

We also need rules to indicate Q_{mass}^{-}, namely that the component does not have a mass malfunction. For these rules the notation is that w_i, w_o is for any one of the ports in a multiport configuration. Using inferences from the momentum equation in the non-separated volumes connected to the separated volume, we have

$$w_i^{/-}\ p^{-} \rightarrow Q_{mass}^{-}$$

$$w_o^{/-}\ p^{-} \rightarrow Q_{mass}^{-}$$

The p's are for the separated gas volume while the ws are from the loop. We also have using the mass balance equation for the separated volume, initiating by turn a pressure disturbance within and without the volume and examining the resultant flow pattern, the rule,

$$T_\ell^- \; w_i^\uparrow \; w_o^\uparrow \rightarrow Q_{mass}^-$$

$$T_\ell^- \; w_i^\downarrow \; w_o^\downarrow \rightarrow Q_{mass}^-$$

It may be that the T_ℓ^- restriction can be relaxed but that requires further analyses.

Energy Conservation

Using the liquid energy balance equation for a volume containing a gas space over liquid inventory,

$$\frac{dmh}{dt} + (wh)_o - (wh)_i - ((wh)_o - (wh)_i)^o = Q_{eng} - Q_{eng}^o. \qquad (3.19)$$

where m = tank liquid mass.

We have to first generate a confluence equation similar to Eq. (3.6) for the non-separated volume from which "all" rules can be derived. Obviously Eq. (3.19) is already in differential form so evidently the confluence is

$$[dmh] + sign\{((wh)_o - (wh)_i) - ((wh_o) - (wh)_i)^o\}[dt] = sign(Q_{eng} - Q_{eng}^o)[dt] \quad (3.20)$$

On the outlet side, the simplification can be made that $h_o = h_\ell$ unless there is significant thermal stratification in the liquid pool. Using [dmh] = [dm] + [dh], [dh] = [dT] for an incompressible liquid and knowledge from the mass balance of Q_m^- gives the rules

$$T_\ell^{/-}\ w_i^-\ h_i^-\ w_o^- \rightarrow Q_{eng}^{/-}$$

$$T_\ell^{\uparrow}\ w_i^-\ h_i^{\downarrow}\ w_o^- \rightarrow Q_{eng}^{\uparrow}$$

$$T_\ell^{\downarrow}\ w_i^-\ h_i^{\uparrow}\ w_o^- \rightarrow Q_{eng}^{\downarrow}$$

As in the case of w_i, we use the shorthand notation $h_i = \Sigma\ w_i\ h_i / \Sigma\ w_i$ for a multiport configuration. We still need a Q_{eng}^- rule which is

$$T_\ell^-\ w_i^-\ h_i^-\ w_o^- \rightarrow Q_{eng}^-$$

3.2.3 CV Rules

CV rules infer the trend status of nonmeasured variables of a process component, based on the trends of other T-H variables and the Q status of the component. Essentially, we are using these rules to fill in the gaps in our knowledge of [w h p ℓ] so that we can fire the Q rules. We, therefore, try to translate and extrapolate available instrument readings by developing rules of the form:

T, ℓ, p trends → w trend

w_1 trend → w_n trend

and

T, ℓ, w trends → p trend

p_1 trend → p_n trend

In our diagnostic strategy with our Q rules, the diagnosis of the malfunction will be very difficult without at least one w signal. The optimum goal for developing the CV rules is to focus on rules which can infer the w trend.

We now discuss physical approximations to reduce the Q dependency on the LHS in certain CV rules [3-8]. We define it so that breaks never occur in junctions. Breaks only occur in pipes. Physically, a junction break would basically be impossible. Essentially then, a leak in a pipe very close to the junction would be our approximation of break problems with a junction. This removes the Q_{mass} dependency for CV rules involving junctions. We do not have to know Q^{-}_{mass} in a junction to apply the junction CV rules. In addition, the Q_{mom} dependency is not present in the mass or energy balance equations for a junction. So these corresponding CV rules will not contain Q_{mom} either. This also holds for some of the non-junction (pipe) rules. There will be no Q_{mom} term in the pipe CV rules for mass and energy. Normally, the ambient surrounding a pipe is at lower pressure than the pipe. So a break will lead only to outflow and not inflow. Since we stop the diagnostics at initiation of two-phase conditions, this means pipe breaks will not affect the enthalpy in the pipe. We therefore can make the approximation that the CV rules for pipe energy (enthalpy transport) will

not include the Q_{mass} dependencies. This will have to be re-examined in future cases if the ambient is not at lower pressures. However, the Q_{mass} dependency has to be present in the CV rules for the pipe mass transport. As with the junction, the Q_{mass} dependency is ignored for an active momentum component. It is assumed that breaks in these cases can also occur only at inlet and outlet piping. We follow below the taxonomy of Fig. 3.4.

3.2.3.1 Non-separated Volume

For the non-separated volume, we have CV rules derived from the EOS, mass conservation, momentum conservation and energy conservation.

Equation of State

For single-phase incompressible fluid,

$$T^{-} \rightarrow h^{-}$$

$$T\uparrow \rightarrow h\uparrow$$

$$T\downarrow \rightarrow h\downarrow$$

Mass Conservation

By reordering the terms in the mass conservation equation expressed in qualitative analysis form, Eq. (3.6), we can derive the following CV rules. These are grouped in Fig. 3.4 by junction or non-junction classes.

a) Non-Junction

There is a further subgrouping by generic component type. Hydraulic time constants are small, so there is some confidence in using $\leftrightharpoons$.[1] Q_{mom} does not appear in the conservation of mass equation so it is not required here.

For mass transport in a pipe using the confluence Eq. (3.6)

$$\bar{Q}_{mass} \quad \uparrow w_{up} \leftrightharpoons \uparrow w_{down}$$

$$\bar{Q}_{mass} \quad \bar{w}_{up} \leftrightharpoons \bar{w}_{down}$$

$$\bar{Q}_{mass} \quad \downarrow w_{up} \leftrightharpoons \downarrow w_{down}$$

For a valve/pump/filter/bearing/seal using the confluence Eq. (3.6)

[1] $\leftrightharpoons$ = the T-H variables such as w_{up} and w_{down} can be transposed.

$$w_{up}^{\uparrow} = w_{down}^{\uparrow}$$

$$w_{up}^{-} = w_{down}^{-}$$

$$w_{up}^{\downarrow} = w_{down}^{\downarrow}$$

For a HX using the confluence Eq. (3.6)

$$Q_{mass}^{-} \quad w_{up}^{\uparrow} = w_{a}^{\uparrow}$$

$$Q_{mass}^{-} \quad w_{up}^{-} = w_{a}^{-}$$

$$Q_{mass}^{-} \quad w_{up}^{\downarrow} = w_{a}^{\downarrow}$$

$$Q_{mass}^{-} \quad w_{down}^{\uparrow} = w_{a}^{\uparrow}$$

$$Q_{mass}^{-} \quad w_{down}^{-} = w_{a}^{-}$$

$$Q_{mass}^{-} \quad w_{down}^{\downarrow} = w_{a}^{\downarrow}$$

where w_a indicates the average mass flow rate through the heat exchanger.

b) Junction

We restrict ourselves to three-way junctions. The two possible configurations were shown in Figs. 3.6 and 3.7. Since liquid water is a very incompressible fluid, we have for configuration (a) the junction mass balance,

$$w_1 = w_2 + w_3 \tag{3.21}$$

The corresponding rules have been derived. However, they have currently not been found to be useful because of questions regarding proximity of instrumentation location to the junction.

For configuration (b) the junction mass balance is,

$$w_3 = w_1 + w_2 \tag{3.22}$$

The corresponding rules have also been derived. However, the junction rules have currently also not been found to be useful because of questions regarding proximity of instrumentation locations to the junctions.

Momentum Conservation

By reordering the terms in the qualitative analysis form, the momentum conservation equations, Eqs. (3.11) and (3.12), we can derive a number of CV rules. Following Fig 3.4, we have three classes;

general, active, and passive rules. General rules are component-independent rules. Q^{-}_{mom} is located between the instrument locations "up" and "down". The general rules are,

$$Q^{-}_{mom}\ p^{\uparrow}_{up} = p^{\uparrow}_{down}$$

$$Q^{-}_{mom}\ p^{-}_{up} = p^{-}_{down}$$

$$Q^{-}_{mom}\ p^{\downarrow}_{up} = p^{\downarrow}_{down}$$

a) Active

Across an active component using the confluence Eq. (3.14),

$$Q^{-}_{mom}\ \Delta p^{\downarrow} \rightarrow w^{\uparrow} \qquad Q^{-}_{mom}\ w^{\uparrow} \rightarrow \Delta p^{\downarrow}$$

$$Q^{-}_{mom}\ \Delta p^{\uparrow} \rightarrow w^{\downarrow} \qquad Q^{-}_{mom}\ w^{\downarrow} \rightarrow \Delta p^{\uparrow}$$

b) Passive

There is a subgrouping by junction or non-junction classes.

Non-Junction

Figure 3.4 shows an additional classification by generic component type.

Across an open valve/filter using the confluence Eq. (3.12),

$$Q^{-}_{mom}\,\Delta p^{\downarrow} \rightarrow w^{\downarrow} \qquad Q^{-}_{mom}\,w^{\downarrow} \rightarrow \Delta p^{\downarrow}$$

$$Q^{-}_{mom}\,\Delta p^{\uparrow} \rightarrow w^{\uparrow} \qquad Q^{-}_{mom}\,w^{\uparrow} \rightarrow \Delta p^{\uparrow}$$

Across a pipe using the confluence Eq. (3.12),

$$Q^{-}_{mass}\,Q^{-}_{mom}\,\Delta p^{\downarrow} \rightarrow w^{\downarrow} \qquad Q^{-}_{mass}\,Q^{-}_{mom}\,w^{\downarrow} \rightarrow \Delta p^{\downarrow}$$

$$Q^{-}_{mass}\,Q^{-}_{mom}\,\Delta p^{\uparrow} \rightarrow w^{\uparrow} \qquad Q^{-}_{mass}\,Q^{-}_{mom}\,w^{\uparrow} \rightarrow \Delta p^{\uparrow}$$

Junction

Currently, none have been found to be of use. Availability of instrumentation is the limiting factor.

Energy Conservation

For the single input/output port control volume shown in Fig. 3.8, rewriting Eq. (3.4) gives us the general energy conservation equation

$$Q_{eng} = w_a(h_{out}-h_{in}) = w_a\,c_p\,(T_{out}-T_{in})$$

where h_{in} and h_{out} are the control volume inlet and outlet enthalpy, respectively, c_p is the specific heat, and Q_{eng} is the energy source/sink term in the energy balance. Transforming Eq. (3.4) into a qualitative differential expression and solving for w_a on the cold side yields the confluence

$$[dQ_{eng}] + [dT_{in}] - [dT_{out}] = [dw_a] \; . \tag{3.23}$$

For the case where the energy source into the control volume is not increasing, the inlet temperature is not increasing, and the outlet temperature is increasing, the confluence infers that the flow rate is decreasing, represented through the rule:

$$\text{If } Q_{eng}^{/\uparrow} \text{ and } T_{in}^{/\uparrow} \text{ and } T_{out}, \text{ then } w_a^{\downarrow} \; .$$

Other CV rules for inference of w_a can be obtained by instantiating the quantities in the left-hand side of the confluence in Eq. (3.23) with different trend combinations. As indicated in Fig. 3.6, the two classes of CV rules are heated or non-heated.

a) Heated

We drop the Q^{-}_{mass} dependency from the rules presented here by making certain that the secondary Q_{mass} rule for a HX is always checked first. Heat transfer is defined as positive into the control volume. Additional notation is that $q^{+} \equiv$ heat into the control volume; $q^{-} \equiv$ heat out of the control volume. Using the confluence Eq. (3.23) we have

$\underline{q^+ \text{ or } q^-}$

$h^{\uparrow}_{out}\ w^{-}_{a}\ Q_{eng}^{-} \rightarrow h_{in}^{\uparrow}$

$h^{\downarrow}_{out}\ w^{-}_{a}\ Q_{eng}^{-} \rightarrow h_{in}^{\downarrow}$

$\underline{q^+}$

$h^{\downarrow}_{out}\ Q_{eng}^{/\downarrow}\ h_{in}^{/\downarrow} \rightarrow w^{\uparrow}_{a}$

$h^{\uparrow}_{out}\ Q_{eng}^{/\uparrow}\ h_{in}^{/\uparrow} \rightarrow w^{\downarrow}_{a}$

$h^{-}_{out}\ Q_{eng}^{\uparrow}\ h_{in}^{-} \rightarrow w^{\uparrow}_{a}$

$h^{-}_{out}\ Q_{eng}^{\downarrow}\ h_{in}^{-} \rightarrow w^{\downarrow}_{a}$

$\underline{q^-}$

$h^{\downarrow}_{out}\ Q_{eng}^{/\downarrow}\ h_{in}^{/\downarrow} \rightarrow w^{\downarrow}_{a}$

$h^{\uparrow}_{out}\ Q_{eng}^{/\uparrow}\ h_{in}^{/\uparrow} \rightarrow w^{\uparrow}_{a}$

$h^{-}_{out}\ Q_{eng}^{\uparrow}\ h^{-}_{in} \rightarrow w_{a}^{\downarrow}$

$h^{-}_{out}\ Q_{eng}^{\downarrow}\ h^{-}_{in} \rightarrow w_{a}^{\uparrow}$

$\underline{q^+ \text{ or } q^-}$

$h^{-}_{out}\ Q_{eng}^{-}\ h_{in}^{-} \rightarrow w^{-}_{a}$

$h^{-}_{out}\ w^{-}_{a}\ Q_{eng}^{-} \rightarrow h_{in}^{-}$

$w^{-}_{a}\ Q_{eng}^{-}\ h_{in}^{-} \rightarrow h^{-}_{out}$

We also use the rule that $h^{/-}_{in}$ indicates an upstream component malfunction unless the time window selected is too long and is greater than a closed loop transport time. A conclusion of $Q_{eng}^{/-}$ is really an indication of a secondary side malfunction. This could be a secondary side mass or momentum malfunction.

b) Non-Heated

The further subgrouping is by junction and non-junction.

Non-junction (pipe)

The notation is that up ≡ upstream and down ≡ downstream. For enthalpy transport in a pipe, we will need to add dynamic effects to the rules:

$\bar{h}_{up} \rightarrow \bar{h}_{down}$ no delay after TWS has accepted $\bar{h}_{up}$ is the correct trend

$\bar{h}'_{up} \rightarrow \bar{h}'_{down}$ after a delay of $\tau_{transport}$ seconds

Junction

The two different junction types are again shown in Fig. 3.9.

At junctions, we have for configuration (a) given in Fig. 3.9,

$$w_1 h_1 = w_2 h_2 + w_3 h_3 \tag{3.24}$$

For configuration (b), we have

$$w_3 h_3 = w_1 h_1 + w_2 h_2 \tag{3.25}$$

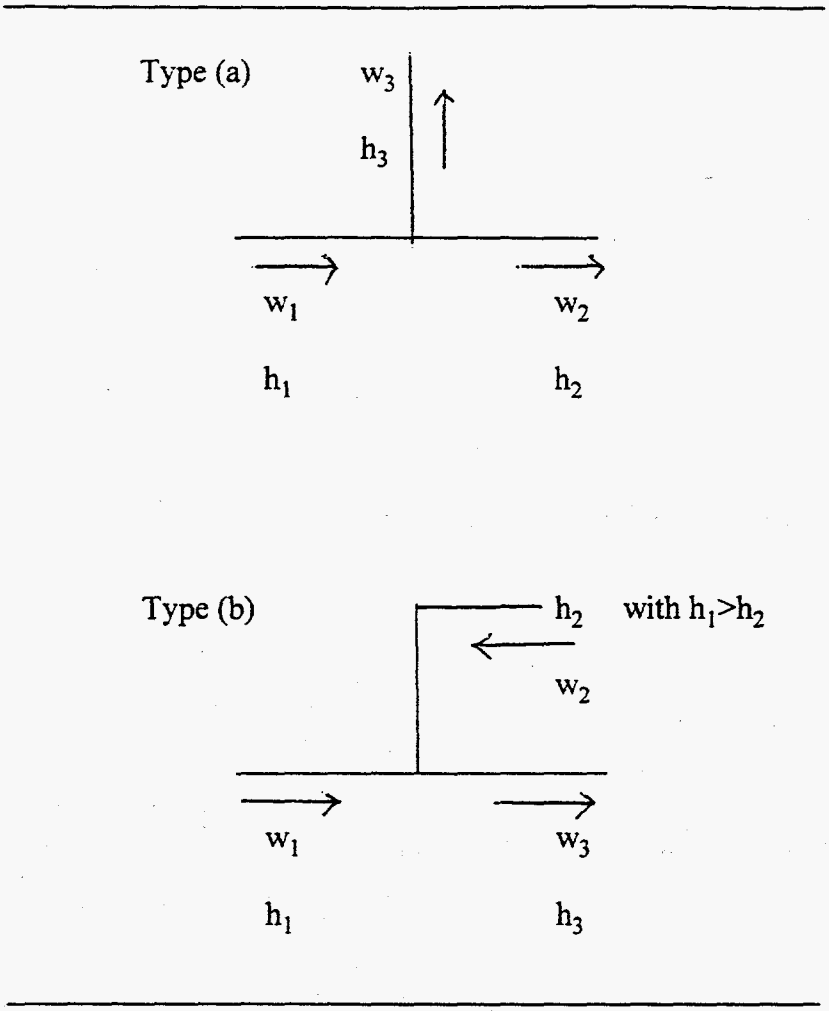

Fig. 3.9. Junction Configurations

The rules for both junction types have been derived. However, they have currently not been found to be useful because of questions regarding the proximity of instrumentation locations to the junctions.

3.2.3.2 Separated Volume

The Q state vector for the separated volume is [Q_{mass}, Q_{eng}, Q_{gas}]. The CV state vector is [$w_{in/out}$ h p ℓ]. We restrict the discussion of the separated volume component to tanks. A tank can have a number of inlet and outlet connections. The notation for the set of rules for a separated volume is that "i" indicates an average or a sum over all inlet connections (except for ICS connected to ECS), while "o" is an average or a sum over all outlet connections (except for ICS connected to ECS); "ℓ" = liquid, "g" = gas.

Mass Conservation

Using the mass balance equation, Eq. (3.17), we can derive from the corresponding confluence Eq. (3.18),

$$T_\ell^- \ \ell\uparrow \ Q^-_{mass} \ w_i^{/\uparrow} \rightarrow w_o^{\downarrow} \qquad T_\ell^- \ \ell^- \ Q^-_{mass} \ w_{in}^- \rightarrow w_o^-$$

$$T_\ell^- \ \ell\downarrow \ Q^-_{mass} \ w_i^{/\downarrow} \rightarrow w_o^{\uparrow} \qquad T_\ell^- \ \ell^- \ Q^-_{mass} \ w_o^- \rightarrow w_{in}^-$$

$$T_\ell^- \ \ell\uparrow \ Q^-_{mass} \ w_o^{/\downarrow} \rightarrow w_i^{\uparrow}$$

$$T_\ell^- \ \ell\downarrow \ Q^-_{mass} \ w_o^{/\uparrow} \rightarrow w_i^{\downarrow}$$

Additional rules have been derived for the multiport configuration, but these currently have not been found to be useful. Availability of instrumentation is the limiting factor.

Energy Conservation

Using the energy balance, Eq. (3.19), we can derive from the corresponding confluence Eq. (3.20),

$$T_\ell^{\uparrow}\ w_i^{-}\ Q_{eng}^{-}\ w_o^{-} \rightarrow h_i^{\uparrow}$$

$$T_\ell^{\downarrow}\ w_i^{-}\ Q_{eng}^{-}\ w_o^{-} \rightarrow h_i^{\downarrow}$$

$$T_\ell^{/-}\ h_i^{-}\ Q_{eng}^{-}\ w_o^{-} \rightarrow w_i^{/-}.$$

Additional rules are available, but availability of instrumentation has been found to be the limiting factor.

3.3 Component Classification Dictionary

We return to the diagnostic strategy tree of Fig. 3.3. The strategy is to break the T-H system up into "independent" generic classes of loops composed of sets of components and then to further break up the set of components into generic classes of component types. The bottom part of the tree is concerned with the decomposition into generic classes of components. This part of the tree is, therefore, the Component Classification Dictionary (CCD). As stated in Section 3.1 discussing the ES taxonomy, each branch point in the tree, where the branching into the different classes occurs, actually consists of formulae and criteria tests which in the ES are implemented as IF-THEN rules. These rules are the PRD rules. The previous section 3.2 derived these rules and filled out that part of the tree in Fig. 3.3. In this section, the different branches into the component classes are filled in with the generic component types. Figure 3.10 shows the lower part of the taxonomy tree of Fig.

3.3 with the generic components listed. This CCD is a living dictionary and as other types of components are processed, they will be assigned a location in the CCD. Obviously the classification of the components into predefined classes is governed by the PRD rules at each point in the tree. The definition of the components is thus directly derived from the conservation equations. Under the Q_{mass} components for non-separated volume, we have T-junction, break, and closed valve. As explained in Section 3.1, junctions are defined to be Q_{mass} sources or sinks. This allows loops to be considered separately and "independently" for the application of the Q_{mass} PRD rules even though the loops do hydraulically intersect at the junctions and are, therefore, hydraulically coupled. A "malfunctioning" junction then points the diagnosis in the direction of the intersecting loops. There are, however, different types of junctions. We limit the junction component used here to a T-junction. Other junction types such as the Y-junction have complicated pressure flow behavior involving venturi effects. These junctions would have to be defined as a separate generic component type at a later date. Physically speaking, a break is not a system component. However, defining a break as a component simplifies the malfunction search procedure significantly. By defining a break as a component the PID can be searched directly for the break location rather than having to maintain a predefined database of all possible break locations. A closed valve is naturally a mass source or sink as its T-H operating function is to either drain inventory from or inject inventory into a system. Its definition as a mass source or sink, however, does show that the initial mode of operation (i.e., closed) could affect the CCD definition of a component. There are a number of generic component subtypes for a closed valve. Figure 3.10 shows these subtypes at one level down. For the case of pressure operated relief valve (PORV), operating conditions are now used to further classify the PORV as either a mass source or a mass sink component depending upon the difference between the

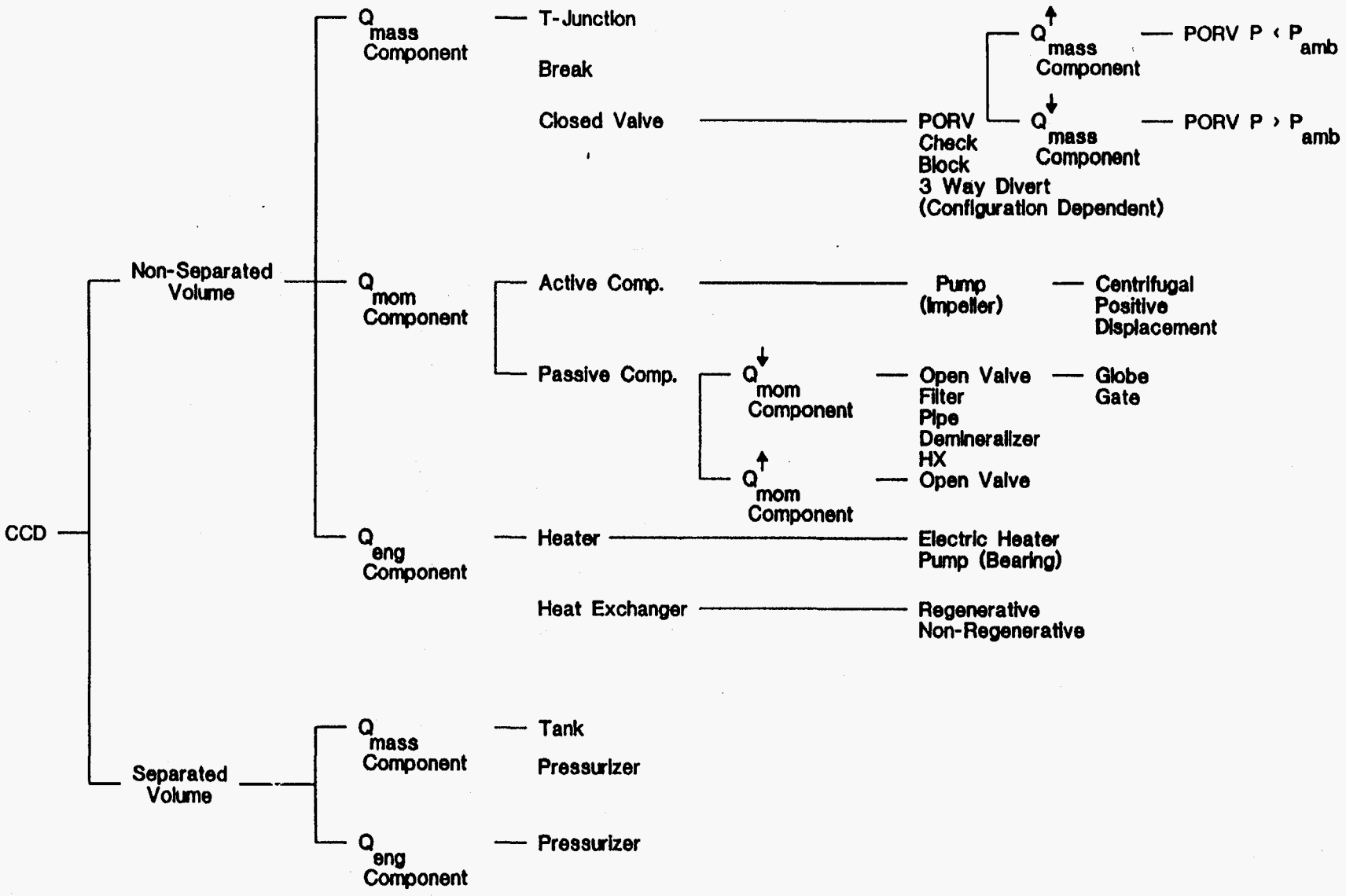

Fig. 3.10. Component Classification Dictionary

ambient pressure and the valve pressure. The operating pressure condition data has to be included in the PID if the distinction between source or sink to be made. The other closed valve type which has been observed to introduce complications for the diagnostic reasoning is the three-way divert valve. The CCD definition of the three-way divert valve appears to have a configuration dependence [3.9]. We prefer to avoid configuration dependence in the CCD if we can.

The three-way divert valve has two possible operating modes at initial steady state.

(a) Fully closed/open: This means that one outlet port is fully closed and the other outlet port is fully open.

(b) Partially closed/open: Both outlet ports are partially closed.

We do not consider mixing valves here which have the opposite function of the divert valves; mixing valves have two inlet ports and one outlet port. We start with mode (a), which is the easier mode to diagnose and is the mode which occurs most frequently. Figure 3.11 shows a configuration in which the end condition pressures are independent. The closed port connects to an ECS, so we do not use the $[w_3\ p_3]$ signals. Unlike the PORV when the closed port #3 opens, extra resistance is added to the open port #2, thereby closing it. We have two situations, depending upon the design values of p_3 and p_2.

For $p_3 > p_2$

$$w_1^{\uparrow}\ w_3^{\downarrow}\ p_3^{\downarrow}\ p_1^{\downarrow} \rightarrow \text{valve 'malfunctions'.}$$

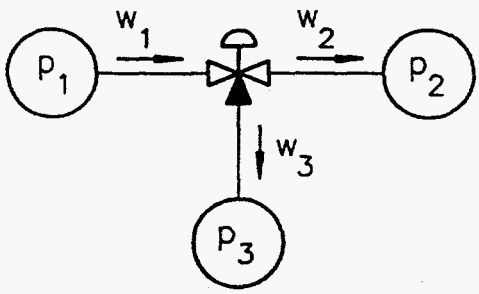

Fig. 3.11. Three-Way Divert Valve

For $p_2 > p_3$

$$w_1^{\downarrow}\ w_3^{\downarrow}\ p_3^{\downarrow}\ p_1^{\uparrow} \rightarrow \text{valve 'malfunctions'.}$$

By 'malfunction,' we mean opening/closing from initial position. By our definition, the three-way divert valve does not leak. From this behavior, we can deduce the following primary Q rules, which we are already currently using with measurements anywhere in the loop

$$w_1^{\uparrow}\ w_n^{\downarrow} \rightarrow Q_{mass}^{/-}$$

$$p_1^{\uparrow}\ p_n^{\downarrow} \rightarrow Q_{mom}^{/-}$$

and define in the CCD

Q_{mass} - three-way divert valve

-

Q_{mom} - three-way divert valve

we can detect a divert valve malfunction. The reason for this joint definition of the three-way divert valve in the CCD is that the design function of a three-way divert valve is to divert flow. Unlike a

PORV which clearly has a Q_{mass} function to increase or decrease system inventory, the divert function of a three-way divert valve could primarily be a Q_{mass} or a Q_{mom} effect depending upon the system T-H design. It is like opening and closing two separate valves simultaneously. Using the above procedure also allows us not to have to modify the Q^- rules for mass and momentum, viz

$$w_1^{\uparrow}\, w_n^{\uparrow} \rightarrow Q_{mass}^{-}$$

$$w_1^{\downarrow}\, w_n^{\downarrow} \rightarrow Q_{mass}^{-}$$

$$p_1^{\uparrow}\, p_n^{\uparrow} \rightarrow Q_{mom}^{-}$$

$$p_1^{\downarrow}\, p_n^{\downarrow} \rightarrow Q_{mom}^{-}$$

For the transients examined so far, it has been appropriate to use in the CCD,

— Q_{mass} — three-way divert valve only.

The secondary Q rule would be similar but not identical to that for a valve, i.e.,

$$\Delta p^{\uparrow}\; w_2^{\downarrow} \rightarrow Q_{mom}^{/-}$$

The partially open/closed valve at steady state, which is mode (b), is more difficult to analyze. Since we normally would not encounter this mode, we will leave it to a future date.

Figure 3.11 showed a configuration where the end condition pressures are independent. If the configuration was modified so that the two end condition pressures p_2 and p_3 are connected, for

example, through a junction, then additional complications arise. The end pressures are no longer independent. Figure 3.12 shows an example of such a configuration. If the divert valve is the malfunction initiator, then the potential difficulty that we have here is the possibility of two $Q^{/-}$'s masking each other. The divert valve malfunction is the initial malfunction, but the injection through the reconnected piping back into the loop at J3 could also be diagnosed as a malfunction. For this transient, $w_1^{\uparrow}$ $w_4^{\uparrow}$. Our rules would then say Q_{mass}^{-} between w_1 and w_4. What, of course, is happening is that $w_1^{\uparrow}$ $w_3^{\downarrow}$ $w_4^{\uparrow}$. There are two $Q_{mass}^{/-}$ occurring in the same loop. If we measured w_3, we would catch it with the divert valve rules. Some special PROLOG logic would have to be

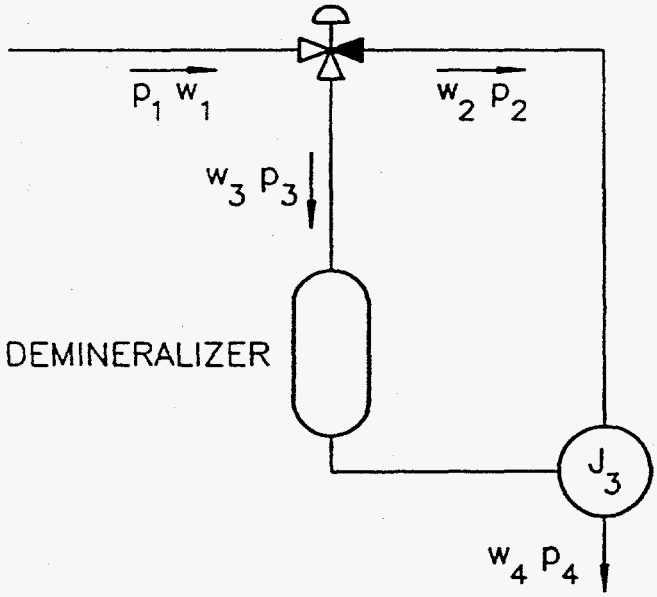

Fig. 3.12. Reconnected Looping with 3-way Divert Valve

written in a future version of PRODIAG to recognize the two $Q_{mass}^{/-}$ possibilities. However, if we do not measure w_3, we may have problems. We will have to rely on the $p_1^{\downarrow}$ $p_4^{\uparrow}$ divert valve rule discussed previously. This may mean that the CCD definition of a divert valve as possibly being $Q_{mom}^{/-}$ as well as $Q_{mass}^{/-}$ will be important here. Even if we do not measure the p's, since we draw

no conclusions if no rules fire, we will still have the possibility of $Q_{mom}^{/-}$ even if we rule out $Q_{mass}^{/-}$ on $w_l^{\uparrow}$ $w_h^{\uparrow}$. We may have to rely on secondary rules to diagnose three-way divert valve malfunctions. The other possibility is to accept the ambiguity of $Q_{mass}^{/-}$ or $Q_{mom}^{/-}$ when a three-way divert valve is involved.

The Q_{mom} components have been further subdivided into active components and passive components subclasses. This is to differentiate between pumps and the other components which can not provide a positive head. The passive components are divided into momentum sources and sinks. The only possible passive source of momentum is an open valve. The open valve could malfunction by opening further and increasing the momentum. As noted previously, the mode of steady-state operation does matter, so the closed valve is defined as a Q_{mass} component while the open valve is defined as a Q_{mom} component. Further classification into globe valves and gate valves is shown in Fig. 3.10 on the basis of large differences in generic valve characteristics. However, this differentiation has not yet been validated through testing. A similar comment can be made for the differentiation made in the CCD between centrifugal pumps and positive displacement pumps on the basis of pump head characteristics. Only two generic types of Q_{eng} components have been identified so far. These are heaters, where the energy input is through external sources and heat exchangers, where the energy input is through heat exchange between two thermal-hydraulic loops. The heat exchanger can be further divided into regenerative and non-regenerative types. Regenerative heat exchangers are so classified when the two heat-exchanging loops are hydraulically connected. Pump bearings produce heat through fluid friction rather than heat exchange and are, therefore, classified as heaters.

Separated volume components, up to this point, have been basically restricted to volumes where internal flow fields are not major factors in the component response. They are, therefore, essentially "end condition" volumes for loops. Examples are tanks and pressurizers. As such, there are, thus, no Q_{mom} components, just Q_{mass} and Q_{eng} components for the class of separated volume components.

3.4 Supervisory Flow Logic

Section 3.2 presented the PRD rules in a prescribed order. Figure 3.4 showed a classification tree structure for the rules. There are a number of rules and these can be grouped and arranged by set in a number of different ways. Various search orderings and arrangements could enhance the reliability of the component malfunction diagnostics and could optimize the speed of the diagnostics. Such an arrangement of the search procedure through the rules will be referred to as the supervisory flow logic.

Figure 3.13 presents an example of this supervisory flow logic. The ordering described here optimizes the reliability of the diagnosis by reducing the probability of a rule misfiring and leading to misdiagnosis. The particular arrangement is, however, not optimized by time performance. Other approaches for the supervisory flow logic are also possible. Volume 2, the PRODIAG Code Manual presents a different approach which was implemented practically using PROLOG. Section 3.2 showed that a minimum number of three variables is required to uniquely diagnose a Q_x malfunction where x = mass, momentum or energy. The supervisory flow logic, therefore, starts out with the $Q^{/-}$ rules which utilize three variables. This is the primary rules set (A) of Section 3.2. For this set, the

rules and the application of the rules are identical for open and closed loops. If the $Q_x^{/-}$ identification can be made at this point, the search in the PRD can be terminated and control of the flow logic is then sent to the search through the PID as detailed in Chapter 2. However, if insufficient signal information is available for three correlated variables, the supervisory flow logic then proceeds to search through primary PRD rule set (B). The rationale for this is that rule set (B) only utilizes two variables. So, if insufficient signal information is available for three variables, there is still the possibility of sufficient signal information being available for a unique $Q_x^{/-}$ identification to be made with the two variable rules. The entire supervisory flow logic is essentially constructed around the principle of searching rules with less signal information requirements later in the process. This should increase the reliability of the diagnostics and increase efficiency. Obviously, the conclusions regarding $Q_x^{/-}$, therefore, also become more ambiguous as the search proceeds down the chain. After primary rule set (B), the secondary $Q^{/-}$ rules for non-separated volumes, set (E), is then searched for a unique $Q_x^{/-}$ identification. The non-separated volume rules are searched before the separated volume rules, as non-separated volumes normally have smaller time constants than separated volumes, so their signal information should probably reach triggering thresholds in the TWS earlier. After set (E), the primary $Q^{/-}$ rules set (C) is then processed. The rules are alternatively referred to as "negative Q logic" as opposed to "positive Q logic" for all the other $Q^{/-}$ rules. The rules do not uniquely identify the $Q_x^{/-}$ malfunction. They point to two possibilities, and in the case of the open loop, also the third possibility of $Q_{EC}^{/-}$. The rules, however, do provide location information for the malfunction. Rule set (E), utilizing single-variable information, provides even more possibilities. However, the decoupling of $Q_{eng}^{/-}$ from $Q_{mom}^{/-}$ or $Q_{mass}^{/-}$ can be established to reduce these possibilities. Establishment of this decoupling is primarily due to the threshold settings on T deviations discussed in Section 3.2. Even if rules in the sets (C) and (D) fire the PRD search

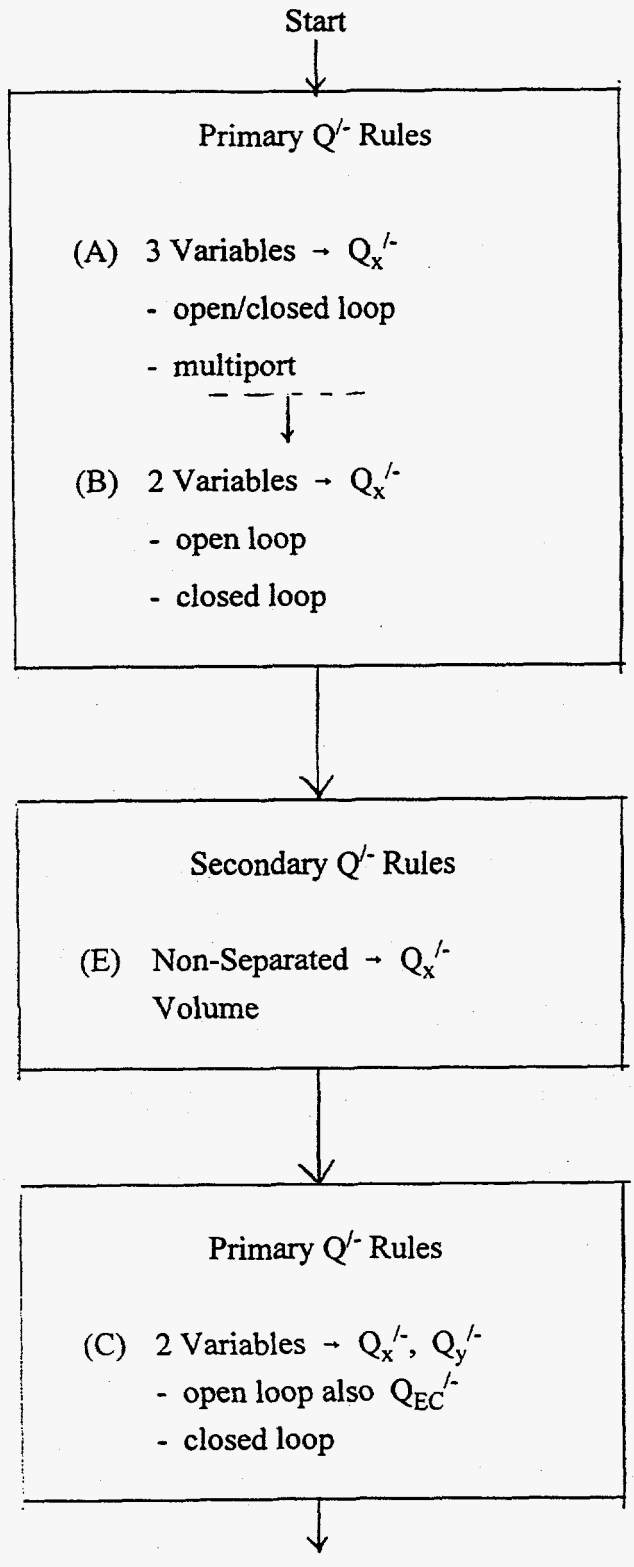

Fig. 3.13. PRD Supervisory Flow Logic

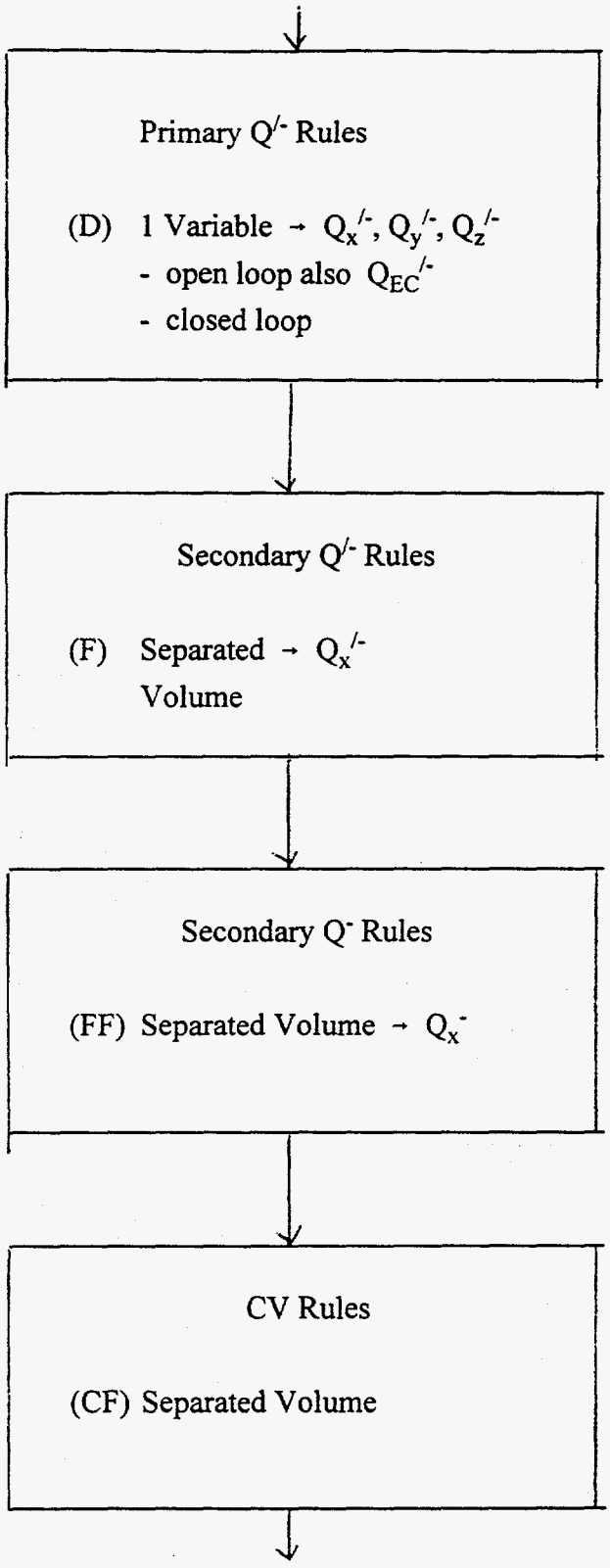

Fig. 3.13. PRD Supervisory Flow Logic (Cont'd.)

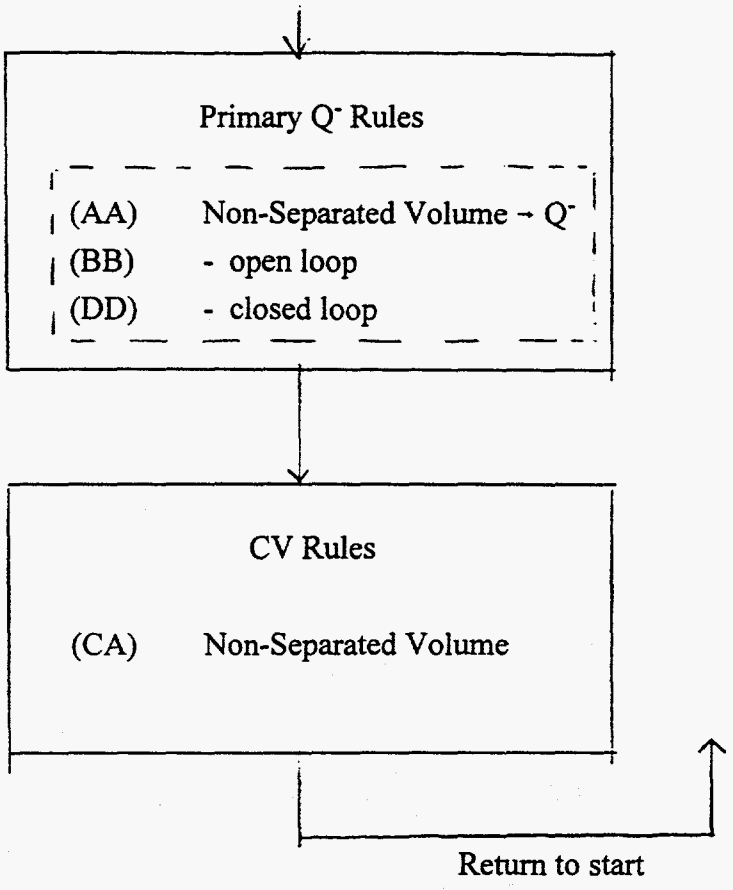

Fig. 3.13. PRD Supervisory Flow Logic (Cont'd.)

must continue as $Q_x^{/-}$ has not been uniquely identified. At this stage in the supervisory flow logic, we have used all the available information from the non-separated volumes in the loops and are now focussing on the separated volumes which form the end conditions for the loops. As mentioned earlier, this ordering is useful where the separated volumes have the longer time constants. The secondary $Q^{/-}$ rules, set (F), for the separated volume are used to try to identify $Q_x^{/-}$. If identification is made then the search returns to the PID. If identification is not made, then the process now becomes one of trying to fill in the gaps in the signal information. This means the CV rules will now have to be used. However, previous to the use of the CV rules, the Q^- status of components have to

be established. The next stage in the supervisory flow logic is to search the secondary Q^- rules for the separated volume, rule set (FF). The information from this stage is then used by the separated volume CV rules, (CF). After the separated volume CV rules are searched, the focus returns to the non-separated volumes. The primary Q^- rule sets, (AA), (BB), and (DD), are first searched for the non-separated volume by open loops and then by closed loops. The applications of these rules are different for the open loop vis a vis the closed loop, as discussed in Section 3.2. Once the Q^- status of the non-separated volume components are established, the CV rules for the non-separated volume are then searched. The supervisory flow logic then returns the control of the search to the start. Additional signal information is now available from the use of the rules to fill in the gaps. A second iteration through the $Q^{/-}$ rules is then made to try to identify the $Q_x^{/-}$. If this proves to be unsuccessful, the supervisory flow logic stops the search before the Q^- and CV rules are reentered.

REFERENCES

[3.1] T. Y. C. Wei, "Diagnostic/Control System Work," Memorandum to J. Reifman and L. L. Briggs, October 1989.

[3.2] Project Staff, "Combined Expert System/Neural Network for Process Fault Diagnosis," Annual Status Report for FY93 (September 1993).

[3.3] T. Y. C. Wei, "Reasoning Algorithm Framework for Combined Expert System/Neural Network for Process Fault Diagnosis," Memorandum to J. Reifman, February 20, 1993.

[3.4] J. Reifman and T. Y. C. Wei, "Systematic Construction of Qualitative Physics-Based Rules for Process Diagnostics," Proceedings of the 7th Portuguese Conference on Artificial Intelligence, pp. 311-322, Funchal, Madeira Island, Portugal, October 3-6, 1995.

[3.5] Project Staff, "Combined Expert System/Neural Network for Process Fault Diagnosis," Annual Status Report for FY94 (September 1994).

[3.6] T. Y. C. Wei, "Modifications to ES Rules Documented in FY93 Report for Generic Problem," Memorandum to J. Reifman, November 30, 1993.

[3.7] T. Y. C. Wei, "Second Pass Through ES Rules," Memorandum to J. Reifman, July 2, 1993.

[3.8] T. Y. C. Wei, "Clarification of Some Issues Relating to First PRODIAG Results," Memorandum to J. Reifman, December 1, 1993.

[3.9] T. Y. C. Wei, "Three-way Divert Valve and Reconnected Looping," Memorandum to J. Reifman, December 16, 1993.

4.0 COMPONENT LEVEL ANN DIAGNOSTICS

4.1 ANN Taxonomy

The hierarchy of ANNs continues the diagnostics where the ES leaves off with the utilization of more complex T-H "numerical" formulas [4.1]. In our approach we are building "parts-of-a-plant" models using ANNs. We use "numerical" in quotes because in our knowledge-base structure, neural networks are used first to perform a limited form of quantitative analysis before detailed mathematical simulation models are used to perform detailed quantitative analysis. This ordering is preferred because neural nets have more fuzziness to their pattern recognition ability than the mathematical models. In a sense, the ES qualitative analysis is even less precise. The ES only needs a signal trend (↑-↓). In principle, the numerical value of the signal derivative is not required by the ES. We become progressively more quantitative with the usage of the neural networks and look for increasing precision. As detailed in Chapter 1.0, the function of the ANN hierarchy in the diagnostic strategy is to perform component level diagnostics. However, as also discussed in Chapter 1.0, the line between the ES and the ANNs is not rigid. The ANNs can also be used to perform some plant-level diagnostics. During the actual implementation and testing of the ANN representations presented in this chapter, it was found possible to acquire only a limited amount of component-level ANN training data. Consequently, only a limited ANN diagnostics capability was actually implemented. This is described in Volume 3 on applications. The set of ANNs which was actually implemented is used to aid the ES in performing plant-level diagnostics. The assistance is given in helping the ES determine whether the malfunction is Q'^{-}_{mass} or Q'^{-}_{mom}.

There are many complicated T-H formulas. We basically want to back out Q' by using measured values of [w p h ℓ] in these formulas. In practice, it is difficult to do so because of the limited instrumentation locations. To back out [Q] from [w p h ℓ] for all possible faults would require many instrumentation locations. The inlet/exit of every component would probably have to be instrumented. This is the problem that previous constraint diagnostic methods have run into. We have to use first-principle physics knowledge here and not rely on brute force mathematics to solve the constraints problem. The solution is to use component characteristics or signatures. Each component has unique T-H signatures. However, the utilization of component characteristics in the diagnostic strategy depends upon the degree of resolution required and quality of instrument involved. By instrument quality, we basically mean time resolution. The structure of our diagnostic technique is to proceed from less time detail (i.e., trend analysis) and more spatial detail (i.e., plant-wide signals) to more time detail (i.e., more Fourier harmonics) and less spatial detail (i.e., individual component). The presence or absence of the component characteristic/signature from the signals should not depend upon the way or extent to which the component malfunctions. By using steady-state operating component characteristics/signatures, we can ignore the effect of component failure extent or component failure history (e.g., how fast and how deeply a malfunctioning valve is shut). Generic and specific steady-state operating component characteristics are to be identified by the ANNs in order to achieve this objective. An added advantage of this approach is that unlike other component-level pattern recognition strategies, we do not have to formulate a matrix of event cases for which malfunction training data are required every time there is a system change. Therefore, in the proposed approach there is no need to train the ANNs to map transient signals to associated component faults. However, it can be seen that our strategy does require component-by-component characteristics data and will, therefore, be T-H system configuration and operating-

condition specific for the ANN training. Unlike the ES which involved the quasistatic balance equations, not all differentiation "formulas" can be identified and implemented in advance of the specific T-H system application. This, therefore, calls for a modular programming approach with hooks put in place for future generic and specific components introduced by different T-H system applications.

As stated in Chapter 1.0 and shown in Fig. 1.2, there are two main questions which our diagnostic technique is structured to answer. In logical order, they are

(1) Which Q_x function, $Q_{mass}^{/-}$ or $Q_{mom}^{/-}$ or $Q_{eng}^{/-}$, is malfunctioning?

(2) Given the identification of the $Q_x^{/-}$, then

(a) which generic component is malfunctioning (e.g., valve or pump)?

Given the generic component,

(b) then which specific component is malfunctioning (e.g., valve A or valve B)?

The ES can answer all these questions if there is enough instrumentation. For less instrumentation, the neural network should be able to answer all these questions with more complicated formulas. But, there is still a minimum instrumentation requirement. For even less instrumentation, we would have to resort to mathematical model simulations with even more complicated formulas. However,

at each level in the diagnosis structure, the deduction may have larger uncertainties as we go from using the ES to the ANN to the FTRS (faster-than-real-time-simulator). This is because the "modelling" has to become more precise and the "model" input requirements become larger as we go from ES to FTRS (i.e., we have to have more quantification data). We now turn to detailing the ANN representations.

There are two preliminary issues:

(a) Deduction of $Q_{eng}^{/-}$ can basically be established by the ES. Typical instrumentation seems adequate for that. So, while some neural networks will be presented here for the $Q_{eng}^{/-}$ branch of the diagnostic tree, use of neural networks to deduce $Q_{eng}^{/-}$ will be limited.

(b) The concept of component characteristics requires definition. The T-H variables are [w p h ℓ]. For non-separated volumes, the hydraulic variables are [w p]. Component characteristics are almost like input-output relations in control theory. For our application, the functional input-output relationships are between one T-H variable and the other T-H variables for the component, e.g.,

$$w = f(p) \tag{4.1}$$

Time does not explicitly appear, but there are time effects which will be discussed later, i.e., w(t) = f(p(t)). In order to arrive at (4.1), one has to select the right set of variables, factor in the first-principles physics contained in the balance equations (2.10)-(2.12), conclude that the general formulas are very complicated, with a number of explicit time-dependent terms such as $\dot{p}$ and determine that more approximations are in order. The best approximations to make are to the time

dependence. In a sense, harmonic analyses are done and formulas are derived for the quasistatic and then for the higher frequency responses. In our technique, we divide each component characteristic in frequency space into two parts: (i) quasistatic; and (ii) higher frequencies. In the language of control theory, the component characteristics we utilize are transfer functions from different parts of the frequency response spectrum.

With these ground rules in mind, we move to the discussion of the specific neural network representations. These are grouped by the specific question in the diagnostic technique structure of Fig. 1.2 they are supposed to answer. The two main questions were listed above. The representations are basically cross-correlations in time systematically derived by using first-principles physics to arrive at the nondimensionalized ANN input groups of T-H variables. Section 4.2 answers the question of $Q_{mass}^{/-}$ or $Q_{mom}^{/-}$ or $Q_{ng}^{/-}$ determination with one Q_{mass} neural net representation and one Q_{eng} neural net representation. The section also answers the question of $Q_{mass}^{/-}$ or $Q_{mom}^{/-}$ determination with a number of quasistatic Q_{mom} neural net representations for both closed and open loop configurations. Section 4.3 addresses the question of identification of components. One neural net representation to differentiate between active and passive components for a specific configuration is discussed. Another neural net representation for PORV identification is presented using quasistatic discharge characteristics. One open valve neural net representation using higher frequency momentum characteristics is also discussed. Nondimensionalization of variables is used to aid in the generation of "generic" ANN topologies.

4.2 Q_x/- Determination

To determine whether the Q_x malfunction is Q_{mass}/- or Q_{nom}/- or Q_{eng}/-, we present two general subsets of ANN representations:

4.2.1 Q_{mass}/- and Q_{eng}/- Determination

We have lumped the two separate determinations of Q_{mass}/- and Q_{eng}/- together because we present a similar type of neural network representation for both for a separated volume. Non-separated volumes are discussed in Section 4.2.2. Conventionally speaking, the term "component characteristics" is normally only used in conjunction with the momentum equations. But it is used here in conjunction with the mass and energy balance equation so that a functional relation similar to Eq. (4.1) can be utilized. Figure 4.1 shows the configuration.

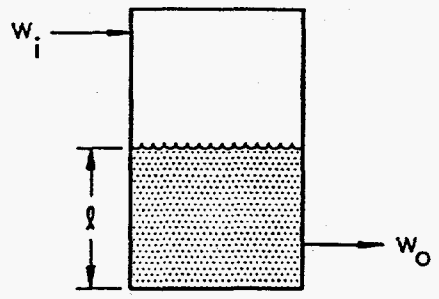

Fig. 4.1. Separated Volume Configuration

For a separated volume, we have the mass balance and energy balance equations

$$\frac{dm}{dt} = w_i - w_o + Q_{mass} \tag{4.2}$$

$$\frac{dmh}{dt} = w_i h_i - w_o h_o + Q_{eng} \tag{4.3}$$

Nondimensionalization of the mass equation (4.2) gives us [4.2], using initial steady state values

$$\frac{dm/m^o}{dt\ w_i^o/m^o} = \frac{w_i}{w_i^o} - \frac{w_o}{w_i^o} + \frac{Q_{mass}}{w_i^o} . \tag{4.4}$$

Rearranging

$$\frac{d\bar{m}}{d\bar{t}} - \bar{w}_i + \bar{w}_o = \frac{\bar{Q}_{mass}}{w_s} , \tag{4.5}$$

where the nondimensional quantities are

$$\bar{m} = m/m^o$$

$$\bar{t} = t w_s/m^o$$

$$\bar{w}_i = w_i/w_i^o \tag{4.6}$$

$$\bar{w}_o = w_o/w_i^o$$

$$\bar{Q}_{mass} = Q_{mass}/w_i^o$$

If we are focusing on a constant liquid density situation, the mass derivative can be replaced with the nondimensionalized level variable. We then have

$$\bar{\ell}'' - \bar{w}_i + \bar{w}_o = \bar{Q}_{mass} . \tag{4.7}$$

This can be looked upon as a functional relationship

$$\overline{Q}_{mass} = f(\bar{\ell}'', \overline{w}_i, \overline{w}_o) \ , \tag{4.8}$$

which can be expressed as the following neural network.

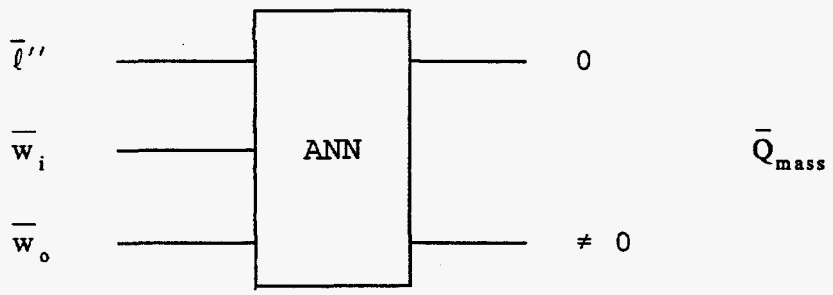

Since from Eq. (4.7) we know that this is a simple linear relationship, three sets of $\left[\bar{\ell}'' \ \overline{w}_i \ \overline{w}_o\right]$ points should be sufficient to define the plane in 3-D space. The ANN will be trained so that if during an actual transient the signal data gives a set of points which is not on the plane, then a non-zero ANN output value will result. This will then indicate that $Q^{/-}_{mass}$. Points on the plane result in an ANN output value of 0, indicating Q^{-}_{mass}. However, given measurement uncertainties and other possibilities within the ± 10% accuracy range, we may want to redefine the region of Q^{-}_{mass} to have some fuzziness in the region around the plane. This would then require more training data and perhaps even system-specific training data. One could also think of variations when, for example, there may be fuzziness if $\bar{\ell}''$ only has the values [↑-↓], but the $\overline{w}_i, \overline{w}_o$ have numerical values and so on. In summary, we have broken up the complete plant problem into parts. This part is the separated volume and, in essence, we are supplying boundary values $\bar{\ell}'' \ \overline{w}_0 \ \overline{w}_i$ to a physical model solver which is implemented in terms of a neural network.

One variation which should be discussed here is the fact that a separated volume (tank) with the mass balance equation, Eq. (4.2), is a natural integrator. It may also be difficult to obtain "smooth" numerical values, so Eq. (4.7) can be integrated to give

$$\bar{\ell} - \int \bar{w}_i dt + \int \bar{w}_o dt = \int \bar{Q}_{mass} dt \ , \tag{4.9}$$

which can be expressed in a neural net as

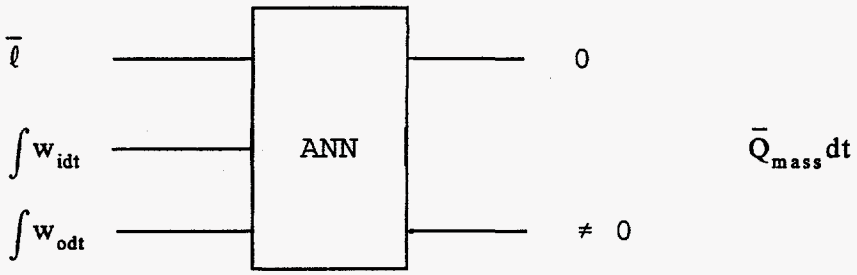

We can also rewrite Eq. (4.9) as a linear relationship

$$\int \bar{Q}_{mass}\, dt = f\left(\bar{\ell}, \int (\bar{w}_i - \bar{w}_o)\, dt\right) . \tag{4.10}$$

Since the TWS algorithm will stop the diagnostics if the behavior of Q_{mass} becomes nonmonotonic, we should be able to drop the integral for Q_{mass}, as there will then be a monotonic relationship between the Q_{mass} trend and the trend of its integral, and use the neural network

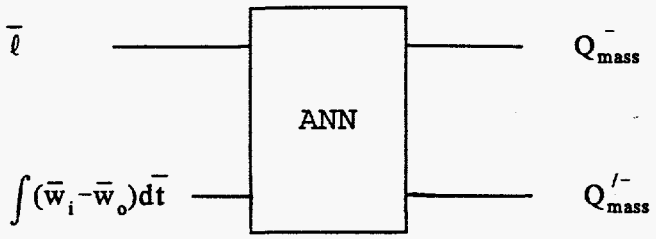

By choosing to use $(\bar{w}_i-\bar{w}_o)$ instead of $\bar{w}_i$ and $\bar{w}_o$ separately, we have reduced the number of independent variables in the choice of the neural network representation.

Similarly, we can express the neural net representation for the energy equation, Eq. (4.3), in functional form

$$\bar{Q}_{eng} = f\left(\overline{m\,h''}, \overline{w_i h_i}, \overline{w_o h_o}\right) \tag{4.11}$$

or

$$= f\left(\overline{m\,h''}, \bar{w}_i, \bar{h}_i, \bar{w}_o, \bar{h}_o\right) \tag{4.12}$$

or

$$= f\left(\bar{T}'', \bar{w}_i, \bar{h}_i, \bar{w}_o, \bar{h}_o\right) \tag{4.13}$$

where $T_{s\ell}$ (liquid saturation temperature) or $h_{s\ell}$ (liquid saturation enthalpy) of the separated volume are used in the nondimensionalization. These are the neural network representations which could be used if the ES PRD rules are unable to draw conclusions about Q_{mass} and Q_{eng}.

4.2.2 Q_{mass}/- or Q_{mom}/- Determination

For non-separated volumes in a loop connecting a pump and a valve, we can write the quasistatic momentum equation between two points 1 and 2 as

$$p_1 - p_2 + \Delta p_{pump} + k_{valve}\, w^2 + k_{pipe}\, w^2 = 0 \ . \tag{4.14}$$

To illustrate the approach, we only consider passive components and only the valve, in which case

$$p_1 - p_2 + k_{valve}\, w^2 = 0 \ . \tag{4.15}$$

Nondimensionalizing gives

$$\frac{p_1 - p_2}{\Delta p^{\circ}} + \frac{k_{valve}}{\Delta p^{\circ}} (w^{\circ})^2 \left(\frac{w}{w^{\circ}} \right)^2 = 0. \tag{4.16}$$

Using the qualitative analysis notation of Eq. (3.9), we define

$$\frac{1}{\overline{Q}_{mom}} = \frac{k_{valve} (w^{\circ})^2}{\Delta p^{\circ}} \ . \tag{4.17}$$

So, Eq. (4.17) becomes

$$-\overline{\Delta p} + \frac{\overline{w^2}}{\overline{Q}_{mom}} = 0 \ . \tag{4.18}$$

where

$$\overline{\Delta p} = (p_2 - p_1)/\Delta p^{\circ}$$

$$\overline{w} = w/w^{\circ}$$

Rearranging gives

$$\overline{Q}_{mom} = \frac{\overline{w}^2}{\overline{\Delta p}} \,. \tag{4.19}$$

We can also write

$$\overline{\Delta p} = \overline{w}^2 / \overline{Q}_{mom} \tag{4.20}$$

In general, for both active and passive hydraulic elements, this shows that

$$\overline{\Delta p} = f(\overline{w}, \overline{Q}_{mom}) \tag{4.21}$$

Since pressure drops are additive, the use of (4.21) can obviously be extended to the full equation, Eq. (4.14). We then have

$$\overline{\Delta p} = \sum_i \left(f_i(\overline{w}) \right) \tag{4.22}$$

where we have dropped the $\overline{Q}_{mom}$ for notational simplicity. We build a stand-alone-parts-of-a-plant model using neural networks instead of standard numerical simulation. But we are building these models to back the component characteristics $f_i(\overline{w})$ out of the instrumentation data. Comparisons with transient data through the use of these types of signal correlations could be more reliable than direct comparisons of individual signal time histories with the transient data.

For a plant model, the configuration geometry is important. There are two generic extremes for geometry: (i) open loop, and (ii) closed loop, with variations in between. We present here ANN representations which can be used for determining whether the malfunction is Q'_{mass} or

Q'_{mom} for specific examples of (i) and (ii) and also for combinations of open and closed loops.

4.2.2.1 Open Loop

We start with (i) the open loop, illustrated in Fig. 4.2. The two pressure end conditions are either boundary conditions or tanks (separated volumes). The following combinations of instrumentation may be present, as shown in Table 4.1.

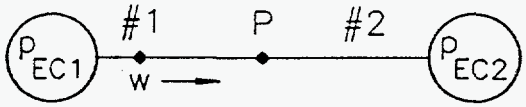

Fig. 4.2. Open Loop

Table 4.1. Possible Instrumentation

1 variable	2 variables
p w	pw pp ww

All combinations of three instruments or more can be formed from the combinations listed in Table 4.1. Going down the table, if we had p(t) or w(t) alone, we can not distinguish between Q'_{mass} or Q'_{mom} without having prior knowledge of the signal histories for the particular malfunction. The combination pp is already treated in the ES where we have,

$p\uparrow\ p\downarrow \rightarrow Q'^{-}_{mom}$ (ES rule already),

$p\uparrow\ p\uparrow$ or $p\downarrow\ p\downarrow \rightarrow Q^{-}_{mom}$ (ES rule already).

The only unique use for a neural network is to see if $p\uparrow\ p\uparrow$ or $p\downarrow\ p\downarrow$ says something about Q_{mass}. However, with quasistatic characteristics alone, this approach is not useful. The situation is similar with ww. The only possibility is the combination pw. Figure 4.2 is drawn with that combination in mind. The end conditions p_{EC1} and p_{EC2} are constant. Segment 1 is the segment between the end condition p_{EC1} and the p measurement. Segment 2 is the rest of the loop. We have the following pressure balances

$$p\text{-}p_{EC2} = p\text{-}p_{EC1} - (p_{EC2} - p_{EC1}) \tag{4.23}$$

$$= -\Delta p_1 - (p_{EC2} - p_{EC1}) = \Delta p \tag{4.24}$$

where the segment momentum characteristics

$$\Delta p_1 = f_1(w) \tag{4.25}$$

$$\Delta p_2 = f_2(w)$$

are the respective characteristics for segments 1 and 2 analogous to Eq. (4.20). Using these characteristics and plotting Eq. (4.24) and the segment 2 characteristic, we have Fig. 4.3.

The intersection of these two formulas gives the operating point. So, if there is a momentum malfunction in segment 1, the characteristics of segment 1 change and the Δp vs w plot traces out $f_2(w)$. If there is a malfunction in segment 2, the same plot traces out $-f_1(w) - (p_{EC2} - p_{EC1})$. This

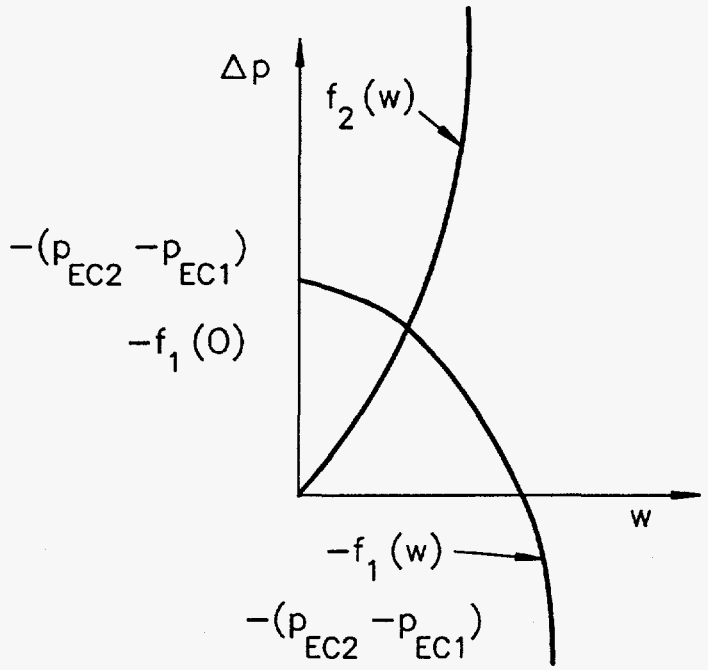

Fig. 4.3. Open Loop Characteristics

conclusion by itself does not add any inferences, since the two-variable [pw] rules in the ES would have drawn the same inference. However, if the malfunction is caused by a leak between p and w, as shown in Fig. 4.4, then the segment 1 characteristics change. Physically speaking, the segment 2 characteristics, pressure drop across the segment as a function of the flow through the segment does not change. However, mathematically speaking, since w is no longer equivalent to the physical flow through segment 2, the mathematical expression $f_2(w)$ will no longer represent the physical pressure drop across the segment. In this sense, the segment 2 characteristics "change." This means that a Δp vs w plot will be different from the initial unperturbed characteristics for both segments. This feature can, therefore, be used to deduce that the malfunction is $Q_{mass}{}^{/-}$ and not $Q_{mom}{}^{/-}$. This is used to produce the corresponding ANN representation shown in Table 4.2. The input/output relationship is between operating point trace and malfunction type.

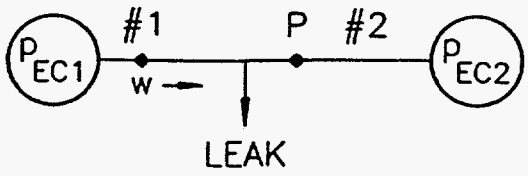

Fig. 4.4. Open Loop with Leak

Table 4.2. Neural Net Representation for Junctionless Open Loop with Constant Boundary Condition

Operating Point	Malfunction
(a) no motion	Q_{mass}^{-} Q_{mom}^{-}
(b) traces out $f_2(w)$	$Q_{mass}^{/-}$ upstream of w or $Q_{mom}^{/-}$ segment 1
(c) traces out $-f_1(w) - (p_{EC2} - p_{EC1})$	$Q_{mass}^{/-}$ or $Q_{mom}^{/-}$ segment 2
(d) none of the above	$Q_{mass}^{/-}$ between p and w segment 1

The method of component characteristics [4.3] can thus be seen as a method of comparing normal operating characteristics with the corresponding characteristic backed out of the transient data. This is a shape comparison. The output results from the ANN could be combined with the logic of the ES to better determine the malfunction location depending upon the location relative to the p and w measurements. We probably need a data uncertainty band. This neural network representation of input/output patterns uses the quasistatic momentum characteristic to narrow the diagnostic beyond the ES with the proper instrumentation location. We could use $\bar{w}^2$ instead of $\bar{w}$, but $\bar{w}$ is probably better for pump characteristics.

This representation which is limited to the configuration of Fig. 4.4 only works if p_{EC1}-p_{EC2} = constant. Changes in (p_{EC1}-p_{EC2}) would also trace out the $f_2(w)$ curve. This means that the end conditions have to be constant boundary conditions or large tank conditions (pressure ≈ constant).

An alternate technique which does not depend upon constant pressure boundary conditions but can be used with time dependent end pressure histories is to make more use of the loop symmetry. Figure 4.5 is the equivalent of Fig. 4.3, but now we define

$$\Delta_B p = -p + p_{EC1} \tag{4.26}$$

in addition to

$$\Delta_A p = p - p_{EC2} \tag{4.27}$$

used previously as Δp_2.

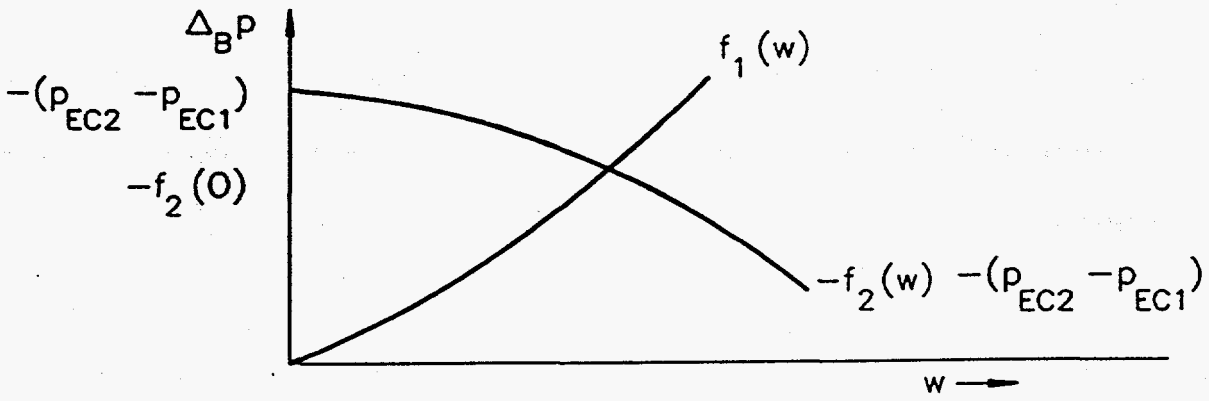

Fig. 4.5. Open Loop Mirror Characteristics

Using both Fig. 4.3 and Fig. 4.5, we arrive at the conclusions in Table 4.3, for malfunction identification.

Table 4.3. Neural Net Representation for Junctionless Open Loop

Malfunctions	Operating Point
(a) Q^{-}_{mass} Q^{-}_{mom}	No Motion
(b) Segment 1 $Q_{mass}^{/-}$ (upstream of w), $Q_{mom}^{/-}$	$\Delta_A p$ moves along $f_2(w)$ $\Delta_B p$ moves along $-f_2(w) - (p_{EC2}-p_{EC1})$
(c) Segment 2 $Q_{mass}^{/-}$, $Q_{mom}^{/-}$	$\Delta_A p$ moves along $-f_1(w) - (p_{EC2}-p_{EC1})$ $\Delta_B p$ moves along $f_1(w)$
(d) $Q^{/-}_{EC1}$, $Q^{/-}_{EC2}$ (changes in boundary conditions)	$\Delta_A p$ moves along $f_2(w)$ $\Delta_B p$ moves along $f_1(w)$
(e) Segment 1 $Q^{/-}_{mass}$ (between p and w)	$\Delta_A p$ does not move along $f_2(w)$, $-f_1(w) - (p_{EC2}-p_{EC1})$ $\Delta_b p$ does not move along $f_1(w)$, $-(p_{EC2}-p_{EC1}) - f_2(w)$

One can see from Table 4.3 that by using the two definitions of Δp one can identify boundary malfunctions. The ANN representation can also be used when the p_{EC}'s are non-separated volume variables and should be more useful for that case than for the case where the p_{EC}'s are separated volume variables.

But, even for open loops, the geometry can be much more complicated. Figure 4.6 shows the next step up in geometrical complication. It includes a junction. The configuration is divided into the segments shown in Fig. 4.6. The presence of the junction now changes the characteristics of segment #1 to

$$f_1(w) = w^2 \left(k_{1a} + k_{1b} \left(1 + \frac{w_3}{w} \right)^2 \right) \qquad (4.28)$$

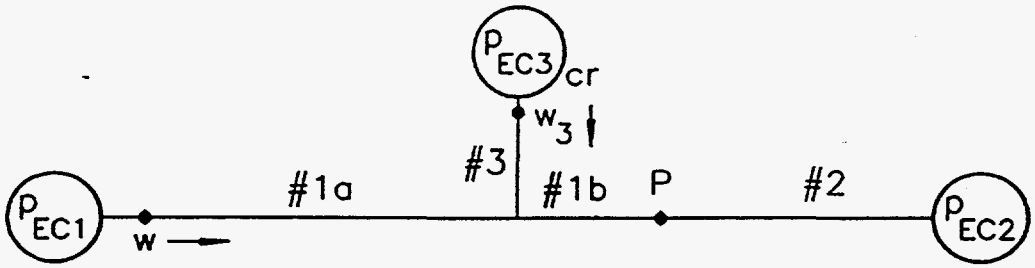

Fig. 4.6. Open Loop with Junction

The same technique/neural network representation used with Fig. 4.4 is used here except that $f_1(w)$ is now given by Eq. (4.28). In the case that w_3 is not measured but p_{EC3} is known instead, then we use the following addition to Eq. (4.28):

$$w_3 = \left[\frac{p_{EC3} - p_{EC1} - k_{1a} w^2}{k_3} \right]^{1/2} \tag{4.29}$$

Equation (4.29) gives the w_3 which is required in Eq. (4.28) for the equivalent segment #1 quasistatic momentum characteristics. It becomes more convenient at this stage to use the $f_i(w)$ notation in the mathematical description as implicit functional dependencies are now encountered.

Using the $f_i(w)$ notation for component characteristics and considering the case of two flow measurements w_1 ($\equiv$ w) and w_3, we have three momentum conservation equations:

$$p_{EC3} - p_{EC2} = f_3(w_3) + f_2(w_1 + w_3) \tag{4.30}$$

$$p_{EC1} - p_{EC2} = f_1(w_1) + f_2(w_1 + w_3) \tag{4.31}$$

$$p_{EC1} - p_{EC3} = f_1(w_1) - f_3(w_3) \tag{4.32}$$

where the one mass balance equation

$$w_2 = w_1 + w_3 \tag{4.33}$$

has been used to eliminate w_2. The set of momentum equations constitute three curves in $w_1 w_3$ space intersecting at one point, the operating point. The curves will be denoted as curves 1-3 in the order of the momentum equations (4.30) - (4.32). Table 4.4 enumerates the list of potential malfunctions, Q_{mass} (mass failure), Q_{mom} (momentum failure) and boundary conditions (p_{EC1}, p_{EC2}, p_{EC3}) changes. Our technique of component characteristics tracks the movement of the operating point when a malfunction occurs. The success of the techniques depends upon selecting the appropriate "measurable" variable space (in this configuration $w_1 w_3$) where the operating point will trace out the steady state momentum characteristic "f" curves [in this case Eqs. (4.30) - (4.32)]. Table 4.5 summarizes the movement of the operating point along the "f" curves for each malfunction. The malfunction numbers correspond to those in Table 4.4. Momentum failure in segment 1, which is malfunction 1 of Table 4.4, causes a change in the $f_1(w_1)$ characteristic. This then changes curves 2 and 3 since Eqs. (4.31) and (4.32) change. The only curve which does not change is curve 1. This means, just as in the previous junctionless open loop configuration, that the operating point in w_1 w_3 space traces out curve 1 as it is the only non-changing curve. Curve 1 is therefore the operating point trace in this space for malfunction 1. The operating point trace for the other malfunctions in Table 4.5 can be similarly derived. The group identifier is required because there are overlaps between operating point traces for different malfunctions. This ambiguity or non-uniqueness reduces the degree of malfunction resolution, as an operating point trace could then correspond to a number of potential malfunctions within a group. Table 4.6 summarizes all of this in the proposed ANN representation for the one junction open loop configuration.

Table 4.4. Potential Malfunctions for One Junction Open Loop

	Malfunction
1.	Momentum failure in segment 1.
2.	Momentum failure in segment 2.
3.	Momentum failure in segment 3.
4.	Mass failure in segment 1 upstream of the w_1 measurement.
5.	Mass failure in segment 2.
6.	Mass failure in segment 3 upstream of the w_3 measurement.
7.	Mass failure in segment 1 downstream of the w_1 measurement.
8.	Mass failure in segment 3 downstream of the w_3 measurement.
9.	End condition p_{EC1} malfunction.
10.	End condition p_{EC2} malfunction.
11.	End condition p_{EC3} malfunction.

Table 4.5. Operating Point Trace for One Junction Open Loop Malfunction

Malfunction	Operating Point Trace w_1w_3 Space	Group
1	Curve 1 since f_1 changes	I
2	Curve 3 since f_2 changes	III
3	Curve 2 since f_3 changes	II
4	Curve 1 since f_1 changes and w_1 measurement still correct	I
5	Curve 3 since f_2 changes	III
6	Curve 2 since f_3 changes and w_2 measurement still correct	II
7	Out (outside the three curves) as f_1 changes but w_3 measurement is incorrect	IV
8	Out as f_3 changes but w_3 measurement is incorrect	IV
9	Curve 1 since the other two curves change	I
10	Curve 3 since the other two curves change	III
11	Curve 2 since the other two curves change	II

Table 4.6. Neural Net Representation for One Junction Open Loop with Two Flow Measurements

Group	Failure	Operating Point in w_1w_3 Space
(I)	1,4,9	Curve 1
(II)	3,6,11	Curve 2
(III)	2,5,10	Curve 3
(IV)	7,8	Out

If, instead of the two flow measurements, one pressure measurement, p, and one flow measurement, w_1, were available in the one junction open loop configuration of Fig. 4.6, the situation becomes more complicated. We want to start with the pw_1 space so the momentum equations to start with are

$$p_{EC1} - p = f_{1a}(w_1) + f_{1b}(w_1+w_3) \tag{4.34}$$

$$p_{EC3} - p = f_3(w_3) + f_{1b}(w_1+w_3) \tag{4.35}$$

$$p - p_{EC2} = f_2(w_1+w_3) \tag{4.36}$$

The notation is that the momentum characteristics of segment 1a and 1b are $f_{1a}(w_1)$ and $f_{1b}(w_1+w_3)$, respectively. The mass balance equation is the same as Eq. (4.33). Rearrangement of these equations to solve for w_3 gives multiple sets of two momentum equations and a "w_3" equation. The first set of two momentum equations and a w_3 equation is,

$$p_{EC1} - p = f_{1a}(w_1) + f_{1b}(w_1+w_3) \tag{4.37}$$

$$p_{EC1} - p = p_{EC1} - p_{EC2} - f_2(w_1+w_3) \tag{4.38}$$

$$f_3(w_3) = f_{1a}(w_1) - p_{EC1} + p_{EC3} \tag{4.39}$$

The two momentum equations in this first set then give curves (1) and (2) in $(p_{EC1}\text{-}p)w_1$ space. The second set of two momentum equations and a w_3 equation is,

$$p - p_{EC2} = f_2(w_1+w_3) \tag{4.40}$$

$$p - p_{EC2} = p_{EC1} - p_{EC2} - f_{1a}(w_1) - f_{1b}(w_1+w_3) \tag{4.41}$$

The w_3 equation is the same as Eq. (4.39)

$$f_3(w_3) = f_{1a}(w_1) - p_{EC1} + p_{EC3} \tag{4.42}$$

The two momentum equations in this second set then give curves (3) and (4) in $(p_{EC2}\text{-}p)w_1$ space. The third set of two momentum equations and a w_3 equation is,

$$p_{EC3} - p = f_3(w_3) + f_{1b}(w_1+w_3) \tag{4.43}$$

$$p_{EC3} - p = p_{EC3} - p_{EC2} - f_2(w_1+w_3) \tag{4.44}$$

The w_3 equation is the same as Eq. (4.39)

$$f_3(w_3) = f_{1a}(w_1) - p_{EC1} + p_{EC3} \tag{4.45}$$

The two momentum equations in the third set then give curves (5) and (6) in $(p_{EC3}\text{-}p)w_1$ space. The fourth set of two momentum equations and a w_3 equation is,

$$p - p_{EC2} = f_2(w_1+w_3) \tag{4.46}$$

$$p - p_{EC2} = p_{EC3} - p_{EC2} - f_3(w_3) - f_{1b}(w_1+w_3) \tag{4.47}$$

The w_3 equation is the same as Eq. (4.39)

$$f_3(w_3) = f_{1a}(w_1) - p_{EC1} + p_{EC3} \tag{4.48}$$

The two momentum equations in this fourth set then give curves (7) and (8) in $(p-p_{EC2})w_1$ space. It can be seen that Eqs. (4.46)-(4.48) duplicate Eqs. (4.40)-(4.42). Curves (7) and (8) are therefore the same as curves (3) and (4) and are hence redundant. The fifth set of two momentum equations and a w_3 equation is,

$$p_{EC1} - p = f_{1a}(w_1) + f_{1b}(w_1+w_3) \tag{4.49}$$

$$p_{EC1} - p = p_{EC1} - p_{EC2} - f_2(w_1+w_3) \tag{4.50}$$

$$f_3(w_3) + f_2(w_1+w_3) + f_{1b}(w_1+w_3) = p_{EC3} - p_{EC2} \tag{4.51}$$

The two momentum equations in this fifth set then give curves (9) and (10) in $(p_{EC1}-p)\ w_1$ space. The sixth set of two momentum equations and a w_3 equation is,

$$p - p_{EC2} = f_2(w_1+w_3) \tag{4.52}$$

$$p - p_{EC2} = p_{EC1} - p_{EC2} - f_{1a}(w_1) - f_{1b}(w_1+w_3) \tag{4.53}$$

The w_3 equation is the same as Eq. (4.51)

$$f_3(w_3) + f_2(w_1+w_3) + f_{1b}(w_1+w_3) = p_{EC1} - p_{EC2}$$

The two momentum equations in this sixth set then give curves (11) and (12) in $(p-p_{EC2})w_1$ space. The seventh set of two momentum equations and a w_3 equation is,

$$p_{EC1} - p = f_{1a}(w_1) + f_{1b}(w_1+w_3) \tag{4.54}$$

$$p_{EC1} - p = f_3(w_3) - f_{1b}(w_1+w_3) + p_{EC1} - p_{EC3} \tag{4.55}$$

The w_3 equation is the same as Eq. (4.51)

$$f_3(w_3) + f_2(w_1+w_3) + f_{1b}(w_1+w_3) = p_{EC1} - p_{EC2}$$

The two momentum equations in this seventh set then give curves (13) and (14) in $(p_{EC1}-p)\ w_1$ space. It can be seen that Eqs. (4.49)-(4.51) duplicate this seventh set of equations. Curves (13) and (14) are therefore the same as curves (9) and (10) and are therefore redundant. The eighth set of two momentum equations and a w_3 equation is,

$$p_{EC3} - p = f_3(w_3) + f_{1b}(w_1+w_3) \tag{4.56}$$

$$p_{EC3} - p = f_{1a}(w_1) + f_{1b}(w_1+w_3) - p_{EC1} + p_{EC3} \tag{4.57}$$

The w_3 equation is the same as Eq. (4.51)

$$f_3(w_3) + f_2(w_1+w_3) + f_{1b}(w_1+w_3) = p_{EC1} - p_{EC2}$$

The two momentum equations in this eighth set then give curves (15) and (16) in (p_{EC3}-p) w_1 space.

The ninth set of two momentum equations and a w_3 equation is,

$$p_{EC3} - p = f_3(w_3) + f_{1b}(w_1+w_3) \tag{4.58}$$

$$p_{EC3} - p = p_{EC3} - p_{EC2} - f_2(w_1+w_3) \tag{4.59}$$

$$f_{1b}(w_1+w_3) + f_2(w_1+w_3) = p_{EC1} - p_{EC2} - f_{1a}(w_1) \tag{4.60}$$

The two momentum equations in this ninth set then give curves (17) and (18) in (p_{EC3}-p) w_1 space.

The tenth set of two momentum equations and a w_3 equation is,

$$p - p_{EC2} = f_2(w_1+w_3) \tag{4.61}$$

$$p - p_{EC2} = p_{EC3} - p_{EC2} - f_3(w_3) - f_{1b}(w_1+w_3) \tag{4.62}$$

The w_3 equation is the same as Eq. (4.60)

$$f_2(w_3+w_1) + f_{1b}(w_1+w_3) = p_{EC1} - p_{EC2} - f_{1a}(w_1)$$

The two momentum equations in this tenth set then give curves (19) and (20) in (p_{EC2}-p)w_1 space.

The eleventh set of two momentum equations and a w_3 equation is,

$$p_{EC1} - p = f_{1a}(w_3) + f_{1b}(w_1+w_3) \tag{4.63}$$

$$p_{EC1} - p = f_3(w_3) + f_{1b}(w_1+w_3) + p_{EC1} - p_{EC3} \tag{4.64}$$

The w_3 equation is the same as Eq. (4.60)

$$f_2(w_3+w_1) + f_{1b}(w_1+w_3) = p_{EC1} - p_{EC2} - f_{1a}(w_1) \quad (4.65)$$

The two momentum equations in this eleventh set then give curves (21) and (22) in $(p_{EC1}-p)w_1$ space. The twelfth set of two momentum equations and a w_3 equation is,

$$p_{EC3} - p = f_3(w_3) + f_{1b}(w_1+w_3) \quad (4.66)$$

$$p_{EC3} - p = f_{1a}(w_1) + f_{1b}(w_1+w_3) - p_{EC1} + p_{EC3} \quad (4.67)$$

This w_3 equation is the same as Eq. (4.60)

$$f_2(w_3+w_1) + f_{1b}(w_1+w_3) = p_{EC1} - p_{EC2} - f_{1a}(w_1) \quad (4.68)$$

The two momentum equations in this twelfth set then give curves (23) and (24) in $(p_{EC3}-p)w_1$ space. It can be seen that Eqs. (4.66)-(4.68) duplicate Eqs. (4.58)-(4.60). Curves (23) and (24) are therefore the same as curves (17) and (18) and are hence redundant.

What we have presented above is essentially a projection of an operating point in multidimensional space onto several two-dimensional spaces. This projection should enable us to correlate certain malfunctions with tracking motion of the operating point along known combinations of f(w)s from the steady state operating data. Table 4.7 enumerates the list of possible malfunctions. Table 4.8 summarizes the movement of the operating point along the "f" curves for each malfunction listed in Table 4.7. The two-dimensional space for each of the curves is listed by columns. Since three different "w_3" equations are used to substitute for w_3 in the momentum equations, the corresponding

Table 4.7. Potential Malfunctions for One Junction Open Loop with One Pressure and One Flow Measurement

	Malfunction
1.	End condition p_{EC3} malfunction
2.	End condition p_{EC1} malfunction
3.	Momentum failure in segment 1a
4.	Momentum failure in segment 3
5.	Mass failure in segment 3
6.	Mass failure in segment 1b
7a.	Mass failure in segment 1a downstream of w_1 measurement
7b.	Mass failure in segment 1a upstream of w_1
8.	Momentum failure in segment 2
9.	Mass failure in segment 2
10.	End condition p_{EC2} malfunction
11.	Momentum failure in segment 1b

Table 4.8. Operating Point Trace for One Junction Open Loop with One Pressure and One Flow Measurement

Malfunction	Operating Point Trace			Group
	"w_3" Eq. (4.39) Space			
	p_{EC1}-p	p-p_{EC2}	p_{EC3}-p	
1	out	out	out	V
2	out	out	out	VI
3	out	out	out	II
4	out	out	out	III
5	out	out	out	III
6	out	out	out	IV
7a	out	out	out	IV
7b	out	out	out	II
8	curve 1	curve 4	curve 5	I
9	curve 1	curve 4	curve 5	I
10	curve 1	curve 3	curve 5	VII
11	curve 2	curve 3	curve 6	VIII

Table 4.8. Operating Point Trace for One Junction Open Loop with One Pressure and One Flow Measurement (Cont'd)

Malfunction	Operating Point Trace			Group
	"w_3" Eq. (4.51)			
	p_{EC1}-p	p-p_{EC2}	p_{EC3}-p	
1	out	out	out	V
2	curve 9	curve 11	curve 15	VI
3	curve 10	curve 11	curve 15	II
4	out	out	out	III
5	out	out	out	III
6	out	out	out	IV
7a	out	out	out	IV
7b	curve 10	curve 11	curve 15	II
8	out	out	out	I
9	out	out	out	I
10	out	out	out	VII
11	out	out	out	VIII

Table 4.8. Operating Point Trace for One Junction Open Loop with One Pressure and One Flow Measurement (Cont'd)

Malfunction	Operating Point Trace			Group
	"w_3" Eq. (4.60)			
	p_{EC3}-p	p-p_{EC2}	p_{EC1}-p	
1	curve 17	curve 19	curve 21	V
2	out	out	out	VI
3	out	out	out	II
4	curve 18	curve 19	curve 21	III
5	curve 18	curve 19	curve 21	III
6	out	out	out	IV
7a	out	out	out	IV
7b	out	out	out	II
8	out	out	out	I
9	out	out	out	I
10	out	out	out	VII
11	out	out	out	VIII

equation numbers are also listed by column to accurately define the two-dimensional space projection. The proposed ANN representation resulting from Table 4.8 for the one junction open loop is shown in Table 4.9. The table shows the groups of malfunctions which can be identified by a common operating point trace when w_1 and p are measured.

Table 4.9. Neural Net Representation for One Junction Open Loop with One Pressure and One Flow Measurement

	Operating Point in Two-Dimensional Space		
Group Failures	w_3 Eq. (4.39)	w_3 Eq. (4.51)	w_3 Eq. (4.60)
(I) 8,9	curves 1, 4, 5	out	out
(II) 3,7b	out	curves 10, 11, 15	out
(III) 4,5	out	out	curves 18, 19, 21
(IV) 6,7a	out	out	out
(V) 1	out	out	curves 17, 19, 21
(VI) 2	out	curves 9, 11, 15	out
(VII) 10	curves 1, 3, 5	out	out
(VIII) 11	curves 2, 3, 6	out	out

4.2.2.2 Closed Loop

We now turn to the closed loop shown in Fig. 4.7. A closed loop must have a pump in it, otherwise the flows will not be in the same direction, and that would violate our definition of a loop. Once again, as in the case of the open loop, the instrumentation combination we start off with from Table 4.1 is pw.

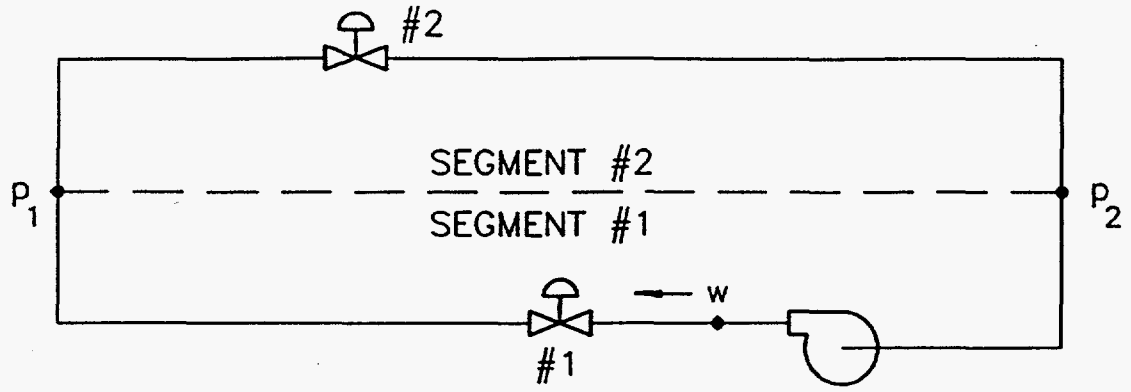

Fig. 4.7. Closed Loop

With the instrument combination pw, using momentum characteristics such as Eqs. (4.20) and (4.21) in the quasistatic momentum balance equation around the loop with w only gives the test whether or not $\Delta p = 0(?)$. There is no tie-in between p and w if only quasistatic momentum characteristics/ balances are used; the combination pw is insufficient to answer the question of $Q_{mass}^{/-}$ or $Q_{mom}^{/-}$. If the test formula $\Delta p = 0(?)$ is used, calculations show that we can not distinguish, based on $\Delta p \lessgtr 0$, between $Q_{mass}^{/-}$ and $Q_{mom}^{/-}$ or even between passive and active momentum element failure. We need one more instrumentation location.

The two additional possibilities are ppw or pww. We start with ppw. For those transients where the trends are too ambiguous to be used by the ES rules, we utilize the ANN with the Δpw instrument combination. This is just as in the case of the open loop. Consider Fig. 4.7 where we have,

$$\Delta p = p_1 - p_2 \tag{4.69}$$

The momentum characteristics of the two segments 1 and 2 are,

$$f_1(w) = f_{pump}(w) + k_1 w^2 \tag{4.70}$$

$$f_2(w) = k_2 w^2 \tag{4.71}$$

Momentum balance between the two segments gives

$$\Delta p \quad = -f_1(w) \quad = f_2(w) \tag{4.72}$$

When Eqs. (4.70)-(4.71) are plotted in Fig. 4.8 for the operating point in Δpw space, we have the closed loop equivalent of Fig. 4.3 for the open loop. The same technique used for the open loop is applied ending up with the same ANN representation which is shown in Table 4.10. Q_{mass} failures are not accounted for in the representation since a Q_{mass} failure will quickly drive the closed loop of Fig. 4.7 into two-phase conditions. Two-phase conditions are currently outside the limits of the diagnostic system.

We could instead use the secondary ES Q rules for the active element and the passive element here to perform the inference. It may be possible to apply the active element (pump) secondary ES Q rule across segment 1. However, the neural net representation has the potential advantage of identifying

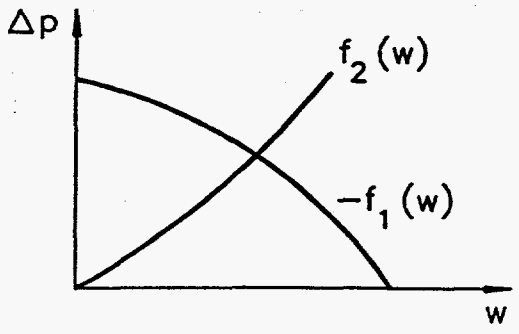

Fig. 4.8. Closed Loop Characteristics

Table 4.10. Neural Net Representation for Junctionless Closed Loop

Malfunction	Operating Point Trace
1) Q^{-}_{mom}	No motion
2) Segment 1 $Q^{/-}_{mom}$	Moves along curve $f_2(w)$
3) Segment 2 $Q^{/-}_{mom}$	Move along curve $-f_1(w)$

a possible $Q_{mass}^{/-}$ if it is located between the p_1 and w measurements for more complicated configurations. For more complicated closed loop configurations with junctions, additional formulas can be derived just as in the case of the open loop. We are using neural networks to implement stand-alone-part plant models which back out component characteristics from the measurements.

ANN representations have been derived for the more complicated closed loop and closed loop/open loop combinations of Figs. 4.9-4.11. Figure 4.9 shows a surge tank attached to a closed loop where p_1, p_2 and w are measured. Figure 4.10 shows a closed loop combined with an open loop with two pressure boundary conditions. Two pressure measurements, p_1 and p_2, and two flow measurements, w_I and w_{II}, are used. Finally, Fig. 4.11 presents a closed loop attached to open loops with three pressure boundary conditions. Only two flow measurements, w_I and w_{II}, are used. We discuss here only the ANN representation for Fig. 4.11.

The steady-state mass balance equations for the flows w_i in segment i are:

$$w_8 = w_{II} - w_I \tag{4.73}$$

$$w_4 = w_I - w_3 \tag{4.74}$$

$$w_1 = w_I \tag{4.75}$$

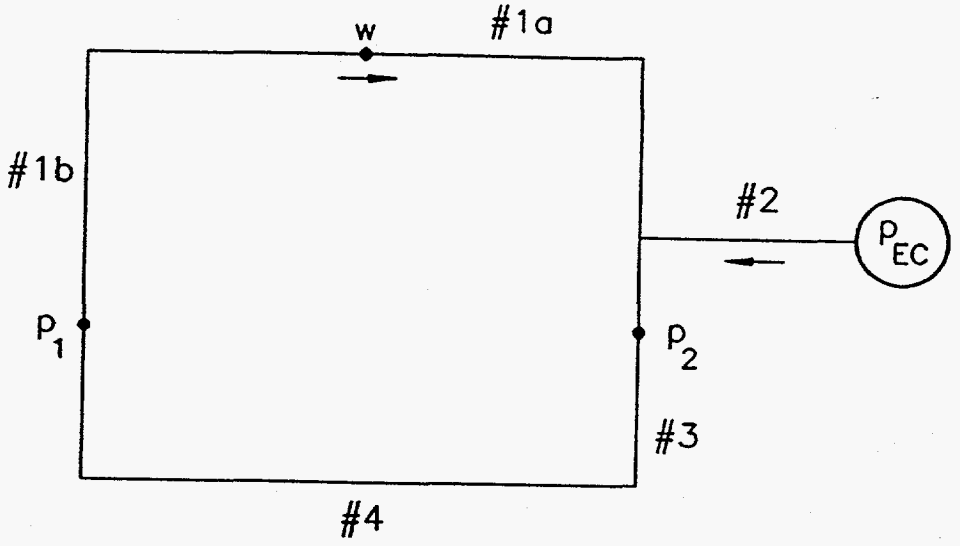

Fig. 4.9. Closed Loop with Surge Tank

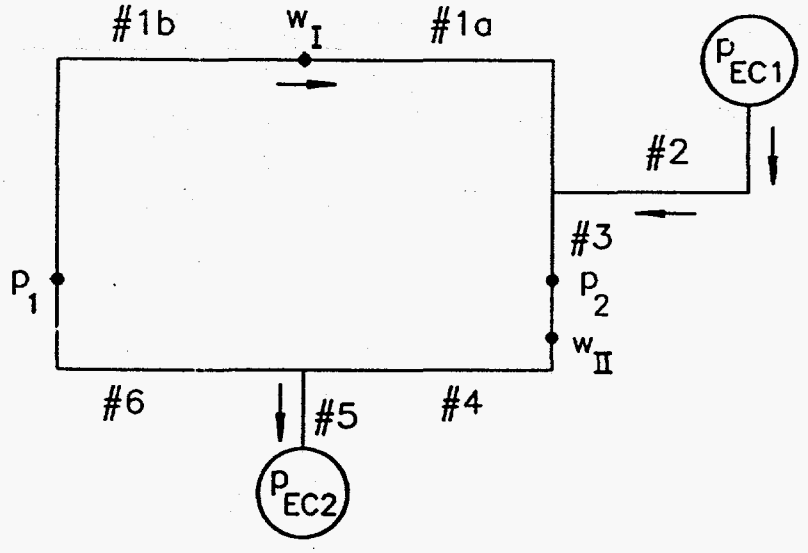

Fig. 4.10. Closed Loop/Open Loop with Two Pressure Boundary Conditions

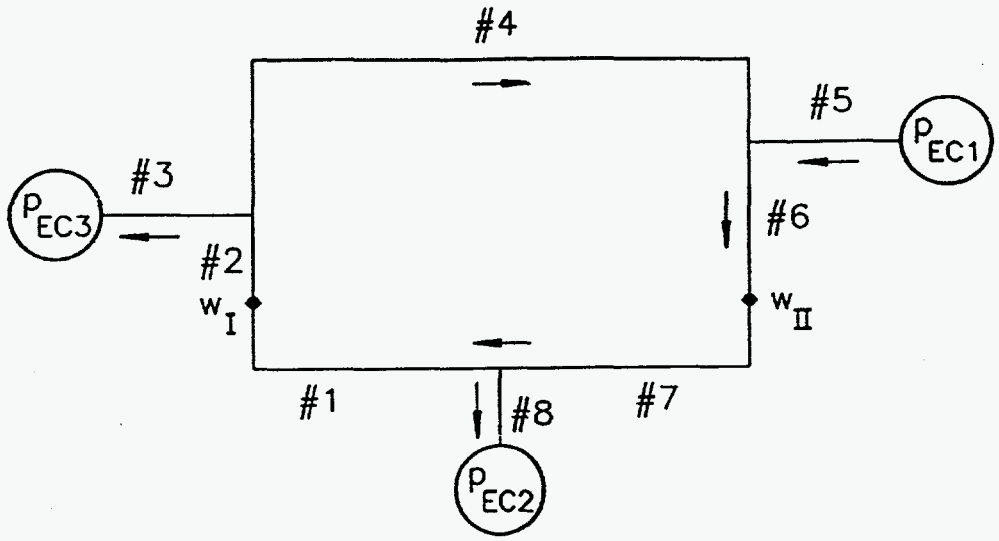

Fig. 4.11. Closed Loop/Open Loop with Three Pressure Boundary Conditions

$$w_2 = w_I \tag{4.75}$$

$$w_5 = w_6 - w_4 = w_{II} - w_I + w_3 \tag{4.77}$$

$$w_6 = w_{II} \tag{4.78}$$

$$w_7 = w_{II} \tag{4.79}$$

As can be seen, these equations can be solved to give only three independent flows, w_I, w_{II}, and w_3. The two-dimensional spaces that we want to use are w_I w_{II} spaces. This requires the elimination of w_3. We now turn to the momentum conservation equations and utilize the momentum characteristics $f_i(w)$ of each segment i together with the results from the mass balance Eqs. (4.73)-(4.79), giving,

$$f_1(w_I) + f_2(w_I) + f_4(w_I - w_3) + f_6(w_{II}) + f_7(w_{II}) = 0 \tag{4.80}$$

$$f_5(w_{II} - w_I + w_3) + f_6(w_{II}) + f_7(w_{II}) + f_8(w_{II} - w_I) = p_{EC1} - p_{EC2} \tag{4.81}$$

$$f_5(w_{II} - w_I + w_3) - f_4(w_I - w_3) - f_2(w_I) - f_1(w_I) + f_8(w_{II} - w_I) = p_{EC1} - p_{EC2} \tag{4.82}$$

$$f_5(w_{II} - w_I + w_3) + f_6(w_{II}) + f_7(w_{II}) + f_1(w_I) + f_2(w_I) + f_3(w_3) = p_{EC1} - p_{EC3} \tag{4.83}$$

$$f_5 (w_{II}-w_I+w_3) - f_4 (w_I-w_3) + f_3 (w_3) = p_{EC1} - p_{EC3} \quad (4.84)$$

$$-f_8 (w_{II}-w_I) + f_1 (w_I) + f_2 (w_I) + f_3 (w_3) = p_{EC2} - p_{EC3} \quad (4.85)$$

$$-f_8 (w_{II}-w_I) - f_6 (w_{II}) - f_7 (w_{II}) - f_4 (w_I-w_3) + f_3 (w_3) = p_{EC2} - p_{EC3} \quad (4.86)$$

Combinations of these momentum equations can be solved to give curves relating w_I and w_{II} by substituting for w_3. Caution must be used since not all of these equations are linearly independent. Since the w_3 substitution involves implicit functions, we can not derive explicit general functional forms for these curves. We resort here to giving the combination of momentum equations which implicitly define each curve.

Curve 1: Eq. (4.80) and Eq. (4.85)

Curve 2: Eq. (4.81) and Eq. (4.85)

Curve 3: Eq. (4.82) and Eq. (4.85)

Curve 4: Eq. (4.80) and Eq. (4.84)

Curve 5: Eq. (4.80) and Eq. (4.81)

Curve 6: Eq. (4.81) and Eq. (4.84)

Other curves in w_I w_{II} space which are linear combinations of these six curves can be derived from the momentum equations, but these linearly independent ones have been found to be the most informative ones for our component-characteristic technique used to diagnose Q_{mass} and Q_{mom} failures.

When Eq. (4.85) is used in the w_3 substitution for Eqs. (4.80), (4.81), and (4.82), it is clear that any two curves of the set, 1, 2, and 3 will uniquely define the operating point in w_I w_{II} space. Only two of the three equations are linearly independent. If this were not the case, the operating point would be overdetermined. Focusing on all the combinations of two curves in this set shows that

- momentum failure in segment 4 leads to the operating point moving along curve 2.

  The characteristic $f_4(w)$ does not appear in Eq. (4.85) which is the "w_3" substitution equation. This means that changes in $f_4(w)$ due to momentum failure in segment 4 will not change the w_3 substitution. Among Eqs. (4.80), (4.81), and (4.82) a change in $f_4(w)$ changes Eqs. (4.80) and (4.82), but does not change Eq. (4.81). Curve 1 is defined by Eqs. (4.80) and (4.85), and curve 3 is defined by Eqs. (4.82) and (4.85). These two curves are therefore changed by segment 4 momentum failures. Curve 2 is defined by Eqs. (4.81) and (4.85). Since these two equations do not change, curve 2 does not change. The operating point, which is moved by the changes in curves 1 and 3, therefore moves along the nonchanged curve, curve 2.

- momentum failure in segment 5 or changes in boundary condition p_{EC1} leads to the operating point moving along curve 1.

  As in the case of momentum failure in segment 4, momentum failure in segment 5 does not change the "w_3" substitution, Eq. (4.85). However, the change in $f_5(w)$ does change Eqs. (4.81) and (4.82). This means that curves 2 and 3 change. However, Eq. (4.80) does not change and, therefore, curve 1 does not change. The operating point therefore moves along curve 1 upon

momentum failure in segment 5. Changes in the boundary condition p_{EC1} would have the same effect on the set of Eqs. (4.80)-(4.82) and Eq. (4.85). The same operating point trace would therefore also be obtained.

- momentum failure in segments 6 or 7 leads to the operating point moving along curve 3. Momentum failure in segments 6 or 7 does not change the "w_3" substitution, Eq. (4.85). Equations (4.80) and (4.81) do change which changes the curves 1 and 2. Equation (4.82), and, therefore, curve 3 does not change. The operating point therefore moves along curve 3.

Similarly, when Eq. (4.84) is used in the w_3 substitution, the set of Eqs. (4.80) and (4.81) give

- momentum failure in segment 8 or change in boundary condition p_{EC2} leads to the operating point following curve 4.
- momentum failure in segments 6 or 7 leads to the operating point following curve 3.
- momentum failure in segments 1 or 2 leads to the operating point following curve 6.

Finally, if Eq. (4.81) is used in the w_3 substitution, the set of equations, Eqs. (4.80) and (4.84) give

- momentum failure in segments 1 or 2 leads to the operating point following curve 6.
- momentum failure in segment 3 or change in boundary condition p_{EC3} leads to the operating point following curve 5.
- momentum failure in segment 4 leads to the operating point following curve 2.

Mass failures require the following logic reasoning to trace the pathway of the operating point.

- Any mass failure within the closed loop will alter the characteristics of segments 4, 6, 7, 1, or 2. This modifies either the equations from which w_3 can be solved in terms of w_I and w_{II} or the equations which w_3 is going to be substituted in. As a consequence, this means that the operating point will not follow any of the curves 1-6. It moves outside.

- For the case of a mass failure in segment 5, if w_3 is known, in principle all the flows are known except for the flow in segment 5 upstream of the mass failure. Of the three equations, Eqs. (4.81), (4.84), and (4.85) used for the w_3 substitution, only Eq. (4.85) remains unchanged with this ambiguity in the segment 5 flow and the change in $f_5(w)$. The only curves in the six curve set which are defined using Eq. (4.85) are the curves 1, 2, and 3. This then points us to the curve set 1, 2, and 3. In this set, only curve 1 is unaffected by the change in f_5 characteristics. This is because Eq. (4.80) does not change while Eqs. (4.81) and (4.82) do. The operating point in w_I w_{II} space, therefore, moves along curve 1.

- For the case of a mass failure in segment 8, the flow in segment 8 now has two values. Of the three equations used for the w_3 substitution, only Eq. (4.84) remains unchanged. This then points us to the curve set 4 and 6. In this set, only curve 4 is unaffected by the malfunction. The operating point in $w_I w_{II}$ space, therefore, moves along curve 4.

- For the case of a mass failure in segment 3, the flow in segment 3 now has two values. Of the three equations used for the w_3 substitution, only Eq. (4.81) remains unchanged. This then points us to the curve set 2, 5, and 6. In this set, only curve 5 is unaffected by the malfunction. The operating point in w_I w_{II} space, therefore, moves along curve 5.

Table 4.11 enumerates the list of possible malfunctions. Table 4.12 summarizes the movement of the operating point along the "f" curves for each malfunction listed in Table 4.11. The proposed ANN representation resulting from Table 4.12 for the closed loop/open loop configuration of Fig. 4.11 is shown in Table 4.13. The table shows the groups of malfunctions which can be identified by a common operating point trace when w_I and w_{II} are the measured variables and are plotted against each other.

Table 4.11. Potential Malfunction for Closed Loop/Open Loop Configuration of Fig. 4.11

Malfunction Number	Malfunction Type
1	Mass failure in segment 4
2	Mass failure in segment 6
3	Mass failure in segment 7
4	Mass failure in segment 1
5	Mass failure in segment 2
6	Momentum failure in segment 1
7	Momentum failure in segment 2
8	Momentum failure in segment 6
9	Momentum failure in segment 7
10	Momentum failure in segment 4
11	Momentum failure in segment 3
12	Mass failure in segment 3
13	End condition p_{EC3} malfunction
14	Momentum failure in segment 5
15	Mass failure in segment 5
16	End condition p_{EC1} malfunction
17	Momentum failure in segment 8
18	Mass failure in segment 8
19	End condition p_{EC2} malfunction

Table 4.12. Operating Point Trace for Closed Loop/Open Loop Configuration of Fig. 4.11

Malfunction Number	Operating Point in w_I w_{II} Space	Group
1	Out (outside the six curves)	I
2	Out	I
3	Out	I
4	Out	I
5	Out	I
6	Curve 6	II
7	Curve 6	II
8	Curve 3	III
9	Curve 3	III
10	Curve 2	IV
11	Curve 5	V
12	Curve 5	V
13	Curve 5	V
14	Curve 1	VI
15	Curve 1	VI
16	Curve 1	VI
17	Curve 4	VII
18	Curve 4	VII
19	Curve 4	VII

Table 4.13. Neural Network Representation for Closed Loop/Open Loop Configuration of Fig. 4.11

Group	Malfunction Number	Operating Point in w_I/w_{II} Space
(I)	1, 2, 3, 4, 5	Out
(II)	6, 7	Curve 6
(III)	8, 9	Curve 3
(IV)	10	Curve 2
(V)	11, 12, 13	Curve 5
(VI)	14, 15, 16	Curve 1
(VII)	17, 18, 19	Curve 4

In these derivations presented here of the step-by-step more complex neural net representations for the step-by-step more complex configurations represented by Figs. 4.6-4.11 and Eqs. (4.28)-(4.29) can be seen the possibility of a general technique and a general theorem [4.4]. The derivation consists of decomposing the T-H loops into segments, at junctions and instrumentation locations, each of which is associated with one momentum characteristic; forming and counting the requisite number of mass and momentum balance equations; and then logically reasoning through the number of equations and variables to determine the number of independent curves in measured variable space which are and are not affected by the set of possible malfunctions. Sets of malfunctions are then grouped according to the curve which the operating point traces during the particular malfunction. It should prove possible to develop a code to automate this logical generation of the neural network representations for different geometrical configurations in this consistent manner.

4:3 Component Identification

As stated in Chapter 1, the diagnostic strategy uses two sets of ANNs to first identify possible generic components which could have malfunctioned and then the specific component within the class of generic components which malfunctioned. We start with the generic component identification.

4.3.1 Generic Component Selection

In the Component Classification Dictionary of Fig. 3.10, once a conclusion of Q'_{mom} diagnostics has been reached by the ES, then a differentiation has to be made in the generic class of Q_{mom}

components between active elements (pump) and passive elements (valves). We consider the two geometrical configurations shown in Fig. 4.12.

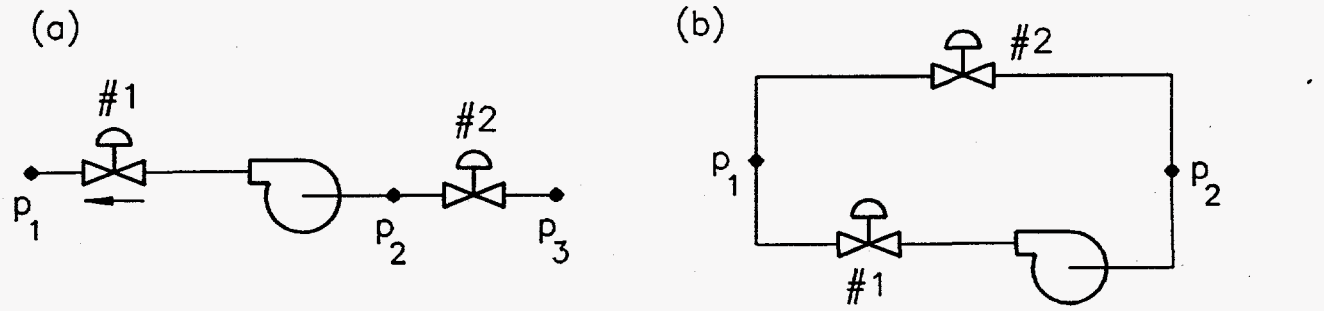

Fig. 4.12. Pump vs Valve Configuration

In configuration (a) of Fig. 4.12, downstream and upstream are distinguishable. In configuration (b), these terms are ambiguous. For Fig. 4.14(a), using a consistent sign definition of pressure difference gives,

$$\begin{aligned} \Delta p &\equiv p_2 - p_3 && \text{across the pump} \\ &\equiv p_1 - p_2 && \text{across valve 1} \\ &\equiv p_1 - p_3 && \text{across the pump + valve 1} \end{aligned} \qquad (4.89)$$

For Fig. 4.12(b), we will use

$$\begin{aligned} \Delta p &\equiv p_1 - p_2 && \text{across valve 2} \\ & && \text{also across the pump + valve 1} \end{aligned} \qquad (4.90)$$

The quasistatic component momentum characteristics for the various combinations shown in each configuration are plotted in Fig. 4.13. If we start with configuration (b), the technique outlined in Section 4.2.2.2 can be used here to distinguish between valve 2 malfunctions and the malfunctions of the combination pump + valve 1. The generic differentiation feature is that the valve characteristic decreases towards zero with decreasing flow, while the combination pump characteristic increases to a maximum with decreasing flow. The ANN is to be trained to recognize this generic differentiation feature. We, therefore, do not need all the specific f(w) component characteristics which are necessary for the resolution of Q'^{-}_{mass} or Q'^{-}_{mom} with the Section 4.2.2.2 techniques. This is a generic characteristics differentiation formula between all valves and all pumps. We move to configuration (a). If we have p_1 p_2 p_3, we can distinguish between valve 1 and pump malfunctions by using the quasistatic momentum characteristics illustrated in Fig. 4.13 and the same techniques detailed in Section 4.2.2.1 with the same generic differentiation feature described for configuration (b). If the possible Q_{mom} malfunction is valve 1 and not valve 2, then we have a different situation. At present, it appears that it is not possible to differentiate between valve 1 malfunctions and pump malfunctions with only quasistatic component momentum characteristics using the instrumentation combinations of Fig. 4.13. There is a configuration/ instrumentation dependence.

4.3.2 Specific Component Identification

Once a generic component class has been identified for the possible malfunction initiator, then differentiation between possible specific components within the generic component class has to be performed. It should be recognized that as the diagnostic strategy proceeds deeper down the tree

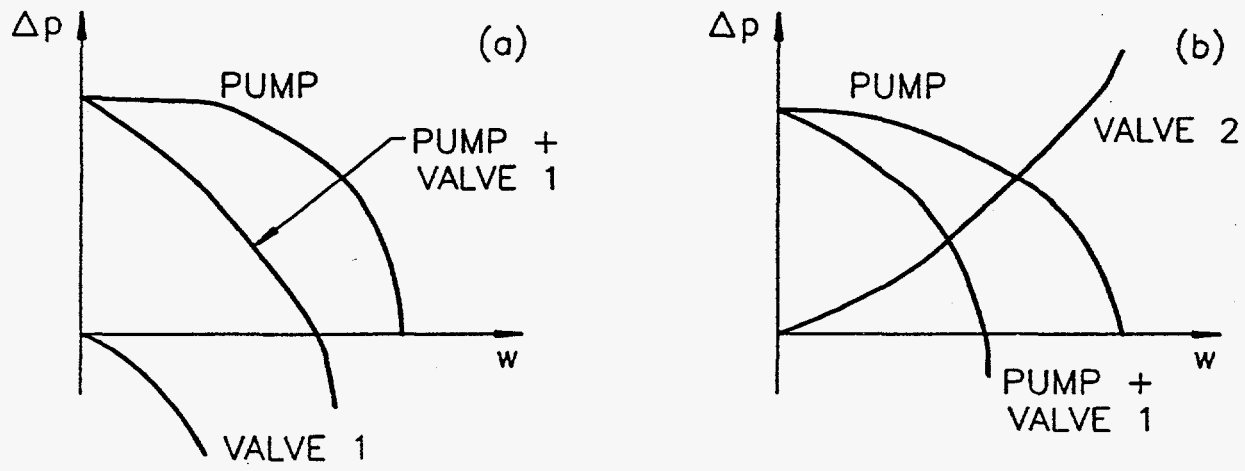

Fig. 4.13. Combination Component Characteristics

structure to identify failure of specific components, many pattern recognition techniques are already available to perform the identification. The tree structure of the diagnostic strategy reduces the number of possibilities which have to be investigated. It may be that the selection of a technique is only one of determining the appropriateness of ANNs for that particular application. We have two neural network-based identifiers here for performing an identification in the case of: (i) PORV a vs PORV b, and (ii) valve a vs valve b. We first consider the specific PORV determination.

4.3.2.1 Specific PORV Determination

We present here a technique for selecting a malfunctioning PORV from a set of candidate PORVs based solely on the PORV discharge characteristics. Once the ES has identified a Q'_{mass} malfunction and once the generic component classifier has decided that the malfunction of an initially closed valve has occurred, this formula will be used to pick the specific PORV from the two possibilities in Fig. 4.14. The PID (or perhaps a separate component characteristic database) has

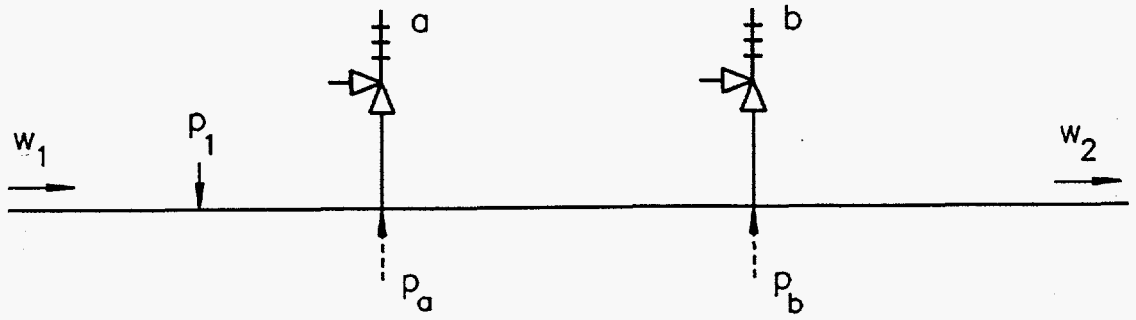

Fig. 4.14. Possible PORV Candidates

stored the PORV discharge characteristics $f_a(P)$ and $f_b(P)$ for the two PORVs. Upon opening of a PORV, the flow w_S through the open unknown PORV is related to p_s, the pressure at the PORV through the discharge characteristics,

$$w_s = f_s(p_s)\,, \tag{4.91}$$

If measurements of w_S and p_s were available, the discharge characteristic $f_s(p_s)$ could be determined. Upon malfunction, we could then compare this $f_S(p_S)$ with $f_a(p)$ and $f_b(p)$ to decide which of the two PORVs is malfunctioning. An ANN will be used here as the equality is not a point equality but a function of pressure, f(p). In other words, a comparison of shapes is once again performed here. The accuracy of this formula depends upon the difference in $f_a(p)$ and $f_b(p)$, and the difference in the locations of the PORVs. With the limitations in instrumentation indicated in Fig. 4.14, only the pressure p_i and the flows w_i and w_o are known. We have to use the quasistatic momentum equation (3.3) for Fig. 4.16, when no pump is present,

$$\Delta p = \sum_j k_j \rho \frac{v_j^2}{2}\,. \tag{4.92}$$

Equation (4.92) can be used to relate, assuming that PORV b is the malfunctioning PORV, the PORV inlet pressure p_b with p_i,

$$p_b = p_i - k_b w_i^2 , \tag{4.93}$$

where k_b = loss coefficient determined by location of PORV b. By mass conservation,

$$w_s = w_i - w_o . \tag{4.94}$$

Alternatively, if system inventory is available, through level measurements for example, Eq. (4.94) can be replaced with

$$w_s = \frac{dm}{dt} . \tag{4.95}$$

These additional equations will provide enough data to allow the comparison of $f_s(p)$ with $f_b(p)$. The procedure is then to equate p_S with p_b, deduce $f_s(p_s)$ using w_s and compare $f_s(p_s)$ with $f_b(p)$. If it is a positive comparison, then the hypothesis that PORV b is the malfunctioning PORV is correct. If the comparison is negative, then the procedure is repeated with PORV a. If it is not PORV a either, then it must be a break. Thus, through a trial-and-error selection process, the specific component classifier can decide whether PORV a or PORV b is the malfunctioning PORV. If the ES and the generic component classifier have performed their functions correctly, the formulation presented here for this specific component should be appropriate. The formula then can be expanded to pick one PORV out of a set of n PORVs in series. It can be seen that here again this will be an iterative search process, with possibilities for optimization. Furthermore, it can be stated that this formula can generally be used to detect the malfunction of any component which is part of the inventory balance in the mass equation. As long as the discharge characteristics f(p) are available for that component, there is conceptually no need to go through the generic component classifier for the Q_{mass} components if all the data are available.

"Generic" relief valve characteristics can also be used instead of specific relief valve characteristics. This means that we are relying on thermal-hydraulic conditions at PORV inlets being different enough so that different parts of the generic relief valve characteristic are used when the PORVs malfunction and open. The different parts of the characteristics will then indicate which PORV has malfunctioned with this method. In order to obtain reasonable resolution, the PORVs cannot be located close together. This is what operational practice has indicated as being exactly the most useful case.

If the PORV flow area is explicitly treated, the PORV quasistatic discharge characteristic is now

$$w_s = A\, f(p_s) \tag{4.96}$$

where

w_s = PORV flow rate

A = flow area

p_s = PORV inlet pressure.

We illustrate with the ideal PORV characteristic shown in Fig. 4.15.

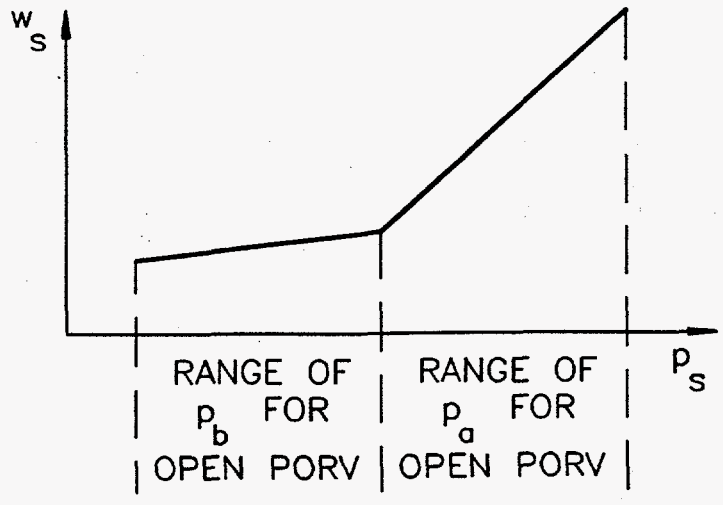

Fig. 4.15. Idealized PORV Characteristic

We have for the configuration of Fig. 4.14

$$p_a = p_i - k_a w_i^2 \tag{4.97}$$

$$p_b = p_i - k_b w_i^2 \tag{4.98}$$

$$w_s = w_i - w_o \tag{4.99}$$

k_a = loss coefficient between p_i location and PORV a

k_b = loss coefficient between p_i location and PORV b

Equations (4.97) and (4.98) assume that no malfunctions have occurred between the $p_i w_i$ locations, and the w_o location. Also, p_i,w_i and w_o are the only available instrumentation. The loss coefficients would have to either be determined from knowing initial pressure distributions or be estimated from knowing the geometrical configurations. When one of the PORVs malfunctions, p_i, w_i and w_o change. The method consists of using Eqs. (4.97) and (4.98) to estimate the valve inlet pressure at the respective PORVs. If there are no breaks, p_a will always be correct, but p_b may or may not be depending upon which valve malfunctioned. This then allows us to have a logical branch to decide which PORV malfunctioned depending upon comparisons with the measured discharge flow w_s.

We then calculate w_a and w_b from

$$w_a = Af(p_a) \tag{4.100}$$

$$w_b = Af(p_b) \tag{4.101}$$

Figure 4.16 shows that the method consists of comparing the calculated w vs calculated p curve, obtained by using p_a and p_b to calculate the PORV flow through Eqs. (4.97)-(4.101) successively, with the measured w_s vs calculated p_s curve, which should follow the PORV characteristic of Fig.

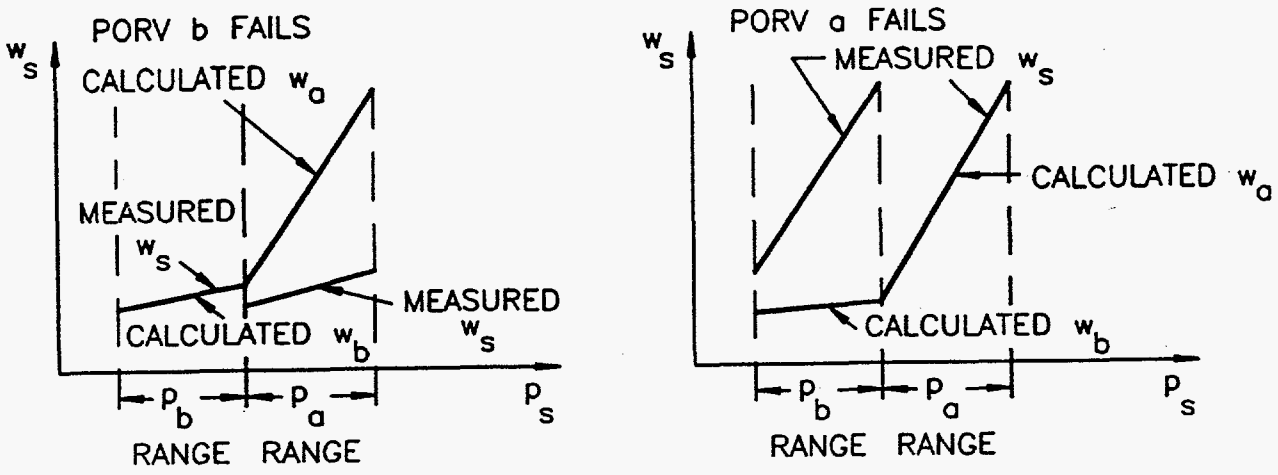

Fig. 4.16. PORV Relief Characteristics Method

4.15. The valve opening area A can be normalized by calibrating to one specific point on the curve and then seeing how well the two shapes compare. Since without a break p_a is always correct, w_a from Eq. (4.100) will be correct (i.e., agree with the measured w_s) only if PORV a malfunctioned. If PORV a is malfunctioning, then the use of p_b, in Eq. (4.101) for the flow, should give a shape from the wrong portion of the characteristic curve of Fig. 4.15, while the use of p_a, Eq. (4.100), should give the shape from the right portion of the characteristic curve. If PORV b malfunctioned, then p_b will be correct and w_b from Eq. (4.101) will be correct (i.e., agree with the measured w_s). However, w_a from Eq. (4.100) will give a shape from the wrong portion of the characteristic curve. It is important to have a characteristic curve with variations. The diagnosis of a break between the two flow measurements would occur if the shape comparison concludes that the mass malfunction is neither PORV a nor PORV b. The proposed neural network representation is given by Table 4.14.

Equations (4.96)-(4.101) are just a means of using a model to obtain comparison data when adequate data is not available. The equations can be used off-line to obtain training data. Neural network

Table 4.14. Specific PORV Neural Net Representation

Malfunction	Operating Point Trace
PORV a	Calculated w_a agrees with measured w_s
PORV b	Calculated w_b agrees with measured w_s
Break	Calculated w_a and w_b do not agree with measured w_s

representations can also be derived for more general configurations such as the one shown below in Fig. 4.17.

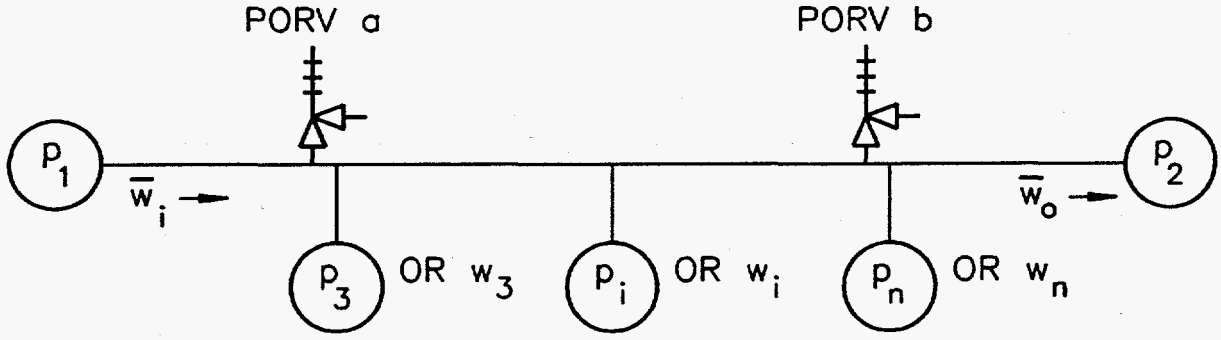

Fig. 4.17. General Configuration for PORV Determination

4.3.2.2 Specific Open Valve Determination

Given that Q'_{mom} and that the generic component classifier determines it is a passive momentum component and not an active momentum component which has malfunctioned, the specific component classifier uses neural nets to pick out the specific passive momentum component which has malfunctioned [4.5]. For illustrative purposes consider the model problem of Fig. 4.18 where

either valve a or valve b has malfunctioned. It should be noted the technique described here is a general technique which can be applied to a number of different passive momentum components arranged in series. Parallel arrangements are handled through the ES rules and the decompositioning into the various loops. Possible techniques depend very much upon the configuration geometry being the geometry defined in Fig. 4.18. This fits in well with the ES first selecting the balance malfunction Q. The whole approach is to break the T-H system up piece by piece.

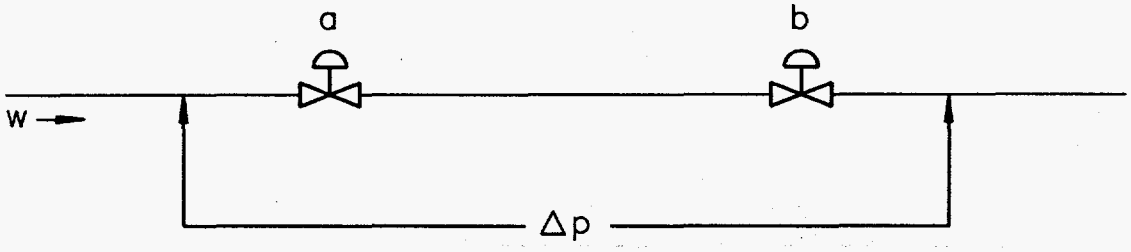

Fig. 4.18. Valve a vs Valve b

Every passive hydraulic component, valve, or filter has a specific component characteristic which can be written as

$$\Delta p = A(w)\, w^2 \qquad (4.102)$$

where Δp = pressure drop across component

w = component mass flow

A(w) is not as strongly dependent upon w as w^2, but the functional dependency normally has a frequency content. Quasistatic valve characteristics are not useful to distinguish between valve a or valve b malfunctions. Higher frequency valve characteristics have to be used in this case.

This limitation on the use of component steady state characteristics means that the next set of T-H formulas in Table 1.1, which summarizes the analytical decomposition strategy, will have to be used. Table 1.1 shows that these are the component transient characteristics. In our use of the component steady state characteristics, quasistatic part-of-a-plant models have been constructed using these characteristics. Implementation has been through the use of ANNs which then allows the pattern recognition comparisons of malfunction data against model data to be made in one step. However, in the case of the use of component transient characteristics, merely modifying the quasistatic part-of-a-plant model approach may not be the optimum route. Two other possibilities already exist and will be utilized in future work on PRODIAG. These are the faster-than-real-time plant numerical simulator (FTRS) and the area of noise signature analysis. Work in the area of FTRS utilizes the standard simulator practice of incorporating the component transient characteristics into numerical dynamic models of the plant. The current research focus then concentrates on multiprocessor algorithms to improve the computing time performance of these numerical models. The area of noise signature analysis is also a field where there is extensive on-going work. Current techniques proposed for diagnosis use the higher frequency characteristics. These techniques essentially perform a Fourier transform to the w(t) and p(t) signals of Fig. 4.18. Cross-correlation and auto correlation methods are used to recognize missing signatures. This is then an identification of a malfunctioning component. ANNs can be used to perform these pattern recognition steps in the procedure but other pattern recognition techniques are being used. However, all these techniques require instrumentation with frequency responses and data sampling rates that appear to be higher than current plant instrumentation can to provide. Higher frequency transponders (e.g., acoustic range) are only available at limited locations in most reactor systems. It would also appear to require a significant amount of prefiltering to separate out the noise in this frequency range.

REFERENCES

[4.1] Project Staff, "Combined Expert System/Neural Network for Process Fault Diagnosis," Annual Status Report for FY93 (September 1993).

[4.2] T. Y. C. Wei, "Nondimensionalization of Variables and Neural Nets," memorandum to J. Reifman, December 10, 1993.

[4.3] T. Y. C. Wei, "Neural Networks Using Component Characteristics," memorandum to J. Reifman, March 10, 1993.

[4.4] Project Staff, "Combined Expert System/Neural Network for Process Fault Diagnosis," Annual Status Report for FY94 (September 1994).

[4.5] T. Y. C. Wei, "Neural Net Representation for Specific Q_{mom} Classifier," memorandum to J. Reifman, December 2, 1993.

ACKNOWLEDGMENTS

We would like to gratefully thank Karen Jenicek for picking up in the middle of this documentation effort and completing it under difficult circumstances. Her effort was indeed commendable.

We would also like to gratefully acknowledge Dr. L. L. Briggs for her constructive review of this document. Her help was much appreciated.